

DEVELOPMENT OF PLASMA FUNCTIONALIZED NANO-ADDITIVES FOR OILS AND
STUDY OF THEIR TRIBOLOGICAL PROPERTIES

by

VINAY SHARMA

DISSERTATION

Submitted in partial fulfillment of the requirements
for the degree of Doctor of Philosophy at
The University of Texas at Arlington

December, 2017

Arlington, Texas

Supervising Committee:

Dr. Pranesh B. Aswath, Supervising Professor

Dr. Richard B. Timmons

Dr. Efstathios "Stathis" I. Meletis,

Dr. Yaowu Hao

Dr. Daejong Kim

Copyright © by

Vinay Sharma

2017

ACKNOWLEDGEMENTS

To all the individuals who have been instrumental in making this dissertation work possible and all those who provided direct or indirect support in this 4 and a half year long graduate school journey ... Thanks you so much!

I would like to include some special mentions here, starting with my research advisor, Dr. Pranesh B. Aswath. He has been a constant source of motivation in the last 4 years and his mentorship has helped me a lot in transforming from a student into a professional. Under his guidance, I have not only gained the knowledge in the subject matter but have also acquired numerous soft skills. He has been a great positive influence in my life and I extend my sincere gratitude to him for providing the incessant support.

The next person who has been pivotal in relation to the success of this dissertation work is Dr. Richard B. Timmons. I consider myself very fortunate to have him as my co-advisor for this research work and this association with him for the past few years has been a great learning experience for me. His contributions to all my academic achievements are most vital and I am very grateful to him for imparting all the knowledge and wisdom.

In continuation, I would also like to thank Dr. Ali Erdemir for providing me the opportunity to work and learn in his research lab at Argonne National Laboratory. It was an honor for me, to have his scientific inputs and recommendations for this doctoral work.

Beside these, I would like to thank the rest of my dissertation committee: Dr. Efstathios "Stathis" I. Meletis, Dr. Dr. Yaowu Hao, and Dr. Daejong Kim, for their words of encouragement and intuitive comments that motivated me to keep a focused perspective toward my research work. In addition, I wish to thank all the faculty and staff members of the material science and

engineering dept. for their valuable contribution throughout my graduate study. A note of thanks to Beth Robinson and Jennifer Standlee for managing all the logistics and graduate school paperwork, to ensure a productive work environment. I also wish to acknowledge the time and efforts of Dr. Brian Edwards, Dr. Jiechao C. Jiang and David Yan who helped to me conduct research related work on different analytical instruments. I thank Dr. Osman Eryilmaz and Dr. Giovanni Ramirez for mentoring me at Argonne National Lab IL. I am also thankful to Dr. Lucia Zuin, Dr. Tom Regier and Dr. Yongfeng Hu of the Canadian Light Source for their help and support with the XANES work.

I would also like to thank all the members of my research group, Dr. Vibhu Sharma, Dr. Felipe Monte, Ami Shah, Kimaya Vyavhare, Tugba Cebe and Kamal Awad who always kept me motivated and helped me to stay focused on my work. The financial support to carry out this dissertation work was provided by Vanderbilt Chemicals it is greatly acknowledged.

I express my gratitude towards my colleagues and friends who have always inspired me with their words of encouragement. At last, I thank my parents, my significant other and my brothers and sisters for their unwavering support and incessant love. Their belief and care helped me go from strength to strength.

DEDICATION

This work is dedicated to the memory
of my uncle,
Dr. R. S. Sharma

LIST OF FIGURES

Chapter 1

- Figure 1.** Greenhouse gas emissions and ILSAC fuel standards. 2

Chapter 2

- Figure 1.** Schematic of the process flow for synthesis of functionalized nanoparticles. 42
- Figure 2.** FTIR spectra for plasma films from HMDSO and HMDSO+O₂ deposited on KBr card (Pressure: 300mT; Flow rate: 2 sccm; Power: 60W; Deposition time: 15 mins. 43
- Figure 3.** Silicon 2p XPS spectrum for functionalized PTFE nanoparticles (PHGM). 44
- Figure 4.** Friction behavior for base oil, oil with ZDDP, PTFE nanoparticles and functionalized PTFE (PHGM) nanoparticles; **(a)** Friction data plot for 1 hour tests; **(b)** Friction outcomes for 4 hours tests. 49
- Figure 5.** Optical profilometry of the cylinders represented in 2D at the center region of the cylinder and the 3D representation is of the area of contact in the cylinders from 1 hour ((i) B.O, (ii) B.O + ZDDP 350, (iii) B.O + ZDDP 350 + 0.33wt% PTFE & (iv) B.O + ZDDP 350 + 0.33wt% PHGM) and 4 hours ((v) B.O+ ZDDP 700 & (vi) B.O+ ZDDP 350 + 0.33wt% PHGM) of tribological testing. 50
- Figure 6.** Optical micrographs of wear surfaces of the flat steel specimens from 1 hour ((i) B.O, (ii) B.O + ZDDP 350, (iii) B.O + ZDDP 350 + 0.33wt% PTFE & 51

(iv) B.O + ZDDP 350 + 0.33wt% PHGM) and 4 hours ((v) B.O+ ZDDP 700 & (vi) B.O+ ZDDP 350 + 0.33wt% PHGM) of tribological testing.

Figure 7. Comparison of wear volume losses for base oil, oil with ZDDP, PTFE nanoparticles and functionalized PTFE (PHGM) nanoparticles; (a) Wear data for 1 hour tests (A,B,C & D); (b) wear volumes for 4 hours tests (E,F & G). 52

Figure 8. XPS spectra for specimens from 1 hour tests; Green plot: B.O + ZDDP 350 + 0.33wt% PHGM; Blue plot: B.O + ZDDP 350. 55

Figure 9. Phosphorus K and L edge XANES TEY spectra of model compounds and tribofilms generated with B.O + ZDDP 350 + 0.33wt% PHGM and B.O + ZDDP 350. 60

Figure 10. Sulfur K edge FLY XANES spectra of model compounds and tribofilms generated with B.O + ZDDP 350 + 0.33wt% PHGM and B.O + ZDDP 350. 61

Figure 11. Sulfur K edge TEY XANES spectra of model compounds and tribofilms generated with B.O + ZDDP 350 + 0.33wt% PHGM and B.O + ZDDP 350. 62

Figure 12. Relative P/S ratios for tribofilms generated with B.O + ZDDP 350 + 0.33wt% PHGM and B.O + ZDDP 350. 63

Figure 13. Phenomenological models for tribofilms generated with (a) B.O + ZDDP 350 + 0.33wt% PHGM and (b) B.O + ZDDP 350. 65

Chapter 3

Figure 1. Coefficient of friction (CoF) as a function of time for the seven formulations: BO, ZD, ZD + PHGM, IL1, IL1 + PHGM, IL2 and IL2 + PHGM. 83

Figure 2. Wear volume losses for pins after tribological testing with BO, ZD, ZD + PHGM, IL1, IL1 + PHGM, IL2 and IL2 + PHGM. 85

Figure 3. 3D SPM images of wear surfaces on flat specimens generated from BO, ZD, ZD + PHGM, IL1, IL1 + PHGM, IL2 and IL2 + PHGM. 87

Figure 4. Phosphorus 2p, Iron 2p, Fluorine 1s and Oxygen 1s XPS spectra for ZD, ZD + PHGM, IL1, IL1 + PHGM, IL2 and IL2 + PHGM. 91

Figure 5. Phosphorus L-edge TEY and Silicon K-edge FLY XANES spectra for ZD + PHGM, IL1 + PHGM and IL2 + PHGM samples. 94

Chapter 4

Figure 1. Coefficient of friction as a function of time for sample A) Base Oil (B.O) ; B) B.O + ZDDP at 700 ppm P level; C) B.O + ZDDP at 350 ppm P level; D) B.O + 0.33wt% TiO₂; E) B.O + ZDDP at 350 ppm P level + 0.33wt% TiO₂; F) B.O + 0.33wt% TiBGM; G) B.O + ZDDP at 350 ppm P level + 0.33wt% TiBGM. 109

Figure 2. Wear volume losses for sample A) Base Oil (B.O) ; B) B.O + ZDDP at 700 ppm P level; C) B.O + ZDDP at 350 ppm P level; D) B.O + 0.33wt% TiO₂; E) B.O + ZDDP at 350 ppm P level + 0.33wt% TiO₂; F) B.O + 0.33wt% TiBGM; G) B.O + ZDDP at 350 ppm P level + 0.33wt% TiBGM. 111

Figure 3. 3D profiles of the worn surfaces after tribological testing for sample A) Base Oil (B.O) ; B) B.O + ZDDP at 700 ppm P level; C) B.O + ZDDP at 350 ppm P level; D) B.O + 0.33wt% TiO₂; E) B.O + ZDDP at 350 ppm P level + 0.33wt% TiO₂; F) B.O + 0.33wt% TiBGM; G) B.O + ZDDP at 350 ppm P level + 0.33wt% TiBGM. 112

Figure 4. Electrical contact resistance (ECR) data plots recorded during tribological testing of sample A) B.O + ZDDP at 700 ppm P level; B) B.O + ZDDP at 350 ppm P level; C) B.O + 0.33wt% TiO₂; D) B.O + ZDDP at 350 ppm P level + 0.33wt% TiO₂; E) B.O + 0.33wt% TiBGM; F) B.O + ZDDP at 350 ppm P level + 0.33wt% TiBGM. 114

Figure 5. XPS spectra (P 2p, Fe 2p, Zn 2p, Ti 2p & O 1s) for samples A) B.O + ZDDP at 350 ppm P level, B) B.O + 0.33wt% TiO₂ and C) B.O + ZDDP at 350 ppm P level + 0.33wt% TiO₂; D) B.O + 0.33wt% TiBGM; E) B.O + ZDDP at 350 ppm P level + 0.33wt% TiBGM. 118

Figure 6. (a) Phosphorus L edge TEY, (b) Zinc L edge TEY and (c) Boron K edge TEY (d) Iron L edge TEY (e) Titanium L edge TEY (f) Oxygen K edge TEY XANES spectra for samples A) B.O + ZDDP at 350 ppm P level, B) B.O + 0.33wt% TiO₂ and C) B.O + ZDDP at 350 ppm P level + 0.33wt% TiO₂; D) B.O + 0.33wt% TiBGM; E) B.O + ZDDP at 350 ppm P level + 0.33wt% TiBGM. 124

Figure 7. Schematics of tribofilms generated from samples A) B.O + ZDDP at 350 ppm P level, B) B.O + 0.33wt% TiO₂ and C) B.O + ZDDP at 350 ppm P level + 0.33wt% TiO₂; D) B.O + 0.33wt% TiBGM; E) B.O + ZDDP at 350 ppm P level + 0.33wt% TiBGM. 127

LIST OF TABLES

Chapter 2

Table 1. Chemical structures and details of the materials used.	40
Table 2. Details of oil formulations for 1 hour tests.	45
Table 3. Details of oil formulations for 4 hour tests.	46

Chapter 3

Table 1. Chemical structures of the additives used for the study.	79
Table 2. Details of the seven formulations used in this study.	80
Table 3. Operating parameters for VLS-PGM and SXRMB beamlines.	82

Chapter 4

Table 1. Details of oil formulations used for tribological tests.	129
--	-----

ABSTRACT

DEVELOPMENT OF PLASMA FUNCTIONALIZED NANO-ADDITIVES FOR OILS AND STUDY OF THEIR TRIBOLOGICAL PROPERTIES

Vinay Sharma, PhD

University of Texas at Arlington, 2017

Supervising Professor: Pranesh B. Aswath

Lubricants used in motor engines contain various chemical species to help enhance energy efficiency and provide increased longevity. Unfortunately, at the same time, these additives become a source of catalytic poisoning, thus increasing emissions from the tailpipe. With growing concern for the negative impacts of human activities on the environment, regulatory bodies for the automobile lubrication industry have set up strict guidelines for chemical compositions of their end products, including engine oils. This research work is a step towards development of a new class of lubricant additives, which are less harmful to the environment and, simultaneously, also reduce friction and wear. A novel approach, employing nanoparticles, has been used to deliver chemical species to tribological contacts to provide improved anti-friction and anti-wear benefits. For this purpose, plasma polymerization technology was used to functionalize nanoparticle additives with chemistries known to provide good tribological outcomes. Different nanoparticles (PTFE and TiO₂) and chemistries (Silicon and Boron rich) were examined and plasma treatment and process protocols were developed. The surface tailored nano-additives derived were dispersed in pure mineral oil and mineral oil containing reduced amounts of zinc dialkyl dithiophosphate

(ZDDP)/Ionic Liquid additives. The resulting solutions were subjected to thorough tribological testing. To help elucidate the lubrication mechanism of these nano-additives optical, and other highly surface sensitive techniques, such as X-ray photoelectron spectroscopy (XPS), X ray absorption near edge spectroscopy (XANES), Surface probe microscopy (SPM), etc., were employed to analyze the tribofilms formed on the wear surfaces. Additionally, the lubrication efficiency of these functionalized nanoparticle/oil mixtures were compared and contrasted with tribological results obtained from unmodified nanoparticle/oil mixtures, as well as with the existing industrial grade additives such as ZDDP. The overall results indicate that plasma functionalized nanoparticles have very promising antifriction and antiwear properties and they exhibit synergistic interaction with traditional additives to give enhanced tribological benefits. This new approach with plasma functionalized nanoparticles is very effective in reducing the harmful levels of phosphorus in the oils and, at the same time, deliver outstanding friction and wear performance.

TABLE OF CONTENTS

ACKNOWLEDGEMENTS	iii
DEDICATION	v
LIST OF FIGURES	vi
LIST OF TABLES	x
ABSTRACT	xi
CHAPTER 1: GENERAL INTRODUCTION	1
Motivation	1
Background	4
Specific Aims	15
Dissertation Structure	18
References	20
CHAPTER 2: Plasma Functionalized PTFE Nanoparticles for Improved Wear in Lubricated Contact	35
Abstract	36
Introduction	37
Experimental	40
Results and Discussion	47
Conclusions	66
References	67

CHAPTER 3: Tribological Interaction of Plasma Functionalized Polytetrafluoroethylene Nanoparticles with ZDDP and Ionic Liquids	75
Abstract	76
Introduction	77
Experimental	79
Results	82
Discussion	94
Conclusions	96
References	97
 CHAPTER 4: Synergistic Effects of Plasma Functionalized TiO ₂ Nanoparticles and ZDDP on Friction and Wear Under Boundary Lubrication	 104
Abstract	105
Introduction	106
Results and Discussion	108
Conclusions	127
Experimental Section	128
References	131
 CHAPTER 5: GENERAL CONCLUSIONS	 137

CHAPTER 1

GENERAL INTRODUCTION

1.1 Motivation

Transportation activities employing internal combustion engines continue to represent an increasingly important aspect of everyday life. As a result, there is a constant demand for more efficient engines. This need has become even more important in terms of current worldwide environmental concerns, especially in light of our growing emphasis on climate changes. As reported by the United States Environmental Protection Agency in year 2014, transportation alone contributes to about 26% of total greenhouse gas emissions and this share cannot be neglected when the demand for automobiles is growing every year. A direct approach to address this situation is to increase the fuel economy which will reduce the overall fuel usage and therefore lower the air pollution. To some extent, with technological and engine design advancements, the internal combustion industry has been able to achieve increased performance, better fuel economy and lower emissions. But, in many cases, these advances have required engines to run under far more severe conditions such as higher speeds, higher working temperatures and higher mechanical stresses. In turn, these more extreme conditions have created demands within the lubrication industry to develop new lubricants having improved properties and performance. For example, new ILSAC GF6 (International Lubricants Standardization and Approval Committee for gasoline fueled vehicles) grade requires the lubrication industry to develop lower viscosity oils with advanced friction and anti-wear additives in order to meet the demand for better fuel economy and to comply with rigorous government regulations on emissions. [1-3]

Figure 1 is a simple representation of the primary motivation behind the development of

advanced lubricant oils with improved additive performance. It highlights the contribution of overall transportation activities towards total green-house emissions (left side) and the constantly changing industrial standards that define the demand for increased fuel economy and better performance.

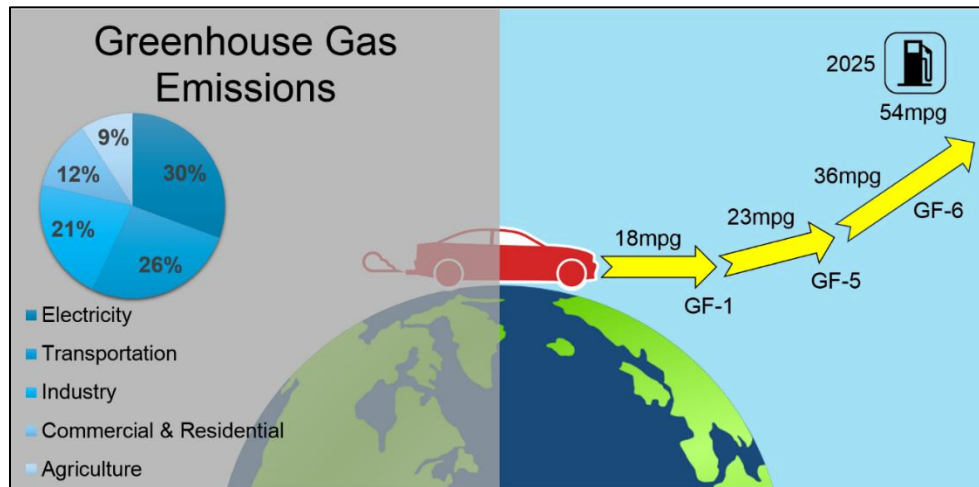


Figure 1. Greenhouse gas emissions and ILSAC fuel standards

Engine oil plays a major role in providing good fuel economy and it also protects the engine parts from wear, thus directly relating to engine durability. In addition, engine oil also helps in reducing the energy loss due to friction in the internal combustion engine which is reported to be around 12% with the current technology. [4] Recent studies have suggested that the current, and speculated future advances in the field of tribology, could lead to significant reduction in these frictional losses in both passenger (~ 18%) and heavy duty (~14%) vehicles. [4,5] Some of the most critical technological advancements in this field include the development of synthetic low viscosity oils, near friction coatings and novel lubricant additives such as ash-less additives, phosphate/borate esters, ionic liquids and nanomaterials. [6-10] Engine oil additives, such as zinc dialkyldithiophosphate (ZDDP), form protective films at the rubbing interfaces and have been shown to provide desired tribological benefits. These films are commonly referred as tribofilms

and are composed mostly of amorphous phosphate glass. [11-13] For several decades, ZDDP has remained the most preferred engine oil additive chemistry in the lubrication industry. Nevertheless, the volatile phosphorus and sulfur species from ZDDP are also known to cause catalytic poisoning which eventually leads to increased emissions at the tail pipe. [14-17]

In light of these clearly undesirable side-effects of existing additive chemistries, coupled with the overall objective to enhance engine efficiency and fuel economy, significant research work has been devoted to development of novel high performance additives. Ash-less additives, such as ionic liquids, boron based compounds and nanostructure chemistries, are among the most promising candidates that have been studied extensively in the recent years for their tribological properties. [9,18-32] Of late, nanostructures such as nanoparticles, nanotubes, nanowires etc. have received significant increased attention for their potential application as lubricant additives. [10,29-35]

The current study explores a unique way of employing nanoparticles for tribological applications to help achieve the highly desired improved fuel efficiency via reductions in friction, wear and emissions. In this approach, nanoparticles are initially functionalized using plasma polymerization techniques, whereby desired chemistries are deposited onto the particles in the form of plasma coatings hence forming a core-shell like structure. This study represents the first efforts to examine the utility of plasma functionalized nanoparticles as additives to improve lubricant oil efficiency. Standard, widely employed, tribological experiments were conducted to quantify their performance as lubricant additives. These experiments included friction and wear testing with steel specimens in a high frequency reciprocating rig configuration, a system which closely mimics the interaction of pistons on liners in engines. Highly surface sensitive techniques such as X-ray photoelectron spectroscopy (XPS) and X-ray absorption near edge spectroscopy

(XANES) were employed to identify the chemical compositions of the tribofilms generated from these additives. Obtaining precise chemical information of these protective surface films is critical in understanding the lubrication mechanism and helps develop a framework for synthesis of new generation lubricant additives. The primary objective of this work is to examine the performance of plasma functionalized nano-additives when used with the low phosphorus oil (ZDDP and/or ionic liquids at 350 ppm P treat rate). The 350 ppm P treat rate employed represents a 50% reduction in the phosphorus currently employed 700 ppm concentration. This approach aims to achieve superior tribological performance at significantly reduced phosphorus content by supplementing the oil with functionalized nanoparticles. The overall information collected for samples from both tribological experiments (friction and wear outcomes) and surface analysis was employed to deduce lubrication mechanisms and phenomenological models for the tribofilms.

1.2 Background

1.2.1 Tribology and Lubrication

Tribology is broadly defined as the science and engineering field which deals with the study of friction, wear and lubrication of the interacting surfaces in relative motion. [36] Tribology has its application in many diverse areas such as simple machinery components, complex assemblies or products, large scale manufacturing processes etc. From an engineering and industrial perspective, tribology has its strong presence in varied areas like, aerospace, automotive, lubrication, agriculture, defense, medical, coatings, energy and cosmetics. In general, the focus is to investigate and understand the various processes and dynamics of interaction between surfaces in contact under relative motion (sliding/rolling/impacting). In discussing surfaces, we need to consider the fact that they are not perfectly flat but possess microscopic features, which is

commonly referred to as roughness. This roughness, along with other physical and chemical aspects of the surfaces, play a critical role in tribology. When two bodies in contact, move relative to each other, they experience a resistance against motion which is called friction. Microscopic forces of molecular abrasion and molecular adhesion are primarily responsible for this resistance. The presence of any other medium between the surfaces dictates the dynamics of friction and wear outcomes. Lubricants (liquid/solid/semi-solid) are such mediums which are designed for specific systems. In case of fluid based lubricants, the fluid film thickness (λ) defines the friction and wear outcomes for the system. In addition, the ratio of film thickness to the roughness of the surfaces, specifies the kind of lubrication regime, as shown in the equation below [37]:

$$\lambda = \frac{h_{\min}}{\sigma^*}$$

where; h_{\min} = minimum thickness of the film; σ^* = root mean square roughness of the surfaces. Depending on λ value, lubrication regimes are classified into 3 types: Hydrodynamic lubrication ($\lambda > 5$); Mixed or Elasto-hydrodynamic lubrication ($1 < \lambda < 5$); and Boundary Lubrication ($\lambda < 1$). A commonly used method of predicting the lubrication regime makes use of a stribeck curve. This curve is a graphical representation of the relation between the friction coefficient and tribological parameters including load, geometry, speed and lubricant's viscosity. [37] For a system in which the speed of relative motion of the surfaces is high and the applied load is low, the rubbing surfaces remain separated, with a thick lubricant film present all the time. This is typically referred as the hydrodynamic lubrication ($\lambda > 5$) regime, wherein the lubrication mechanism is primarily dependent on fluid characteristics such as viscosity, traction and load bearing capability and friction and wear is minimum. In case of mixed or elasto-hydrodynamic lubrication ($1 < \lambda < 5$) regime, the load is relatively higher and speed is slower. As a result of the increased pressure the viscosity of the lubricant increases and the sufficiently high load leads to elastic deformation of

the surfaces during the hydrodynamic course. Even though the fluid film remains thick enough to keep the surfaces apart, there is some occasional contact between tallest surface asperities which can protrude through the fluid film. Finally, boundary lubrication is the condition where λ is smaller than 1. This takes place at very high load and very slow speed of motion between the interacting surfaces. The fluid film has negligible thickness and, as a result, the surface asperities are in considerable contact. This interaction causes both elastic and plastic deformation of the surfaces and under these circumstances the bulk properties of the lubricant become insignificant. [38-40] However, at the same time, the chemical properties of the lubricant additives and the base lubricant itself become very critical for providing desired tribological performance such as reduced friction and enhanced surface protection. Under boundary lubrication conditions, the surface asperities are always in contact and the lubricant chemistry interacts with surfaces to form thin protective films commingle called “tribofilms”. Typically, the thickness of tribofilms is in the range of 100 to 400 nanometers. [11,12,41-43] These films constantly minimize direct contact of the rubbing surfaces, thus decreasing frictional resistance against motion, as well as material removal due to wear. [13,44]

1.2.2 Lubricant Additives and Tribofilms

Depending on the application, lubricants usually contain additives that perform designated functions at the rubbing surfaces. Lubricants serve to reduce friction, heat transfer and, in addition, with the aid of additive packages they promote the formation of protective films at the interfaces to keep materials wear loss to a minimum. For example, for automotive applications, engine oils are formulated using a base stock and an additive package, in which the latter component is custom designed to provide the base oil with enhanced performance in a particular tribological environment. A typical additive package may contain different chemical species each selected to

provide a specific task such as anti-wear, friction modifiers, anti-oxidants, detergents, dispersants, corrosion inhibitors, anti-foaming agents etc. [45-48] For engine parts where there is significant metal to metal contact, the anti-wear additives play a key role in forming protective tribofilms. These additives undergo thermal decomposition under high temperature and pressure conditions. The thermal degradation process provides reactive ions and other chemical species that react with activated rubbing surfaces and form tribofilms to minimize the wear. [13] These surface films are sacrificial in nature and, in an ideal scenario, they are continuously formed and replaced under the shear forces. [41] The most accepted mechanism for tribofilm formation from lubricant additives suggests that, under boundary lubrication, the interaction of surface asperities generate very high temperature and pressure at the points of contact. These conditions favor the thermo-mechanical decomposition and reaction of chemical species from the lubricant additives that subsequently forms tribofilms at the surfaces. [13,21,49-51] The mechanism of formation of tribofilm is still not completely understood as there are many different variables involved in the process such as amount of additive chemistry in the lubricant, geometry and surface roughness of the surfaces, sliding frequency and duration of contact. A majority of the studies focused on exploration of the mechanism of tribofilm formation have been conducted using ZDDP (zinc dialkyldithiophosphate) additive. It has remained the gold standard for anti-wear additives in the lubrication industry for several decades. A recent study done by Spike et al. supports the mechanochemical model for ZDDP tribofilm formation. [52] In this study, they showed that shear stress experienced by the ZDDP additive in the lubricant, dictates the tribofilm growth rate at the interacting surfaces. In addition, their findings also suggest that shear stresses can significantly bring down the thermal activation barrier for ZDDP tribofilm formation up to 50%. Similarly, many other studies have also provided significant scientific evidence to support the importance of mechanochemistry in

tribology. [13,49,52-57]

1.2.3 Zinc Dialkyldithiophosphate (ZDDP)

As noted above, among the diverse class of anti-wear additives, the most important one is Zinc Dialkyldithiophosphates (ZDDPs), which has been used for over seventy years. It plays many different roles in the oil, including important anti-wear and anti-oxidation functions. [13,44,52,58] Despite a wide range of experimental studies to identify improved anti-wear additives, the lubrication industry has remained dominated by ZDDP. Many scientific studies have been devoted to elucidation of the mechanism by which ZDDP functions as an anti-wear agent. [11,13,49,52,59] The results from such studies suggest that, at high temperatures and stresses, the ZDDP breaks down and its subsequent reaction with steel surfaces leads to formation of an amorphous film which consists of zinc and iron poly phosphates, sulfates and sulfides. [11,12,60-63] Researchers have also focused on altering the chemistry of ZDDP by incorporation of fluorine and these fluorinated forms of ZDDP have demonstrated improved anti-wear performance. [58,64] Detailed studies were conducted using fluorinated ZDDP to understand the lubrication mechanism and the resulting tribofilm's composition. The enhanced wear performance was found to be linked with the formation of more durable tribofilms at the surfaces compared to regular ZDDP. Extensive characterizations of ZDDP tribofilms, including use of high-end techniques such as XANES and XPS, have revealed that the outer layer of these amorphous films is composed primarily of long chain polyphosphates, whereas inner layers are made up of short chain polyphosphates. [19,61,65] Unfortunately, decomposition of ZDDP in the engine becomes a source of volatile phosphorus species and ash in the engine oils. Furthermore, at the downstream end, they damage the catalytic convertors in the exhausts system, which are primarily designed to convert harmful chemical compounds into harmless gases prior to their release in the environment. [14-16] In recognition of

these discoveries, very strict regulations have been implemented to restrict the level of certain potential harmful chemical species, such as phosphorus, sulfur etc., in engine oils. This in turn, has produced regulations which have reduced the amount of ZDDP in the engine oils thus compromising the anti-wear properties and significantly reducing the durability of the engines. In light of these more restrictive regulations and restrictions on the use of ZDDP in engine oils, scientists have attempted to identify a better approach to anti-wear lubricants such as ionic liquids, boron based additives, nanomaterials etc. [9,27,51,66,67]

1.2.4 Ionic Liquids and Boron Based Additives

Ionic liquids (ILs) are usually composed of an inorganic anion and asymmetric organic cation. These molecules are relatively large in size and, due to these large sizes and the low charges on the ions, there are reduced electrostatic forces between the ions and therefore they can remain stable in liquid state at room temperature. One of the earliest known application of ILs was as an electrolyte in batteries. As they were investigated further for their unique properties such as thermal stability, low volatility, miscibility with organic molecules, they have become widely used as green solvents. [68] Depending on the specific application, ILs can be designed by choosing the desired cationic and anionic moieties and due to this added flexibility in design they have been explored for their use in many different fields. One of the most recent application of ILs has been in the field of tribology and lubrication. [69-71] The first reported work is from year 2001 in which Ye at al. investigated the properties and performance of ILs as lubricants. [68] Many studies involving ILs as lubricants have shown that their unique set of properties such as high thermal stability, low volatility and low flammability make them a promising candidate for use in tribological applications. The ILs investigated for their tribological behavior mostly contain phosphorus, sulfur or boron ions which can react with metal surfaces to form protective

tribofilms. [9,24,51,72] The list of some of most commonly studied ILs includes imidazolium, ammonium, phosphonium and tetrafluoroborate etc. [9,73-76]

The initial work with ILs as lubricant additives focused on PF₆ and BF₄ anions and they performed better than the existing lubricants. [68] Later, due to some problems with PF₆ and BF₄ reaction byproducts, the focus shifted to some other fluorine based ILs that have better hydrolytical stability, as well as improved wear performance. [77,78] In addition, phosphorus containing ILs such as dimethylphosphate and phosphonium-phosphates were investigated for their use as lubricant additives in base oil to mimic the existing ZDDP. [79] The results published in a recent study by Qu et al. suggest that phosphonium IL has superior or, at least, similar anti-wear properties compared to the traditional ZDDP in the base oil. [80]

The majority of studies involving ILs have used XPS and XANES techniques to identify the elemental composition of the tribofilm, as well as to understand the underlying lubrication mechanism. For example, XPS results from one of the studies using phosphonium ILs, conducted by Liu et al., revealed that the protective films were composed of oxides, hydroxides and fluorides of aluminum, as well as boron oxide and aluminum phosphates. [81] In the most recent study done by Vibhu et al., XANES analysis was used to investigate the tribochemistry of the worn surfaces. [51] The results provide strong evidence in support of ILs participation in the tribochemical reaction at the rubbing interfaces and in formation of phosphate rich tribofilms. In addition, some studies have also reported synergistic interactions between ILs and ZDDP, providing enhanced tribological benefits. [25]

Just like ILs, boron based additives also represent environmentally friendly lubricants. They are being used for multiple tribological applications such as antiwear additives, friction modifiers, corrosion inhibitors and antioxidants. [82] There are many different ways in which boron

compounds can be used for tribological applications. For example, boron nitride and boric acid are used as solid lubricants due to unique lamellar lattice structures. [83-85] Organic borates are extensively used as anti-wear, anti-friction, extreme pressure additives and corrosion inhibitors due to their high thermal stability and good miscibility with oils. [86,87] In a study conducted by Philippon et al., the XPS results showed that the tribochemical reactions between trimethylborate and steel surfaces lead to the formation of a borate–iron glass network in the tribofilms by digestion of the abrasive iron oxide. [86] Similarly, inorganic borates such as boric acid, hexagonal boron nitride, titanium borate, zinc borate etc. have also been used in lubricating oils as additives. [83,85,88,89]

1.2.5 Nanomaterials/Nanoparticles in Tribology

Nanotechnology has significantly contributed to the development of novel nanomaterial based lubricants and/or lubricant additives. Nano-additives belong to the new class of lubricant additives which are now being explored for use in tribological applications. Nanomaterials possess some very specific characteristics that have made them promising candidates for use as lubricants/additives. One of the most critical features is their size that allows them to enter the surface asperities or the contact area between the rubbing interfaces. In one of recent article by Spikes, some of the most important advantages of nano-additives are highlighted which include insolubility in base oil, high chemical and thermal stability and the ability to form surface films. [90] These nanoparticles based additives are available in many different shapes, sizes and chemistries and, each form can serve many different functions at tribological interfaces. In a broad sense, nanoparticles can be classified as metal, metal oxides, chalcoganides, carbon based, inorganic fullerenes, boron based, ceramic, composite and, polymeric nanoparticles. [10,29-32,91-96] Accompanying the increased use of nanoparticles as lubricants, there have been a number of

lubrication mechanisms proposed by researchers. These mechanisms include, but are not limited, to ball bearing effect, tribofilm formation effect, mending effect and polishing effect. For ball bearing effect, the nanoparticles undergo rolling action between the contacting surfaces when the contact loads are not very high and where the nanoparticles can maintain their dimensions. [97] Tribofilm formation effect comes into the picture when there is an active participation of nanoparticles in the tribochemical reaction at the rubbing contacts. The protective film forms as a result of interaction between the different additive chemistries and its properties are dependent on tribological conditions, as well as the chemical environment of the lubrication system under study. [98] The mending and polishing effect are secondary effects that are observed as a result of surface modification due to the nanoparticles. [32] There is compensational physical material transfer from nanoparticles on to the rubbing surfaces in mending or repairing effect. However, in case of polishing effect, the nanoparticles reduce the roughness of the contacting surfaces via nanoparticle-facilitated abrasion.

Extensive work has been done involving metal nanoparticles for tribological applications. For example, Padgurskas et al reported the anti-wear effect of Fe, Cu and Co nanoparticles, in which the Cu nanoparticles gave the best anti-wear and anti-friction outcomes. [99] Studies have been done with TiO₂ nanoparticles where they are found to stabilize the friction and also form TiO₂ films on the contacting surfaces. [93,100,101] Kao et al. investigated the effect of TiO₂ nanofluid on engine oil and friction reduction in a real engine. [102] The engine oil with TiO₂ nanoparticles displayed reduced friction compared to the original oil. Similarly, boron nitride, silicon dioxide and molybdenum disulfide nanoparticles have also been explored for their use in lubricant oils as nano-additives. [27,103-106] Nano sized derivatives of carbon, such as graphite, diamond, graphene and carbon nanotubes, have also displayed promising tribological behavior.

[10,106] In the class of polymeric nanoparticles, one of the extensively studied candidates for tribological applications are polytetrafluoroethylene (Teflon) nanoparticles due to their exceptional frictional properties, and thermal and chemical stability. For example, M.K. Dubey and co-workers have investigated the tribological performance of oils containing different sized PTFE nanoparticles at different concentrations. [35,96] In addition, they also reported the effect of polyisobutylene succinimide (PIBSI) dispersant in improving the tribological performance of PTFE nanoparticles in the virgin oil. [107] A major issue concerned with nanoparticle use in oil involves their formation of stable, uniform dispersions. Many methods and techniques have been proposed overtime to modify the surface of nanoparticles to keep them dispersed in oil for extended period of times. [108-110] Some of the most recent studies have also focused on interaction of nanoparticle based additives with conventional lubricant additives such as ZDDP, ILs etc. [66,106,111,112] These studies aim to understand the lubrication mechanism for the additive mixtures to promote the use of nano-additives in fully formulated oils. Many approaches are being employed by the researchers to improve the tribological performance of different nano-additive based lubricants. A novel approach, and the one examined in this thesis, is plasma surface functionalization of nanoparticles as described is explained in detail in the following section.

1.2.6 Plasma Polymerization

As the name suggests, this technique is employed to deposit polymeric materials under plasma conditions [113]. The deposited coatings are generally highly cross linked in nature and usually have good adhesion to the substrate materials. Also, due to the high crosslinking density, plasma deposited coatings generally show good stability against chemical solvents. During the plasma deposition process, the growth of the film is uniform and conformal in nature. Monomers introduced into the plasma reactor are dissociated into reactive species by the high energy electrons

created in the discharge. These reactive species produce deposition of polymer films on the reactor walls and on substrates inside the reactor. The composition of these polymer films can be readily varied by appropriate choice of monomer and by the plasma discharge operating parameters employed, such as reactor design, placement of electrodes, RF power, pressure, flow rate, deposition time and duty cycle. Interestingly, the variable duty cycle pulsed plasmas provide excellent control of the polymer film compositions. [113-115] A precise control over the chemistry of the film is of prime importance during plasma deposition. When operating the plasma deposition under continuous wave, the ratio of power to monomer flow rate can be varied to achieve some film chemistry control. Yasuda has shown that there can be huge differences in the residual free radical concentration by comparing CW and pulsed plasma films, with these differences being strongly monomer dependent. [115] In one study, Timmons and co-workers clearly demonstrated the effect of variation of RF duty cycle (ratio of plasma on time to off time) on plasma polymer compositions in a study of allyl alcohol. [116] Their studies have also shown that the pulsed plasma technique not only provides better control of the film chemistry but can also be employed to improve the adhesion of the film to the substrate via use of a gradient layering technique.

Use of plasma polymerization for nanoparticle functionalization is also an established technique. [117,118] But it has never been used for nanoparticles and chemistries that may potentially be used for tribological applications. In the present study, this technique is used to functionalize NPs shown to have favorable tribological behavior such as PTFE and TiO₂. The monomer chemistry chosen for the plasma polymerization is also known to provide anti-friction and anti-wear properties. Overall, this represents a novel approach to deliver chemistries at the tribological interfaces involving the use of nanoparticles. These nano-additives show a promising way to reduce the amount of ZDDP in the oil, thus reducing the aforementioned catalytic

poisoning, while simultaneously improving the anti-wear and anti-friction performances. The potential scope of this new technology is not restricted to a particular nanoparticle-additive system and thus it can be explored further with many different systems that may have even better tribological benefits.

1.3 Specific Aims

The principle goal of this research project is to explore a novel approach involving surface modified nanoparticles based additives as a potential route to improving the lubricant properties of oils. We believe that this approach has enormous potential to provide better lubricant additives for oils than the existing ones, at the same time, prove to be more environmentally friendly by reducing harmful automobile emissions. This approach focuses on the use of plasma polymerization technology to functionalize nanoparticles with chemistries known to be favorable for tribological applications. These functionalized nanoparticles are mixed with oils and evaluated using standard ASTM tribological testing procedures. A variety of analytical tools are employed to investigate the mechanism of lubrication and chemical make-up of the protective tribofilms formed at the surfaces.

Hypothesis

It is well documented, in the scientific literature that the major effectiveness of lubricant additives results from protective tribofilms that form at contacting surfaces under high temperature and high shear forces. These films are mostly amorphous glasses in nature. For example, ZDDP (Zinc dialkyl dithiophosphates), a widely used oil additive, is known to provide anti-wear performance by forming glassy films of phosphates, sulfates and sulfides. The role of phosphorus and sulfur in ZDDP's activity highlights the importance of chemical processes occurring on these

surfaces. In addition, in the past few years, nanotechnology has provided an opportunity to use a variety of nanoparticles as lubricant oil additives and they have proven to be potential candidates towards reducing friction and improving anti-wear properties.

This research work centers on examination of a novel nanotechnology based approach to create improved chemical modification of these engine interfaces. Specifically, it involves initial plasma surface treatments to tailor the surface chemistries of nanoparticle additives via deposition of thin polymeric films. This approach is very general in nature in that it can be applied to a wide variety of nanoparticles and, dependent on the nature of the monomer selected, can provide a wide range of polymeric chemical films. Nanoparticles will initially be functionalized with chemistries similar to those that have been shown to provide favorable tribological applications. Subsequently, detailed experiments will be carried out to quantify their tribological properties, followed by thorough analytical chemical analysis of wear surfaces to provide an understanding of the underlying lubrication mechanism.

1.3.1 Functionalization of nanoparticles using plasma polymerization technology

An obvious critical, 1st step, aspect of this work was selection of both nanoparticles and monomers to achieve the desired chemistry. Nanoparticles that have already been reported to show good anti-wear and anti-friction properties, such as PTFE and TiO_2 , were selected. Hexamethyldisiloxane (HMDSO), trimethylboroaxine (TMB) and glycidyl methacrylate were the monomers used for plasma deposition of thin films in order to develop core-shell structures from nanoparticles. Various process parameters, such as flow rate, monomer pressure, RF power input, and duty cycle in pulsed plasma runs were optimized to get the coatings with desired chemistries. The process optimization work was performed using silicon wafers as substrate material to

examine film deposition rates and FTIR analysis of the plasma coatings on KBr discs to identify presence of various chemical functional groups. Additional valuable chemical composition data were acquired using XPS, an especially important instrument in dealing with surface chemical analyses.

1.3.2 Evaluation of Tribological Performance

Molecularly tailored nano-additives developed by plasma functionalization were blended with different oil formulations and then these blends were tested using standard tribological experimental setups. ZDDP is the most widely used additive in the lubrication industry, despite the fact that it has a down side due to its negative impact on the environment by contributing to automobile catalytic deactivation. Thus an important aspect of this study was to examine the possibility of improving anti-wear properties via use of nanoparticles accompanied by significant reductions in the amount of ZDDP additives currently employed. Similarly, oil formulations containing ionic liquids and plasma functionalized nano-additives were also evaluated for their tribological performance.

1.3.3 Understanding the mechanism of tribofilms formation with nanoadditives

The wear surfaces generated from the tribological testing were subjected to high end surface characterization techniques such as white light interferometry, XPS and XANES to explore the physical and chemical properties of the tribofilms. All information gathered from the experimental test data and surface characterization tools was used to help comprehend the mechanistic process of nano-additives lubrication. The chemical composition of the tribofilms provided an insight into how nanoparticles function in terms of reducing friction and wear. Mechanistic and physical models were proposed for the tribofilms based on the overall findings.

1.3.4 Application of same approach with different nanoparticle-chemistry-additive combination

In order to validate the proposed hypothesis, the plasma functionalization approach was employed for two different nanoparticles (PTFE and TiO₂) and two monomer chemistries (HMDSO and TMB). In addition, the interaction of these nano-additives was investigated with two existing additive chemistries namely ZDDP and ILs. Tribological results from these different nanoparticle-chemistry-additive combinations provide strong evidence of enhanced anti-friction and anti-wear performance.

1.4 Dissertation Structure

The following paragraphs provide an overview and summary of the five chapters of this dissertation. In addition, the relevance and contribution of each chapter to the central theme of the dissertation will be highlighted.

Chapter 1, General Introduction: This chapter starts with the information regarding the fundamental motivation for this research work and it is followed with a detailed background including information about tribology, lubrication, lubricant additives (ZDDP, Ionic Liquids, Boron Additives, Nanomaterials), tribofilms and most importantly plasma polymerization technique which forms the core of this dissertation work. The specific aims of the research work are also mentioned towards the end of this chapter. Overall, the introduction chapter covers all the essential scientific information that forms the basis for the following chapters of this dissertation.

Chapter 2, includes the study directed towards the development of plasma functionalized PTFE nanoparticles for improved wear in lubricated contact. This chapter provides the detailed experimental procedure for development of plasma functionalized PTFE nanoparticles. The monomers used for the functionalization process were HMDSO and methacrylate. The tribological

results of this study provide substantial evidence in support of the use of plasma functionalized nanoparticles as lubricant additives as proposed in the hypothesis. The synergistic interaction of functionalized PTFE with significantly reduced amount of ZDDP in the oil is the highlight of this study. The tribofilms generated with these nanoadditives were examined employing XPS and XANES techniques and phenomenological models were developed for the same.

Chapter 3 explores the tribological interaction of plasma functionalized PTFE nanoparticles with ionic liquids. The findings of the prior work described in chapter 2 formed the basis of the studies done in this chapter. The synergistic interaction of functionalized PTFE nanoparticles with ZDDP stimulated the idea to investigate their interaction with a totally different class of anti-wear additive i.e. ionic liquids. And again, the results suggested that functionalized PTFE nanoparticles were interacting synergistically with both ionic liquids employed in the study and displayed enhanced friction and wear behavior. The information from XPS and XANES experiments revealed the crucial difference in chemical architecture of the tribofilms generated from different additive mixtures.

Chapter 4, is a significant extension of the approach that was successfully demonstrated in chapters 2 and 3. The central idea behind this study was to experimentally extend and validate the proposed hypothesis. This chapter provides the details of the study focused on development of plasma functionalized TiO₂ nanoparticles using the same approach as chapter 2. For this work, a new nanoparticle-monomer combination was studied. A boron rich monomer (Trimethylboroxine) was used for plasma functionalization of the TiO₂ nanoparticles. These nanoadditives were examined for their tribological interaction with and without ZDDP in the base oil. Interestingly, the TiO₂ nanoparticles by themselves showed incompatibility with ZDDP and gave severe wear outcomes. However, when plasma functionalized TiO₂ nanoparticles were employed with ZDDP,

there was a substantial reduction in the wear volume loss compared to the non-functionalized one. ECR, XPS and XANES data gave detailed insight into the mechanism of tribofilm formation and the chemistry of the tribofilms formed at the rubbing surfaces.

Combined, the studies done in chapters 2, 3 and 4 provide strong quantitative experimental evidence in support of the proposed hypothesis of this dissertation work that plasma functionalized nanoparticles can be used as lubricant additives to achieve superior tribological performance.

Chapter 5 presents the final conclusions of this dissertation work. This chapter summarizes the major findings of this research and also provides an insight into how the results of each chapter are interconnected to each other and to the central idea of the dissertation.

1.5 References

- [1] 2017 and Later Model Year Light-Duty Vehicle Greenhouse Gas Emissions and Corporate Average Fuel Economy Standards, Final Rule. In: Anonymous Federal Register, National Archive and Records Administration: Environmental Protection Agency and Department of Transportation National Highway Traffic Safety Administration; 2012, p. 62623.
- [2] Federal Emission Standards Reference Guide.
- [3] Ferrick Kevin. Technical Bulletin 1 API 1509, Engine Oil Licensing and Certification System. ;2010.
- [4] Holmberg K, Andersson P, Erdemir A. Global energy consumption due to friction in passenger cars. Tribol Int 2012;47:221-34.
- [5] Holmberg K, Andersson P, Nylund N, Mäkelä K, Erdemir A. Global energy consumption due to friction in trucks and buses. Tribol Int 2014;78:94-114.

- [6] Tormos B, Ramírez L, Johansson J, Björklund M, Larsson R. Fuel consumption and friction benefits of low viscosity engine oils for heavy duty applications. *Tribol Int* 2017;110:23-34.
- [7] Ala' A, Eryilmaz O, Erdemir A, Kim SH. Nano-texture for a wear-resistant and near-frictionless diamond-like carbon. *Carbon* 2014;73:403-12.
- [8] Kim B, Sharma V, Aswath PB. Chemical and mechanistic interpretation of thermal films formed by dithiophosphates using XANES. *Tribol Int* 2017;114:15-26.
- [9] Sharma V, Dorr N, Erdemir A, Aswath P. Interaction of phosphonium ionic liquids with borate esters at tribological interfaces. *RSC Adv* 2016;6:53148-61.
- [10] Gautam Anand and PS. A review on graphite and hybrid nano-materials as lubricant additives. *IOP Conference Series: Materials Science and Engineering* 2016;149:012201.
- [11] Mourhatch R, Aswath PB. Tribological behavior and nature of tribofilms generated from fluorinated ZDDP in comparison to ZDDP under extreme pressure conditions---Part 1: Structure and chemistry of tribofilms. *Tribol Int* 2011;44:187-200.
- [12] Mourhatch R, Aswath PB. Tribological behavior and nature of tribofilms generated from fluorinated ZDDP in comparison to ZDDP under extreme pressure conditions—Part II: Morphology and nanoscale properties of tribofilms. *Tribol Int* 2011;44:201-10.
- [13] Spikes HA. The history and mechanisms of ZDDP. *Trib Lett* 2004;17:469-489.
- [14] Forzatti P, Lietti L. Catalyst deactivation. *Catalysis Today* 1999;52:165-81.
- [15] Buwono HP, Minami S, Uemura K, Machida M. Surface Properties of Rh/AlPO₄ Catalyst Providing High Resistance to Sulfur and Phosphorus Poisoning. *Ind Eng Chem Res* 2015;54:7233-40.

- [16] Williamson WB, Perry J, Gandhi HS, Bomback JL. Effects of oil phosphorus on deactivation of monolithic three-way catalysts. *Applied Catalysis* 1985;15:277-92.
- [17] Williamson W, Perry J, Goss R, Gandhi H, Beason R. Catalyst deactivation due to glaze formation from oil-derived phosphorus and zinc 1984.
- [18] Farng LO. Ashless antiwear and extreme-pressure additives. In: Rudnick LR, editor. *Lubricant Additives-Chemistry and Applications*, 2nd Edition, Chemical Industries 124, Danvers, MA, U.S.A.: CRC Press; 2009, p. 213-249.
- [19] Sharma V, Erdemir A, Aswath PB. An analytical study of tribofilms generated by the interaction of ashless antiwear additives with ZDDP using XANES and nano-indentation. *Tribol Int* 2015;82:43-57.
- [20] Chen X, Elsenbaumer RL, Aswath PB. Synthesis and Tribological Behavior of Ashless Alkylphosphorofluoridothioates. *Tribol Int* 2013;69:114-24.
- [21] Kim BH, Jiang J, Aswath PB. Mechanism of Wear at Extreme Loads and Boundary Conditions with Ashless Anti-wear Additives: Analysis of Wear Surfaces and Wear Debris. *Wear* 2011;270(3-4):181-94.
- [22] Kim B, Jiang JC, Aswath PB. Mechanism of wear at extreme load and boundary conditions with ashless anti-wear additives: Analysis of wear surfaces and wear debris. *Wear* 2011;270:181-94.
- [23] Zhou Y, Qu J. Ionic Liquids as Lubricant Additives: A Review. *ACS Appl Mater Interfaces* 2017;9:3209-22.

- [24] González R, Bartolomé M, Blanco D, Viesca J, Fernández-González A, Battez AH. Effectiveness of phosphonium cation-based ionic liquids as lubricant additive. *Tribol Int* 2016;98:82-93.
- [25] Qu J, Barnhill WC, Luo H, Meyer HM, Leonard DN, Landauer AK et al. Synergistic Effects Between Phosphonium-Alkylphosphate Ionic Liquids and Zinc Dialkyldithiophosphate (ZDDP) as Lubricant Additives. *Adv Mater* 2015.
- [26] García A, González R, Hernández Battez A, Viesca JL, Monge R, Fernández-González A et al. Ionic liquids as a neat lubricant applied to steel–steel contacts. *Tribol Int* 2014;72:42-50.
- [27] Shah FU, Glavatskih S, Antzutkin ON. Boron in tribology: from borates to ionic liquids. *Tribology letters* 2013;51:281-301.
- [28] Greco A, Mistry K, Sista V, Eryilmaz O, Erdemir A. Friction and wear behaviour of boron based surface treatment and nano-particle lubricant additives for wind turbine gearbox applications. *Wear* 2011;271:1754-60.
- [29] - Kong L, - Sun J, - Bao Y. - Preparation, characterization and tribological mechanism of nanofluids. - *RSC Adv*:- 12599.
- [30] Bakunin VN, Suslov AY, Kuzmina GN, Parenago OP, Topchiev AV. Synthesis and Application of Inorganic Nanoparticles as Lubricant Components – a Review. *Journal of Nanoparticle Research* 2004;6:273-84.
- [31] Chen J. Tribological Properties of Polytetrafluoroethylene, Nano-Titanium Dioxide, and Nano-Silicon Dioxide as Additives in Mixed Oil-Based Titanium Complex Grease. *Tribology Letters* 2010;38:217-24.

- [32] Drummond C, Alcantar N, Israelachvili J, Tenne R, Golan Y. Microtribology and Friction-Induced Material Transfer in WS₂ Nanoparticle Additives. *Advanced Functional Materials* 2001;11:348-54.
- [33] Chen CS, Chen XH, Xu LS, Yang Z, Li WH. Modification of multi-walled carbon nanotubes with fatty acid and their tribological properties as lubricant additive. *Carbon* 2005;43:1660-6.
- [34] Berman D, Deshmukh SA, Sankaranarayanan SKRS, Erdemir A, Sumant AV. Extraordinary Macroscale Wear Resistance of One Atom Thick Graphene Layer. *Advanced Functional Materials* 2014;24:6640-6.
- [35] Dubey MK, Bijwe J, Ramakumar SSV. Nano-PTFE: New entrant as a very promising EP additive. *Tribol Int* 2015;87:121-31.
- [36] Elango B, Bornmann L, Kannan G. Detecting the historical roots of tribology research: a bibliometric analysis. *arXiv preprint arXiv:1601.00141* 2016.
- [37] Parekh K. Interactions between antiwear agent and novel additive in engine oils. 2007.
- [38] Bhushan B. *Modern Tribology Handbook, Two Volume Set.* : CRC, 2000.
- [39] Bhushan B. Nanotribology and nanomechanics. *Wear* 2005;259:1507-31.
- [40] Dowson D. Developments in lubrication - the thinning film. *J Phys D* 1992;25:334,334-339.
- [41] Nehme G, Mourhatch R, Aswath PB. Effect of contact load and lubricant volume on the properties of tribofilms formed under boundary lubrication in a fully formulated oil under extreme load conditions. *Wear* 2010;268 (9-10):1129-47.

- [42] Somayaji A, Mourhatch R, Aswath PB. Nanoscale Properties of Tribofilms from ZDDP and Fluorinated ZDDP in the Presence and Absence of Antioxidants. *Journal of Nanoscience and Nanotechnology* 2007;7:4378-4390.
- [43] Fujita H, Spikes HA. The formation of zinc dithiophosphate antiwear films. *Proc Inst Mech Eng Part J* 2004;218:265-77.
- [44] Barnes AM, Bartle KD, Thibon VRA. A review of zinc dialkyldithiophosphates (ZDDPS): characterisation and role in the lubricating oil. *Tribol Int* 2001;34:389-95.
- [45] Dodd JC. Gas engine lubricating oil composition. 2015.
- [46] SAE International. SAE J300, Engine Oil Viscosity Classification, Fuels and lubricants, TC1, Engine Lubricants. 2015.
- [47] Ratoi M, Niste VB, Alghawel H, Suen YF, Nelson K. The impact of organic friction modifiers on engine oil tribofilms. *RSC advances* 2014;4:4278; 4278,4285; 4285.
- [48] Topolovec-Miklozic K, Forbus TR, Spikes H. Film Forming and Friction Properties of Overbased Calcium Sulphonate Detergents. *Tribology Letters* 2008;29:33.
- [49] Gosvami NN, Bares JA, Mangolini F, Konicek AR, Yablon DG, Carpick RW. Tribology. Mechanisms of antiwear tribofilm growth revealed in situ by single-asperity sliding contacts. *Science* 2015;348:102-6.
- [50] Qu J, Meyer HM, Cai Z, Ma C, Luo H. Characterization of ZDDP and ionic liquid tribofilms on non-metallic coatings providing insights of tribofilm formation mechanisms. *Wear* 2015;332:1273-85.

- [51] Sharma V, Gabler C, Doerr N, Aswath PB. Mechanism of tribofilm formation with P and S containing ionic liquids. Tribol Int 2015;92:353-64.
- [52] Zhang J, Spikes H. On the Mechanism of ZDDP Antiwear Film Formation. Tribology Letters 2016;63:24.
- [53] Ito K, Martin JM, Minfray C, Kato K. Formation mechanism of a low friction ZDDP tribofilm on iron oxide. Tribol Trans 2007;50:211-6.
- [54] Mourhatch R, Aswath PB. Mechanism of Boundary Lubrication with Zinc Dialkyl Dithiophosphate. Proceedings of the STLE/ASME International Joint Tribology Conference 2006;San Antonio, TX, USA:IJTC-12054.
- [55] Bancroft GM, Kasrai M, Fuller M, Yin Z, Fyfe K, Tan KH. Mechanisms of tribochemical film formation: stability of tribo- and thermally-generated ZDDP films. Trib Lett 1997;3:47,47-51.
- [56] Wu YL, Dacre B. Effects of lubricant-additives on the kinetics and mechanisms of ZDDP adsorption on steel surfaces. Tribol Int 1997;30:445-53.
- [57] Spedding H, Watkins RC. Antiwear Mechanisms of ZDDP's - 1. Tribol Int 1982;15:9-12.
- [58] Somayaji A, Aswath PB. Antiwear perforce of ZDDP and fluorinated ZDDP in the presence of antioxidants. Tribology Transactions Under Review (2006).
- [59] Willermet PA, Dailey DP, Carter RO,III, Schmitz PJ, Zhu W. Mechanism of formation of antiwear films from zinc dialkyldithiophosphates. Tribology International 1995;28:177-87.

- [60] Kim B, Mourhatch R, Aswath PB. Properties of tribofilms formed with ashless dithiophosphate and zinc dialkyl dithiophosphate under extreme pressure conditions. *Wear* 2010;268:579-91.
- [61] Li Y, Pereira G, Lachenwitzer A, Kasrai M, Norton PR. Studies on ZDDP Thermal Film Formation by XANES Spectroscopy, Atomic Force Microscopy, FIB/SEM and ³¹P NMR. *Tribol Lett* 2008;29:11-22.
- [62] Li Y, Pereira G, Lachenwitzer A, Kasrai M, Norton PR. X-ray absorption spectroscopy and morphology study on antiwear films derived from ZDDP under different sliding frequencies. *Tribology Letters* 2007;27:245-53.
- [63] Zhang Z, Yamaguchi E, Kasrai M, Bancroft G, Liu X, Fleet M. Tribofilms generated from ZDDP and DDP on steel surfaces: Part 2, chemistry. *Tribology Letters* 2005;19:221-9.
- [64] Parekh K, Chen X, Aswath PB. Synthesis of Fluorinated ZDDP Compounds. *Tribol Lett* 2009;34:141-53.
- [65] Li Y, Pereira G, Kasrai M, Norton PR. Studies on ZDDP anti-wear films formed under different conditions by XANES spectroscopy, atomic force microscopy and ³¹P NMR. *Tribology Letters* 2007;28:319-28.
- [66] Sharma V, Timmons R, Erdemir A, Aswath PB. Plasma-Functionalized Polytetrafluoroethylene Nanoparticles for Improved Wear in Lubricated Contact. *ACS Appl Mater Interfaces* 2017;9:25631-41.

- [67] Nicholaos G. Demas, Robert A. Erck, Cinta Lorenzo-Martin, Oyelayo O. Ajayi, and George R. Fenske. Experimental Evaluation of Oxide Nanoparticles as Friction and Wear Improvement Additives in Motor Oil. *Journal of Nanomaterials* 2017;Volume 2017 (2017), Article ID 8425782.
- [68] Ye C, Liu W, Chen Y, Yu L. Room-temperature ionic liquids: a novel versatile lubricant. *Chem Commun* 2001:2244-5.
- [69] Amiril SAS, Rahim EA, Syahrullail S. A review on ionic liquids as sustainable lubricants in manufacturing and engineering: Recent research, performance, and applications. *Journal of Cleaner Production* 2017.
- [70] Zhou Y, Qu J. Ionic Liquids as Lubricant Additives: A Review. *ACS Appl Mater Interfaces* 2017;9:3209-22.
- [71] Somers EA, Howlett CP, MacFarlane RD, Forsyth M. A Review of Ionic Liquid Lubricants. *Lubricants* 2013;1.
- [72] Taher M, Shah FU, Filippov A, de Baets P, Glavatskih S, Antzutkin ON. Halogen-free pyrrolidinium bis (mandelato) borate ionic liquids: some physicochemical properties and lubrication performance as additives to polyethylene glycol. *RSC Advances* 2014;4:30617-23.
- [73] Gabler C, Dörr N, Allmaier G. Influence of cationic moieties on the tribolayer constitution shown for bis(trifluoromethylsulfonyl)imide based ionic liquids studied by X-ray photoelectron spectroscopy. *Tribol Int* 2014;80:90-7.
- [74] Zhang C, Zhang S, Yu L, Zhang P, Zhang Z, Wu Z. Tribological behavior of 1-methyl-3-hexadecylimidazolium tetrafluoroborate ionic liquid crystal as a neat lubricant and as an additive of liquid paraffin. *Tribology Letters* 2012;46:49-54.

- [75] Gusain R, Gupta P, Saran S, Khatri OP. Halogen-Free Bis (imidazolium)/Bis (ammonium)-Di [bis (salicylato) borate] Ionic Liquids As Energy Efficient and Environment-Friendly Lubricant Additives. *ACS applied materials & interfaces* 2014;6 (17):15318-28.
- [76] Pisarova L, Gabler C, Dörr N, Pittenauer E, Allmaier G. Thermo-oxidative stability and corrosion properties of ammonium based ionic liquids. *Tribol Int* 2012;46:73-83.
- [77] Lu Q, Wang H, Ye C, Liu W, Xue Q. Room temperature ionic liquid 1-ethyl-3-hexylimidazolium-bis(trifluoromethylsulfonyl)-imide as lubricant for steel–steel contact. *Tribol Int* 2004;37:547-52.
- [78] Minami I, Kita M, Kubo T, Nanao H, Mori S. The tribological properties of ionic liquids composed of trifluorotris (pentafluoroethyl) phosphate as a hydrophobic anion. *Tribology Letters* 2008;30:215-23.
- [79] Minami I, Inada T, Sasaki R, Nanao H. Tribo-chemistry of phosphonium-derived ionic liquids. *Tribology letters* 2010;40:225-35.
- [80] Qu J, Luo H, Chi M, Ma C, Blau PJ, Dai S et al. Comparison of an oil-miscible ionic liquid and ZDDP as a lubricant anti-wear additive. *Tribol Int* 2014;71:88-97.
- [81] Liu X, Zhou F, Liang Y, Liu W. Tribological performance of phosphonium based ionic liquids for an aluminum-on-steel system and opinions on lubrication mechanism. *Wear* 2006;261:1174-9.
- [82] Herdan JM. Friction modifiers in engine and gear oils. *Lubr Sci* 2000;12:265-76.
- [83] Rowe GW. Some observations on the frictional behaviour of boron nitride and of graphite. *Wear* 1960;3:274-85.

- [84] Deshmukh P, Lovell M, Sawyer WG, Mobley A. On the friction and wear performance of boric acid lubricant combinations in extended duration operations. *Wear* 2006;260:1295-304.
- [85] Erdemir A, Fenske G, Erck R. A study of the formation and self-lubrication mechanisms of boric acid films on boric oxide coatings. *Surface and coatings technology* 1990;43:588-96.
- [86] Philippon D, De Barros-Bouchet M-, Lerasle O, Le Mogne T, Martin J-. Experimental Simulation of Tribochemical Reactions Between Borates Esters and Steel Surface. *Tribology Letters* 2011;41:73-82.
- [87] Kreuz KL, Fein RS, Dundy M. EP Films from Borate Lubricants. *A S L E Transactions* 1967;10:67-76.
- [88] Hu ZS, Dong JX. Study on antiwear and reducing friction additive of nanometer titanium borate. *Wear* 1998;216:87-91.
- [89] Dong JX, Hu ZS. A study of the anti-wear and friction-reducing properties of the lubricant additive, nanometer zinc borate. *Tribology International* 1998;31:219-23.
- [90] Spikes H. Friction Modifier Additives. *Tribology Letters* 2015;60:5.
- [91] Sunqing Q, Junxiu D, Guoxu C. A review of ultrafine particles as antiwear additives and friction modifiers in lubricating oils. *Lubr Sci* 1999;11:217-26.
- [92] Joly-Pottuz L, Dassenoy F, Belin M, Vacher B, Martin JM, Fleischer N. Ultralow-friction and wear properties of IF-WS₂ under boundary lubrication. *Tribology Letters* 2005;18:477-85.
- [93] Ilie F, Covaliu C. Tribological Properties of the Lubricant Containing Titanium Dioxide Nanoparticles as an Additive. *Lubricants* 2016;4.

- [94] Greco A, Mistry K, Sista V, Eryilmaz O, Erdemir A. Friction and wear behaviour of boron based surface treatment and nano-particle lubricant additives for wind turbine gearbox applications. *Wear* 2011;271:1754-60.
- [95] Luo T, Wei X, Zhao H, Cai G, Zheng X. Tribology properties of Al₂O₃/TiO₂ nanocomposites as lubricant additives. *Ceram Int* 2014;40:10103-9.
- [96] Kumar Dubey M, Bijwe J, Ramakumar SSV. PTFE based nano-lubricants. *Wear* 2013;306:80-8.
- [97] Chiniñas-Castillo F, Spikes HA. Mechanism of Action of Colloidal Solid Dispersions. *Journal of Tribology* 2003;125:552-7.
- [98] Jenei IZ, Svahn F, Csillag S. Correlation Studies of WS₂ Fullerene-Like Nanoparticles Enhanced Tribofilms: A Scanning Electron Microscopy Analysis. *Tribology Letters* 2013;51:461-8.
- [99] Padgurskas J, Rukuiza R, Prosycevas I, Kreivaitis R. Tribological properties of lubricant additives of Fe, Cu and Co nanoparticles. *Tribol Int* 2013;60:224-32.
- [100] Ingole S, Charanpahari A, Kakade A, Umare SS, Bhatt DV, Menghani J. Tribological behavior of nano TiO₂ as an additive in base oil. *Wear* 2013;301:776-85.
- [101] Jaiswal V, Kalyani, Umrao S, Rastogi RB, Kumar R, Srivastava A. Synthesis, Characterization, and Tribological Evaluation of TiO₂-Reinforced Boron and Nitrogen co-Doped Reduced Graphene Oxide Based Hybrid Nanomaterials as Efficient Antiwear Lubricant Additives. *ACS Appl Mater Interfaces* 2016;8:11698-710.

- [102] Yuh-Yih Wu, Mu-Jung Kao. Using TiO₂ nanofluid additive for engine lubrication oil. *Ind Lubr Tribol* 2011;63:440-5.
- [103] Kimura Y, Wakabayashi T, Okada K, Wada T, Nishikawa H. Boron nitride as a lubricant additive. *Wear* 1999;232:199-206.
- [104] Jiao D, Zheng S, Wang Y, Guan R, Cao B. The tribology properties of alumina/silica composite nanoparticles as lubricant additives. *Appl Surf Sci* 2011;257:5720-5.
- [105] Li X, Cao Z, Zhang Z, Dang H. Surface-modification in situ of nano-SiO₂ and its structure and tribological properties. *Appl Surf Sci* 2006;252:7856-61.
- [106] Tomala A, Vengudusamy B, Rodríguez Ripoll M, Naveira Suarez A, Remájková M, Rosentsveig R. Interaction Between Selected MoS₂ Nanoparticles and ZDDP Tribofilms. *Tribology Letters* 2015;59:26.
- [107] Dubey MK, Bijwe J, Ramakumar SSV. Effect of dispersant on nano-PTFE based lubricants on tribo-performance in fretting wear mode. *RSC Adv* 2016;6:22604-14.
- [108] López TD, González AF, Del Reguero A, Matos M, Díaz-García M.E., Badalá-R. Engineered silica nanoparticles as additives in lubricant oils. *Science and Technology of Advanced Materials* 2015;16:055005.
- [109] YANG G, CHAI S, XIONG X, ZHANG S, YU L, ZHANG P. Preparation and tribological properties of surface modified Cu nanoparticles. *Transactions of Nonferrous Metals Society of China* 2012;22:366-72.

- [110] Gulzar M, Masjuki HH, Kalam MA, Varman M, Zulkifli NWM, Mufti RA et al. Tribological performance of nanoparticles as lubricating oil additives. *Journal of Nanoparticle Research* 2016;18:223.
- [111] Morina A, Neville A, Priest M, Green JH. ZDDP and MoDTC interactions and their effect on tribological performance – tribofilm characteristics and its evolution. *Tribology Letters* 2006;24:243-56.
- [112] Aldana PU, Vacher B, Le Mogne T, Belin M, Thiebaut B, Dassenoy F. Action Mechanism of WS₂ Nanoparticles with ZDDP Additive in Boundary Lubrication Regime. *Tribology Letters* 2014;56:249-58.
- [113] Yasuda HK. Some Important Aspects of Plasma Polymerization. *Plasma Processes and Polymers* 2005;2:293-304.
- [114] Beck AJ, Jones FR, Short RD. Plasma copolymerization as a route to the fabrication of new surfaces with controlled amounts of specific chemical functionality. *Polymer* 1996;37:5537-9.
- [115] Yasuda H, Hsu T. Some aspects of plasma polymerization investigated by pulsed R.F. discharge. *Journal of Polymer Science: Polymer Chemistry Edition* 1977;15:81-97.
- [116] Rinsch CL, Chen X, Panchalingam V, Eberhart RC, Wang J, Timmons RB. Pulsed Radio Frequency Plasma Polymerization of Allyl Alcohol-Controlled Deposition of Surface Hydroxyl Groups. *Langmuir* 1996;12:2995-3002.
- [117] Savage CR, Timmons RB, Lin JW. Molecular control of surface film compositions via pulsed radio-frequency plasma deposition of perfluoropropylene oxide. *Chem Mater* 1991;3:575-7.

[118] Sumitsawan S, Cho J FAU - Sattler, Melanie,L., FAU SM, Timmons RB. Plasma surface modified TiO₂ nanoparticles: improved photocatalytic oxidation of gaseous m-xylene. Environmental science & technology JID - 0213155 1207.

CHAPTER 2

PLASMA FUNCTIONALIZED PTFE NANOPARTICLES FOR IMPROVED WEAR IN LUBRICATED CONTACT *

Vinay Sharma, Richard Timmons, Ali Erdemir and Pranesh B. Aswath

ACS Applied Materials and Interfaces, 2017, 9 (30), pp 25631–25641

DOI: 10.1021/acsami.7b06453

Publication Date (Web): June 28, 2017

Copyright © 2017 American Chemical Society

*Used with permission of the publisher, 2017.

ABSTRACT

Plasma functionalized poly tetra fluoroethylene (PTFE) nanoparticles were employed to evaluate their utility in improving the lubrication property of a group III mineral oil with significantly low amount of zinc dialky dithiophosphate (ZDDP). The particles were coated with two consecutive films, the initial coating contained silica to enhance amorphous glassy tribofilm formation, followed by a methacrylate film to protect the silica coating and enhance dispersability in the oil. The functionalized nanoparticles were evaluated for their tribological performance using high-frequency reciprocating rig, in a cylinder on flat configuration. The oil formulations containing ZDDP (350ppm phosphorus level) and the functionalized nanoparticles resulted in dramatic reductions in friction coefficient and overall wear compared to the samples containing non-functionalized PTFE nanoparticles, ZDDP (350 ppm P) and samples devoid of nanoparticles but containing ZDDP with 700 ppm P treat rate. XPS and XANES spectroscopy were employed to characterize the tribological films formed on the test samples. The samples with functionalized particles and ZDDP clearly exhibited tribofilms with Si and F doped polyphosphates of Zn coupled with the presence of ZnS at the metal tribofilm interface. On the other hand, oils without the functionalized nanoparticles have oxides of Fe and to a lesser extent short chain phosphates of Zn. The overall results suggest that the synergism between plasma coated PTFE nanoparticles and ZDDP contributed to the development of protective tribofilms even at reduced amount of phosphorus in the oil. This new method of employing nanoparticles to deliver novel anti-friction and antiwear chemistries at the tribological interfaces stands out to be a promising approach to further reduce P levels in oils without compromising friction and wear performance.

1. INTRODUCTION

Increasing worldwide concern of global warming has lately accelerated efforts to further reduce overall greenhouse gas emissions. In terms of Greenhouse gas (GHG) production, it is well recognized that transportation activities represent a major, and increasing, contribution to this problem. For example, in a report published by EPA it was estimated that in the USA, transportation vehicles were responsible for 26% of overall GHG emissions in 2014. Despite increasing efforts to reduce these emissions, via the development of more efficient engines and increased uses of electric vehicles, it is clear that further advances are urgently needed.

Towards this end, an active area of tribological research has lately been focusing on the development of much improved lubricants in order to further reduce friction and wear-related losses in internal combustion engines thus enhancing their fuel efficiency, durability, and, simultaneously, reducing GHG emissions.¹⁻⁴ These studies have included reducing oil viscosity and the use of various additives that adversely impair the functionality of after-treatment catalysts in engines.^{2, 5-9} As one such example, the much used zinc dialkyldithiophosphate (ZDDP), while very effective in helping to form a highly protective tribofilms,¹⁰⁻¹⁸ has also been shown to contribute to emissions that compromise the catalytic converter's efficiency.¹⁹⁻²¹ This and some of the other additives in engine oils also help control friction, oxidation and host of several other properties that insure smooth and long-lasting operations of engine.^{2, 8, 12, 22-24} Over the past several decades, great strides have been made in controlling friction and wear of sliding engine components but mainly because of increasingly more stringent operating conditions and desire to further curtail GHGs, however, further advances are obviously needed. In particular, development of new breed of more effective additives that do not create undesirable environmental concerns will be very desirable.

In light of the above considerations, a wide variety of other additives have been and are continuing to be evaluated to help improve internal combustion engine efficiency, while simultaneously minimizing the undesirable environmental side effects. Examples of such work include a multitude of studies involving the uses of a diverse range of phosphorus and sulfur containing organic compounds,^{12, 16, 25-27} their halogenated derivatives^{16, 28} nanoparticles,²⁹⁻³² boron based additives³³⁻³⁵ and ionic liquids additives.^{9, 23, 36, 37} Although, these compounds have exhibited some promising tribological performance there are some disadvantages associated with their use such as: Halogenated additives may cause pitting corrosion, boron based additives get depleted rapidly, ionic liquids are not well understood yet and nanoparticles have issues with dispersibility in the oil. The present paper involves a systematic study of a suite of functionalized PTFE nanoparticles. In the past, numerous other nanoparticles have been developed and proposed as a new class of anti-friction and -wear additives for a wide range of tribological applications. Some of unique features that make them good candidates for their uses as additives include their comparable sizes to surface asperities, increasingly cheaper, more diverse, and larger-volume availability of nanoparticles of different kinds in recent years, their desirable chemical and thermal stabilities at the temperature ranges where typical engine oils are used.³⁰⁻³² Broadly, the types of nanoparticles evaluated for enhanced lubrication purposes can be categorized as metal, metal oxide, metal sulfides, carbon based, carbonates and organic solids. Particularly, many previous studies have evaluated the anti-friction and -wear potentials of Cu, Fe, Co, TiO₂, WS₂ and Sn nanoparticles.^{29, 30, 38, 39} In other research works, nanoparticles of BN, MoS₂, SiO₂ and a number of metal oxides and their composite nanoparticles have also been studied and reported to exhibit superior tribological properties.^{32, 35, 40-43} Wei et al. reported that a composite mixture of Al₂O₃/TiO₂ nanoparticles provided much superior anti-wear and anti-friction properties than the

individual nanoparticles.⁴⁴ Nano sized derivatives of carbon, such as graphite, diamond, graphene and carbon nanotubes,⁴⁵⁻⁴⁷ have also shown very promising outcomes for some specific applications. Polytetrafluoroethylene (PTFE) is a polymer and is well known for its outstanding frictional properties, thermal and chemical stability. Some recent studies involving PTFE nanoparticles have examined the effect of their size and concentration on mineral oil on their tribological performance.⁴⁸⁻⁵³ Considering the thermo-mechanical properties, lower market price and easy availability of PTFE nanoparticles, they were selected as the suitable candidate for the current investigation.

A distinguishing feature of this study is that the PTFE nanoparticles employed were initially surface modified using a plasma-based thin film deposition process. For this purpose, two films were deposited on PTFE nanoparticles. The initial film was from polymerization of hexamethydisiloxane, which was followed by the deposition of a thin coating of polymerized glycidyl methacrylate. Plasma polymerization is an established technique and it can be used to have a precise control over the composition of the deposited film.⁵⁴⁻⁵⁷ In this study, plasma functionalized PTFE nanoparticles were subsequently dispersed in different oil formulations and subjected to extensive friction and wear experiments in boundary lubrication regime. The very aim of this study was to investigate the performance of these functionalized nanoparticles in the oil containing reduced amount of ZDDP and their interaction. Some recent studies have also focused on exploring the interaction of different nanoparticles with ZDDP to develop an understanding of how they will behave in a fully formulated motor oil.^{58, 59} In addition to the measurements of friction coefficients and wear volumes, the metal surfaces were subjected to a wide range of chemical analyses including X-ray photoelectron spectroscopy (XPS) and X-ray absorption near edge spectroscopy (XANES) spectroscopy in order to determine the compositions of the thin

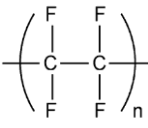
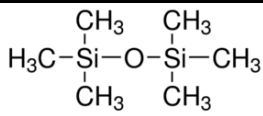
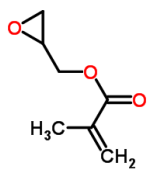
boundary films formed during testing. Phenomenological models were deduced using the chemical and analytical information derived from sample characterization. It was discovered that these tribological thin films provided a remarkably large decrease in both friction coefficients and overall surface wear as detailed herein.

2. EXPERIMENTAL

2.1 Materials

All the materials used in the preparation of plasma functionalized nanoparticles were analytical reagent grades. Polyfluortetraethylene (PTFE, $(\text{CF}_2\text{CF}_2)_n$) nanoparticles (MP1150), having an average size of 200 nm, were procured from the Dupont Corporation. Hexamethyldisiloxane (HMDSO, $(\text{CH}_3)_3\text{SiOSi}(\text{CH}_3)_3$) and glycidyl methacrylate ($\text{C}_7\text{H}_{10}\text{O}_3$) were used as purchased from Sigma-Aldrich. Zinc dialkyldithiophosphate (ZDDP) was supplied by Oronite. Details regarding the materials are provided in table 1.

Table 1. Chemical structures and details of the materials used.

Material Name	Chemical Structure
Polyfluortetraethylene (PTFE)	 $\left(\begin{array}{cc} \text{F} & \text{F} \\ & \\ -\text{C} & - & \text{C}- \\ & \\ \text{F} & \text{F} \end{array} \right)_n$
Hexamethyldisiloxane (HMDSO)	 $\begin{array}{c} \text{CH}_3 \quad \text{CH}_3 \\ \quad \\ \text{H}_3\text{C}-\text{Si}-\text{O}-\text{Si}-\text{CH}_3 \\ \quad \\ \text{CH}_3 \quad \text{CH}_3 \end{array}$
Glycidyl methacrylate	

Zinc dialkyldithiophosphate (ZDDP)	
PTFE nanoparticles, functionalized with both HMDSO and methacrylate plasma coatings	PHGM

2.2 Synthesis of Plasma Functionalized Nanoparticles

Figure 1 shows the schematic of the process flow for the production of functionalized PTFE nanoparticles. Specifically, a homebuilt 360° rotatable plasma reactor was employed to modify the surfaces of the nanoparticles. A rotary reactor was chosen for this purpose to help overcome the severe tendency for particle aggregation when dealing with nanoparticles and thus achieve more uniform surface modification during plasma processing. The nanoparticles of PTFE were coated with films containing siliceous functional groups by using a mixture of oxygen and the monomer hexamethyldisiloxane (HMDSO) as the siliceous precursor. Typically, the gas mixture of HMDSO and oxygen was in a 1:2 ratio and deposition was carried out at an RF frequency of 13.56 MHz. The science behind mixing oxygen gas to the monomer is well established and it has been shown that oxygen helps to achieve silica rich film by knocking out the carbon in the form of carbon dioxide.

Fourier transform infrared spectroscopy (FTIR) (Thermo Nicolet 6700 FTIR Spectrometer) was conducted on the plasma processed films. Figure 2 depicts the change in FTIR spectra for the plasma-processed films from HMDSO with the addition of the oxygen gas. The initial deposition was done using continuous wave (CW) plasma followed with progressively lower duty cycle pulsed plasmas. The continuous wave plasma deposits a film strongly adhered to the substrate and the lower duty cycles provide a gradient layer structure, with each layer tightly bound to the other. The flow rate was kept at 2 sccm and pressure was kept at 300mT throughout

the process. Total deposition time was 75 min initially employing a CW plasma discharge, followed by a sequence of pulsed plasmas in which the plasma on : plasma off times were 50:20 followed by 50 : 50 (times in ms) with each sequence lasting for 15 min. The peak RF power was kept at 60W for both CW and Pulsed Plasma. Subsequently, thin polymer films containing methacrylate ligands were deposited on top of the siliceous coated nanoparticles to assist the subsequent dispersion of the particles in the oils. The latter deposition was done for 1 hour at 100mT pressure, 100W RF power, with the plasma on: plasma off ratio maintained at 20:50(in ms). The PTFE nanoparticles, functionalized with both HMDSO and methacrylate plasma coatings are identified PHGM particles in the write-up.

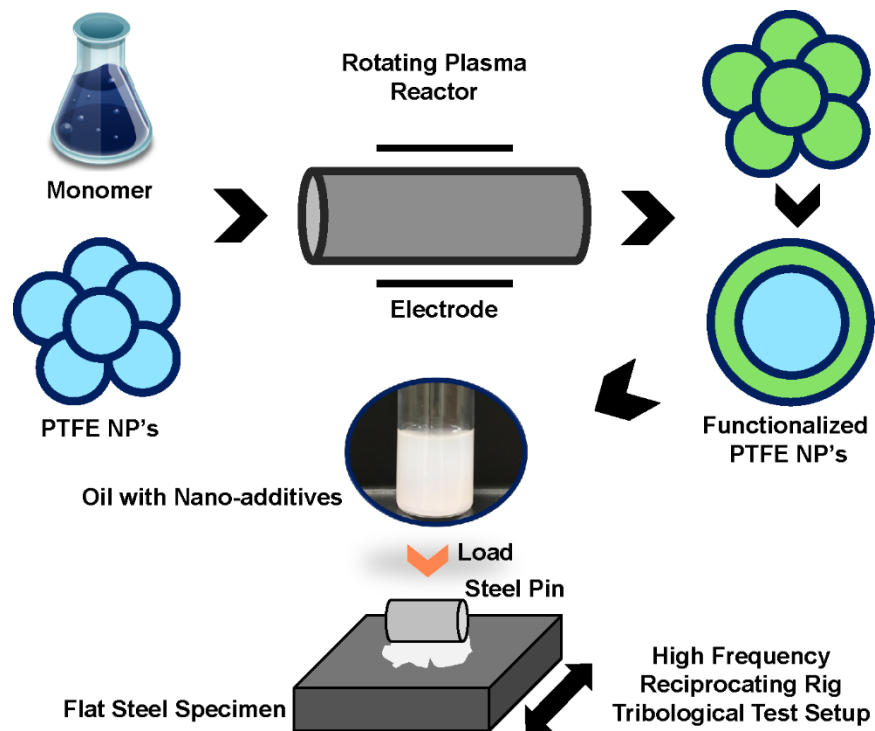


Figure 1. Schematic of the process flow for synthesis of functionalized nanoparticles.

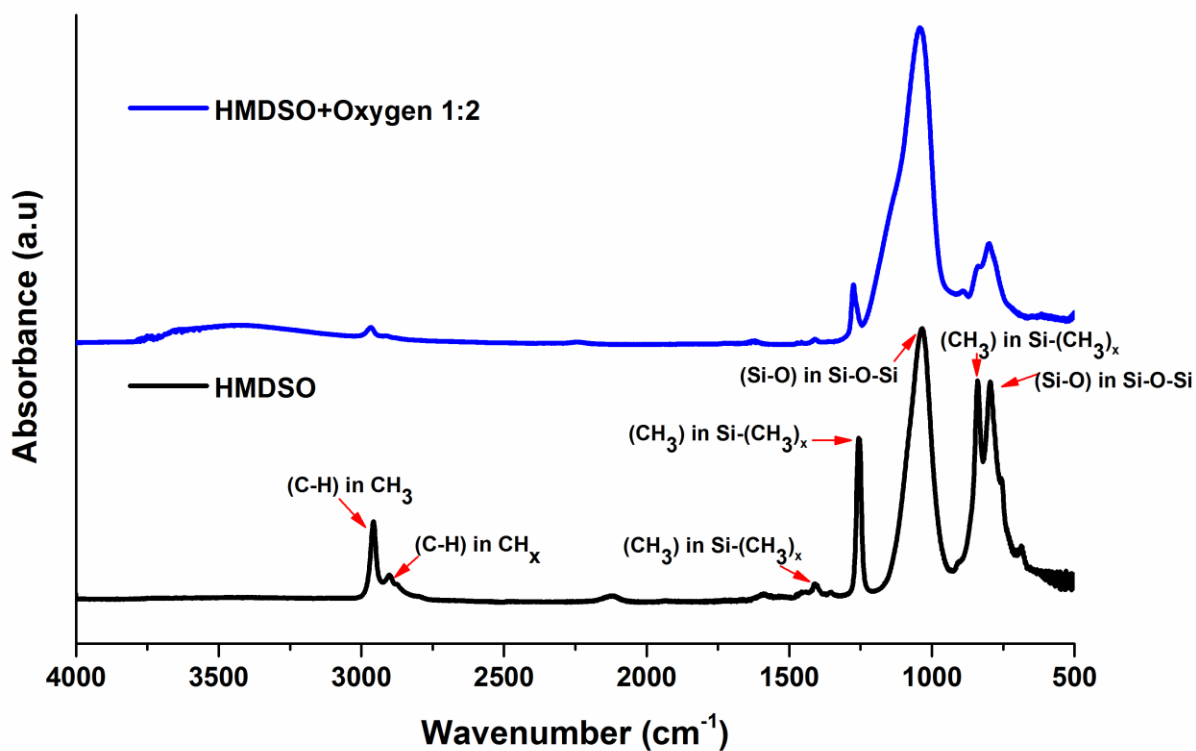


Figure 2. FTIR spectra for plasma films from HMDSO and HMDSO+O₂ deposited on KBr card (Pressure: 300mT; Flow rate: 2 sccm; Power: 60W; Deposition time: 15 min).

2.3 Functionalized Nanoparticles Characterization

The PTFE nanoparticles harvested from the reactor after plasma functionalization with HMDSO monomer were characterized using XPS (Kratos Axis Ultra system using monochromatic Al K_α X-ray source). Figure 3 shows the Silicon 2p XPS spectra for PHGM particles. The peaks around 101 eV binding energy represent the presence of siliceous plasma coating on the surface of PTFE nanoparticles.

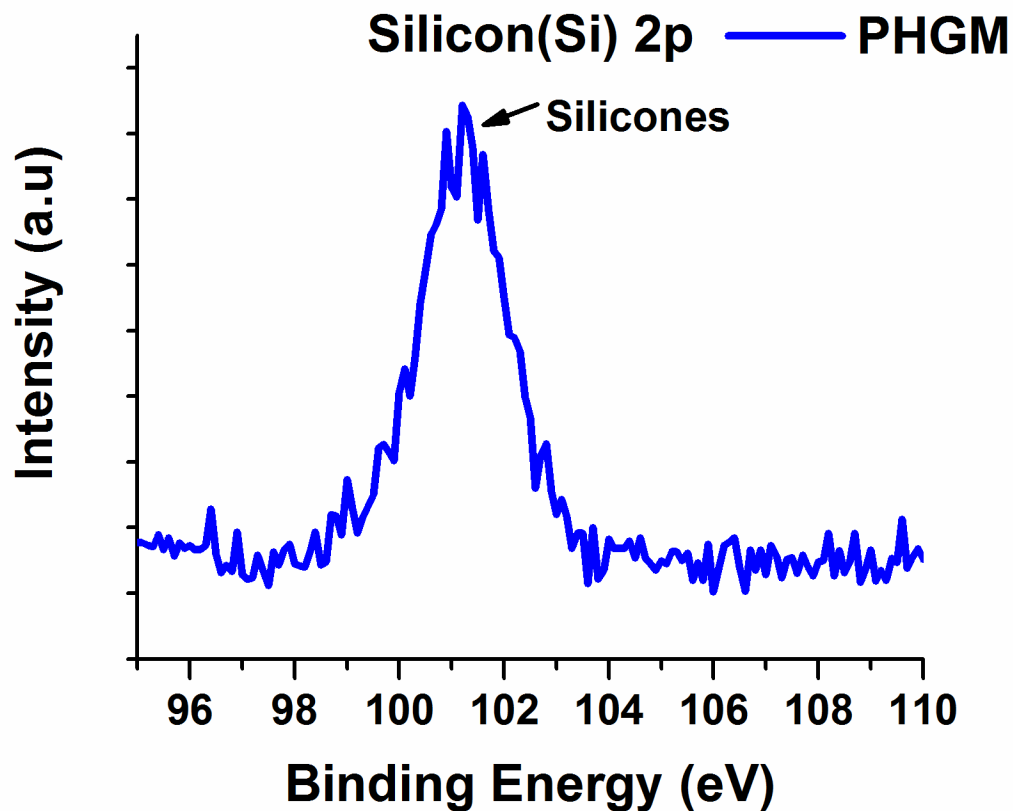


Figure 3. Silicon 2p XPS spectrum for functionalized PTFE nanoparticles (PHGM).

2.4 Tribological Evaluation

1 Hour Tests: Group III base stock (GS Caltex Kixx Lubo 4 cSt) was used as the carrier oil for all the tests performed in our study. Phosphorus level for ZDDP was kept at 350 ppm and four different oil formulations were prepared and the details about each test formulation is shown table 2. To make a homogenous mixture and achieve uniform dispersion of functionalized nano-additives in base oil, each blend was subjected to probe sonication for about 30 mins just before the test and 2-3 drops of this mix were used for testing. The test configuration selected was high-frequency reciprocating cylinder on flat surface (Ra 13 nm), which closely simulates the

tribological interaction of piston ring on liner in the actual automobile engines. The results for tribological tests shown in this work were performed using a Bruker's UMT machine under 82 N load, which results in an initial Hertzian contact pressure of 500MPa. Tests were run at 5Hz reciprocation speed for a duration of 60 minutes for each formulation at 100⁰ C. Stroke length was 6 mm and both cylinder (4mm X 6mm) and flat (14mm X 14 mm) were 52100 hardened steel. Data acquisition was done using Bruker's UMT software. All test specimens were cleaned thoroughly prior to the tests using Stoddard solvent, isopropanol and acetone to get rid of any residue of oil and other contaminants from the surfaces. The samples were cleaned with heptane after the tests and the rubbed surfaces were then preserved by submerging in PAO oil.

4 Hours Tests: Three different oil formulations were prepared using the same approach as mentioned above. Phosphorus level was kept at 700 ppm in one formulation and 350 ppm in another and rest of the details are shown in table 3. Other than the duration of the test i.e. 4 hours, rest of the parameters and conditions were kept the same. Repeats were carried out for all the tests (1 hour and 4 hours) to see the reproducibility of the experiments. In order to conduct an assessment of wear volume losses, the cylinders after the tests were first cleaned with heptane and then examined under optical microscope and 3D optical interferometer.

Table 2. Details of oil formulations for 1 hour tests.

Test	Name used in figures	Formulation
A.	B.O	Group III Base oil (B.O): B.O
B.	B.O + ZDDP 350	B.O+ZDDP with 350 ppm of Phosphorus treat rate: B.O + ZDDP 350
C.	B.O + ZDDP 350 + 0.33wt% PTFE	B.O+ZDDP with 350 ppm of Phosphorus treat rate + 0.33 wt% PTFE

D.	B.O + ZDDP 350 + 0.33wt% PHGM	B.O+ZDDP with 350 ppm of Phosphorus treat rate + 0.33 wt% PHGM
----	-------------------------------	---

Table 3. Details of oil formulations for 4 hour tests.

Test	Name used in figures	Formulation
E.	B.O	Group III Base oil (B.O)
F.	B.O + ZDDP 700	B.O+ZDDP with 700 ppm of Phosphorus treat rate
G.	B.O + ZDDP 350 + 0.33wt% PHGM	B.O+ZDDP with 350 ppm of Phosphorus treat rate + 0.33 wt% PHGM

2.5 Tribofilms Characterization Procedure

To understand the tribochemistry of the boundary films formed at the sliding interfaces, surface sensitive techniques such as XPS and XANES were employed. XPS analysis were performed with the Kratos Axis Ultra system using monochromatic Al K_α X-ray source. This spectroscopic technique reveals the presence of an element, its abundance on the sample surface (typical detection depth ~5 nm) and the chemical bonding state. For analysis, steel flat specimens were first cleaned with hexane to remove the oil from the surface and then loaded on the sample holder. Before data collection each specimen was sputter cleaned using ion gun (beam energy 4.20 keV) for about 10 mins and then the x-ray gun was slowly ramped up to 150 W power before data accumulation. The spot size of the x-ray beam for data collection was kept at 300 μm x 700 μm.

XANES work was performed at Canadian Light Source synchrotron facility at Saskatoon Canada. This study was particularly helpful in looking at phosphorus and sulfur species in the tribofilms of the samples at different depths of penetration. Phosphorus and sulfur K-edge spectra

were collected at Soft X-ray Microcharacterization Beamline (SXRMB) beam station which provides with an energy range from 1.7 keV to 10 keV, a photon resolution of 3.3×10^{-4} InSb (111) and was operated using 1 mm x 2 mm spot size. The phosphorus L-edge data was collected at Variable Line Spacing Plane Grating Monochromator (VLSPGM) beam station. This beam line has a photon resolution of greater than 10,000 $E/\Delta E$ and the energy range from 5.5 eV to 250 eV. For our experiments, the spot size of the photon beam was kept at 100 μm x 100 μm .

3. RESULTS AND DISCUSSION

3.1 Friction and wear volume

For 1 hour tests, the base oil (A), oil with only ZDDP (B), and oil with ZDDP and non-functionalized PTFE (C) particles samples exhibited essentially the same friction profile. However, in sharp contrast with these three samples, the friction coefficient obtained for the oil formulation with ZDDP and functionalized PTFE nanoparticles (D) exhibited dramatically lowered and stable values as shown in figure 4 (a). In a study by Dassenoy et al.⁵⁸ that involved a dispersion of PAO, WS₂ nanoparticles and ZDDP, it was reported that synergistic effects between nanoparticles and ZDDP enhanced tribological performance. In the current study, the ZDDP and PTFE nanoparticles when used together in the oil did not yield any synergistic effects. However, when functionalized PTFE (PHGM) was mixed in with ZDDP, lower friction coefficient is seen due to synergism between additives.^{8, 58-61} In addition, for 4 hours tests, the oil with ZDDP 350 + 0.33wt% PHGM nanoparticles exhibited stable friction behavior. It has lower values for friction coefficient at the beginning of the test and towards the end the values are almost similar to the oil with higher amount of ZDDP (700 ppm of P level) as shown in figure 4 (b).

Figure 5 shows the optical profilometry of the cylinders represented in 2D at the center region of the cylinder and the 3D representation is of the area of contact in the cylinders after

tribological tests. It is evident that the oil with ZDDP and functionalized PTFE nanoparticles (PHGM) exhibited better wear characteristics for both 1 and 4 hours tests. In addition, the wear surface on the flat specimen have visually distinguishable features that reveal oil with ZDDP and PHGM offered excellent wear protection as shown in figure 6. The wear volume was calculated by measuring the wear scar on the cylinder using an optical microscope. The wear results were promising for the oil formulation with the PHGM that demonstrated significant reduction in wear volume compared to the other samples, the results are shown in figures 7 (a) & (b) . The presence of PTFE nanoparticles coated with siliceous chemistry enhanced the anti-wear properties of ZDDP even at reduced amount of phosphorus in the oil.^{8, 58-61}

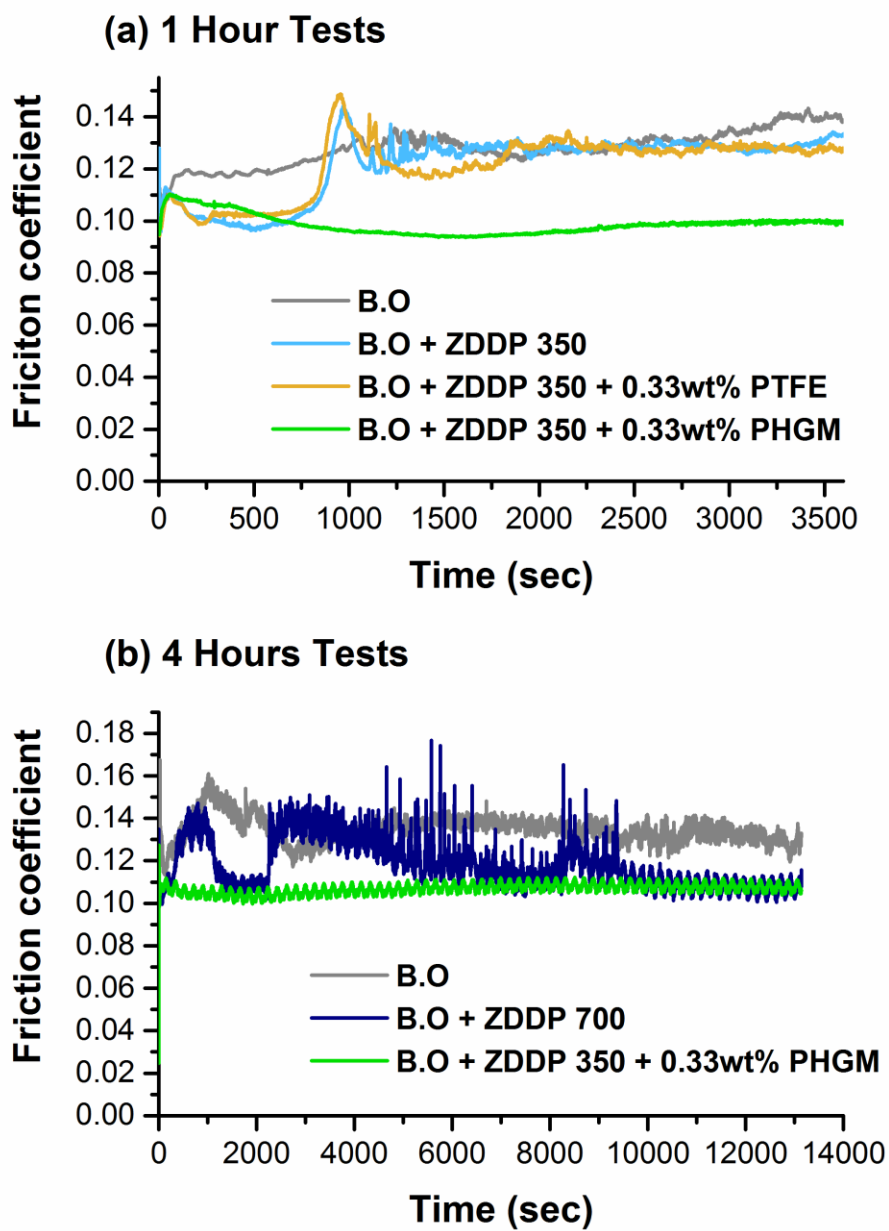


Figure 4. Friction behavior for base oil, oil with ZDDP, PTFE nanoparticles and functionalized PTFE (PHGM) nanoparticles; **(a)** Friction data plot for 1 hour tests; **(b)** Friction outcomes for 4 hours tests.

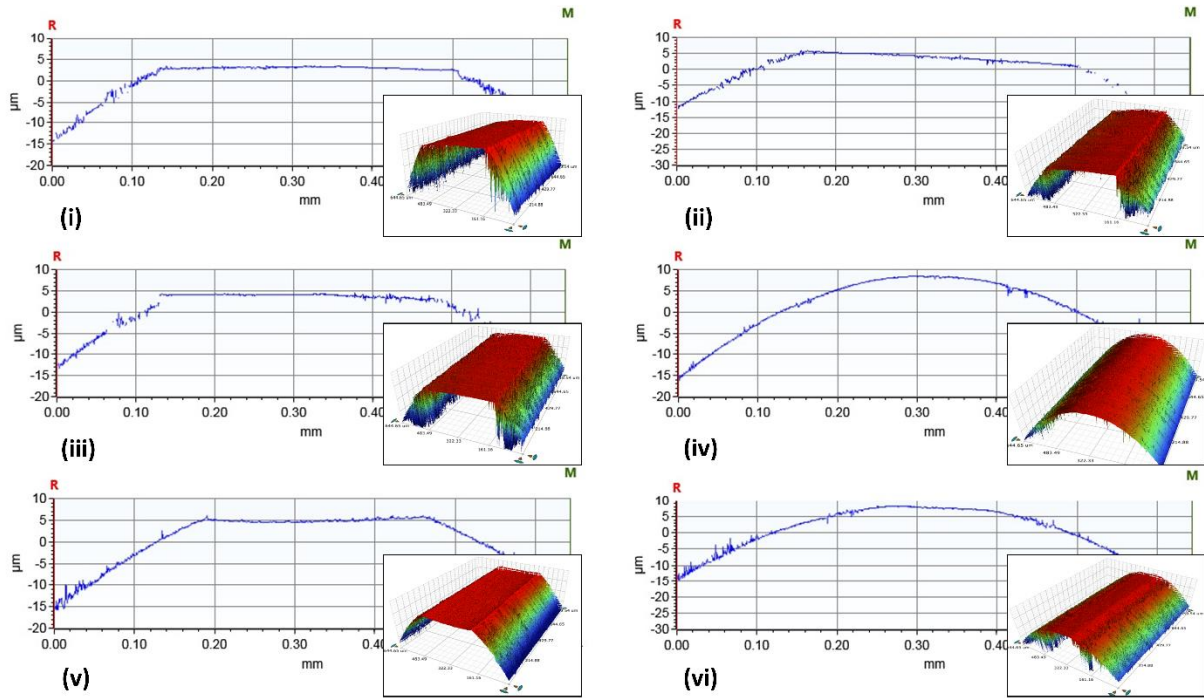


Figure 5. Optical profilometry of the cylinders represented in 2D at the center region of the cylinder and the 3D representation is of the area of contact in the cylinders from 1 hour ((i) B.O, (ii) B.O + ZDDP 350, (iii) B.O + ZDDP 350 + 0.33wt% PTFE & (iv) B.O + ZDDP 350 + 0.33wt% PHGM) and 4 hours ((v) B.O+ ZDDP 700 & (vi) B.O+ ZDDP 350 + 0.33wt% PHGM) of tribological testing.

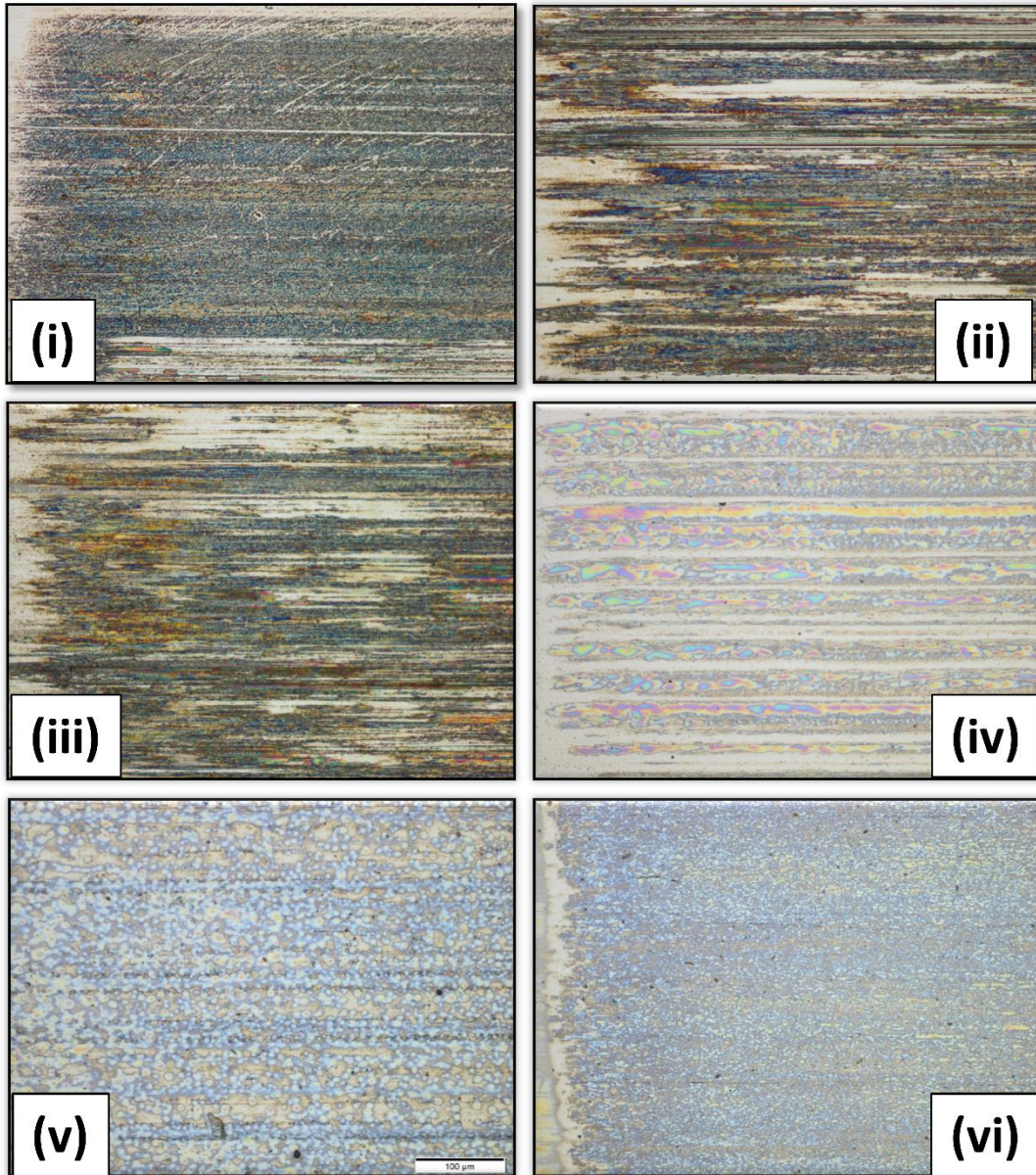


Figure 6. Optical micrographs of wear surfaces of the flat steel specimens from 1 hour ((i) B.O, (ii) B.O + ZDDP 350, (iii) B.O + ZDDP 350 + 0.33wt% PTFE & (iv) B.O + ZDDP 350 + 0.33wt% PHGM) and 4 hours ((v) B.O+ ZDDP 700 & (vi) B.O+ ZDDP 350 + 0.33wt% PHGM) of tribological testing.

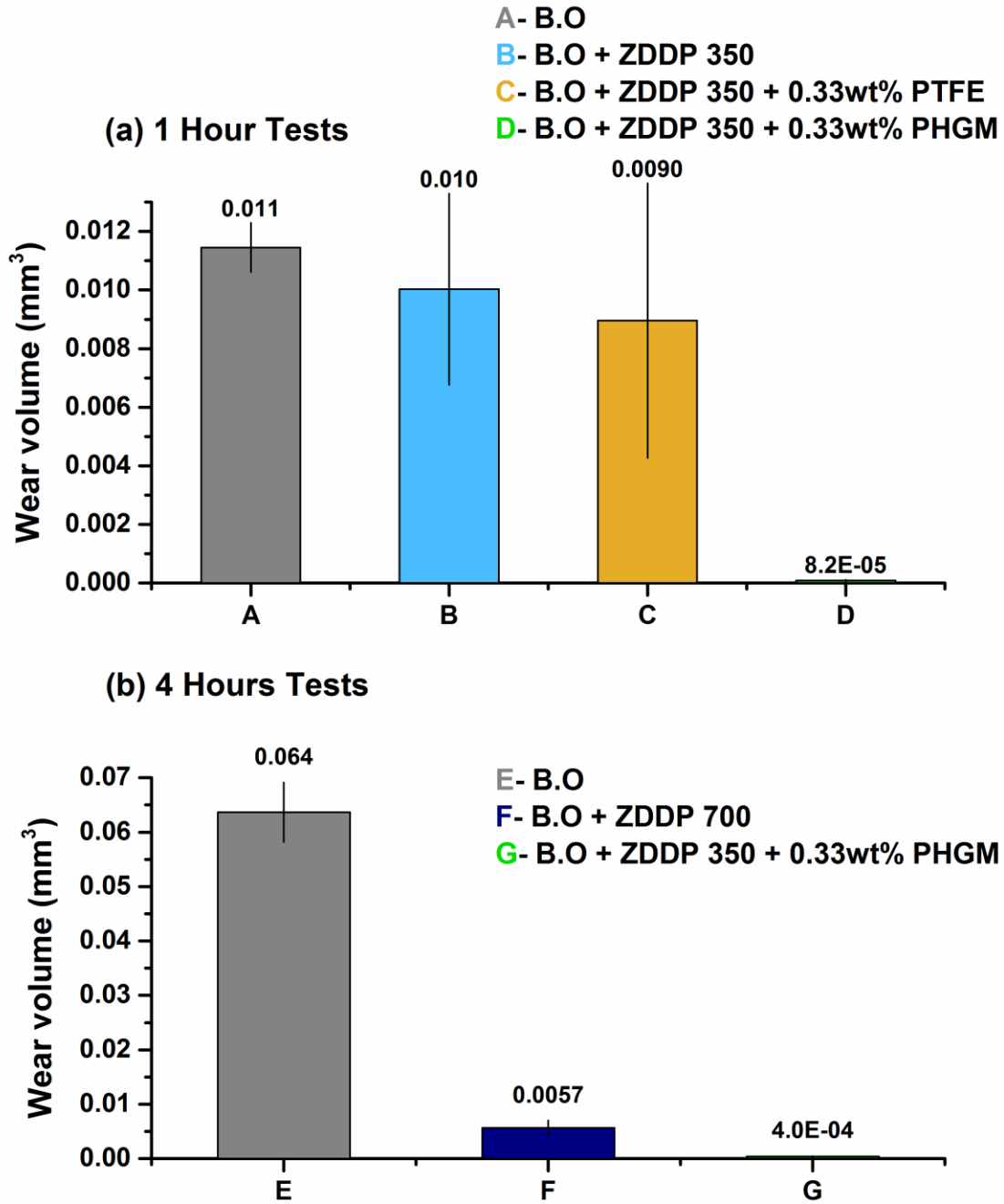


Figure 7. Comparison of wear volume losses for base oil, oil with ZDDP, PTFE nanoparticles and functionalized PTFE (PHGM) nanoparticles; (a) Wear data for 1 hour tests (A,B,C & D); (b) wear volumes for 4 hours tests (E,F & G).

3.2 Tribochemical Characterization

An extensive comparative study of the tribochemistry of the films was performed which includes specimens from one hour tests; test **B** (B.O + ZDDP 350) and test **D** (B.O + ZDDP 350 + 0.33wt% PHGM).

3.2.1 XPS analysis

X-ray photoelectron spectroscopy (XPS) was used for elemental analysis of the samples after tribological testing. The results obtained are shown in Figure 8. Each graph provides a contrast between the sample which contained only the base oil and ZDDP (350ppm P-level) and the sample containing the base oil with ZDDP (350ppm P-level) and 0.33wt% PHGM [added plasma surface functionalized PTFE nanoparticle]. As depicted earlier in the wear measurement results, a very dramatic difference is observed in contrasting these samples. For zinc 2p and phosphorus 2p, we see sharp peaks (~ 1022.6 eV & ~ 1045.7 eV for Zn 2p; ~ 134.3 eV for P 2p) in the sample tested with oil containing functionalized nanoparticles when compared to the sample consisting only of base oil and ZDDP. This sample also exhibits very low intensity peaks for Fe 2p as compared to the other. This clearly indicates the presence of stable tribofilms containing both zinc and phosphorus on the surface. Whereas the overall concentration of oxygen looks relatively similar in O 2p spectra for both samples, there is a distinct shift in peak shape, with an increased presence of higher binding energy electrons from the sample containing the functionalized nanoparticles. The peak for the sample without nanoparticles is at lower binding energy (~ 530.1 eV) and corresponds to oxides of iron whereas for the sample with functionalized nanoparticles there is a shift in the peak position towards higher binding energy values (~ 531.9 eV & ~ 533.8 eV). The phosphorus and silicon species bound to oxygen contribute to this peak shift and this again confirms the presence of phosphates protecting the surface and reducing the wear.

The peaks in spectra for Si 2p (~103 eV) and F 1s (~689.4 eV) show the presence of siliceous (Si-O) and carbon bound fluorine chemical species in the tribofilm for sample with ZDDP and PHGM nanoparticles whereas the other sample fails to show any evidence for both the elements. These results suggest that functionalized PTFE nanoparticles were successfully able to deliver the siliceous chemistry to the interacting interfaces and contributed to the formation of protective films by acting in synergy with ZDDP in the oil.

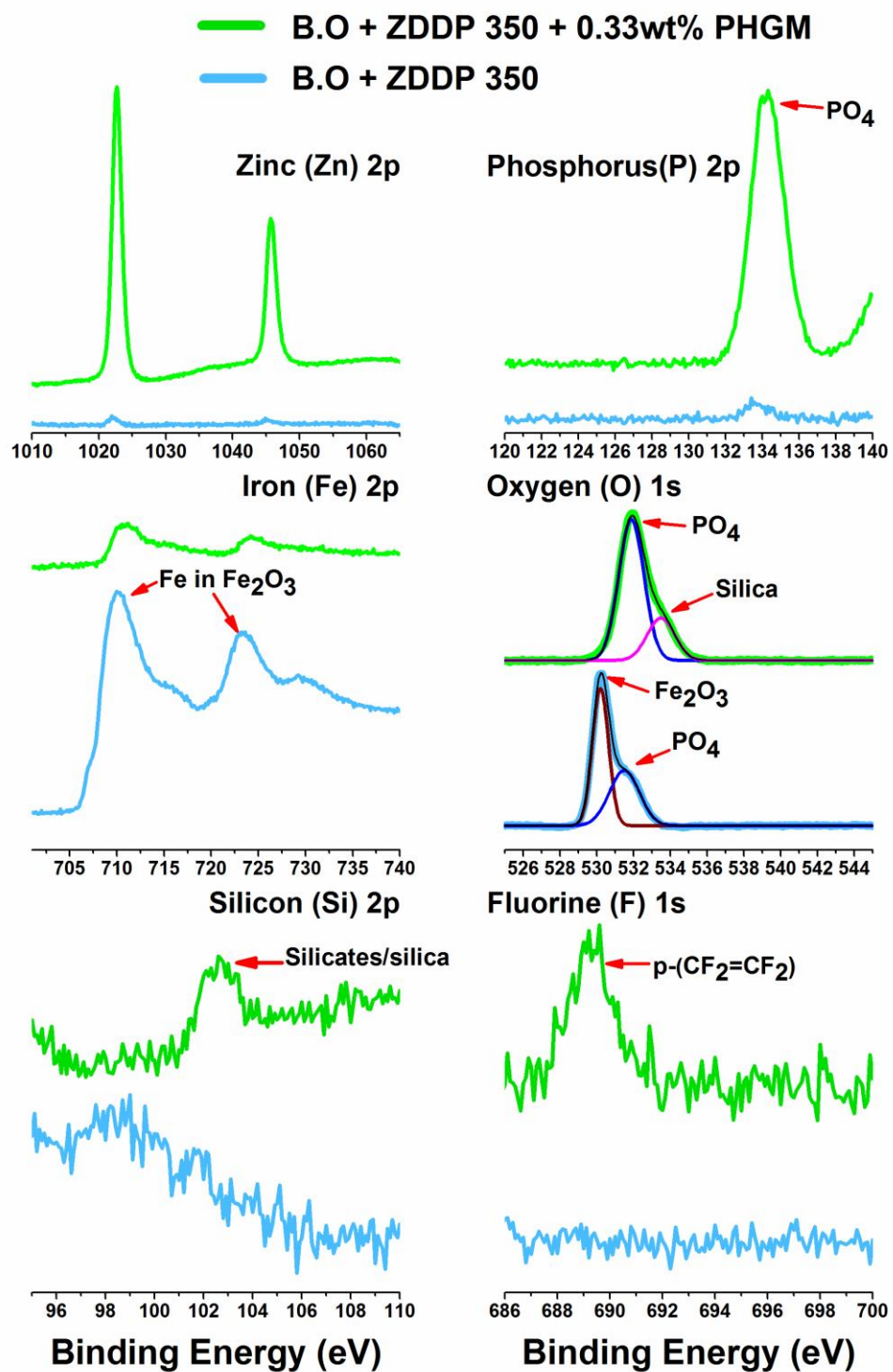


Figure 8. XPS spectra for specimens from 1 hour tests; **Green plot:** B.O + ZDDP 350 + 0.33wt% PHGM; **Blue plot:** B.O + ZDDP 350.

3.2.2 XANES analysis

X-ray absorption near edge structure spectroscopy, normally identified simply as XANES, is an analytical technique wherein absorption spectra involving core electron excitation to higher energy unoccupied states are obtained. It is used to determine the local coordination of the elements and the information can be obtained from both surface and bulk of the sample. XANES spectra provide detailed information concerning both the geometric make up and electronic structure of the absorbing atom.^{62, 63} XANES analyses have played a particularly significant role in tribological studies and it has been broadly employed in investigating the chemical composition of the tribofilms formed from different oil additives.^{8, 27, 27, 36, 61, 64, 65} In the present case, the XANES study focused on phosphorus and sulfur chemistry in the tribofilms. It included fluorescence yield (FLY) mode spectra, which gives information from bulk of the sample and total electron yield (TEY) mode spectra, which is more surface sensitive, for both K and L shell electrons. As shown in Figures 9, 10 & 11, there are important differences observed in contrasting the phosphorus L and K edge spectra, and sulfur K edge spectra obtained from one hour test specimens with oils that contain Base Oil + ZDDP (350 ppm of P level) and Base Oil+ ZDDP (350 ppm of P level)+ 0.33wt% PHGM. For phosphorus K and L edge, the initial two spectra in each graph are those obtained for pure samples of zinc phosphate and iron (III) phosphate, obtained for both K (Fig. 9a) and L (Fig. 9b) level electrons. In each case there is a clear energy shift of the phosphorus fluorescence to higher value for the P atoms associated with Zn, compared to Fe. For sulfur K edge, there are two sets of spectra obtained from pure samples in FLY (Fig. 10) and TEY (Fig. 11) mode. First set of spectra is from sulfide compounds namely zinc sulfide, iron sulfide and pyrite, and the second set is from sulfate species like zinc sulfate, ferrous sulfate and ferric sulfate.

Phosphorus K and L edge

Phosphorous K-edge TEY spectra for model compounds, shown in the figure 9(a), have peaks **c** (2152.2 eV) and **c'** (2153.22) that correspond to electronic transition from 1s to vacant p state. The energy for peak **c** (for zinc phosphate) is slightly lower than peak **c'** (for iron oxide). The peak position of the spectra from the specimen tested with ZDDP and functionalized nanoparticles (PHGM) overlaps exactly with that of zinc phosphate model compound. Whereas the specimen tested with only ZDDP has peak position overlapping with iron phosphate. Clearly, the K-edge spectra from the tested samples provide further confirmation that stable tribofilms of zinc phosphate are prominently present only on the surface of sample which contained the added functionalized nanoparticles.

Phosphorous L-edge TEY XANES spectra provides us with significant additional chemical information as the sampling depth is around 5-15 nm. As shown in the figure the different peak positions for model compounds are marked as **a**, **b**, **c**, **c'** and **d**. Each peak has its own significance assigned to specific electronic transitions. Peak **a** can be correlated with zinc phosphate's P 2p spin orbital splitting, whereas peaks assigned as **c** and **c'** correspond to transitions to the t_2^* molecular orbital in zinc and iron phosphate respectively.⁶⁶ The peak **d**, around 146.0 eV, is characteristic of various different types of phosphates present in both samples.⁶⁷ Again, from the plots in figure 9(b), it can be deduced that tribofilms generated on the flat specimen tested with oil containing plasma functionalized PTFE nanoparticles is primarily composed of zinc phosphate as all the peak positions (**a**, **b** & **c**) align with the peaks for zinc phosphate model compound. The peaks for other sample (ZDDP 350 only) line up with those of iron phosphate model compound and is indicative of respective chemistry in the tribofilm. Phosphorus L-edge spectra is also very useful for the estimation of chain length of polyphosphates present in the tribofilm on the surface and for this purpose, the ratio of peak intensities of peak **a** and **c** is calculated. A peak height a/c ratio up to 0.3

to 0.4 corresponds to the presence of short chain polyphosphates and a/c ratio above 0.6 represents long chain polyphosphates.^{36, 61, 68, 69} The spectra for sample with PHGM as additive has a/c ratio of ~0.5 which indicates medium chain polyphosphates are present in the top 5-15 nm of the tribofilm. It is quite evident in the plots that tribofilms for the sample with functionalized nanoparticles has phosphorus mainly in the form of zinc phosphate (medium chain) whereas the other sample, i.e. the one without nanoparticles, has phosphorus present as iron phosphate.

Sulfur K edge

The sulfur K edge spectra for model compounds are shown in both FLY (Fig. 10) and TEY (Fig. 11) mode. The peak position for each kind of sulfide compound is easily distinguishable from the other. The main peak positions for FeS (peak **a**), FeS₂ (peak **a'**) and ZnS (peak **b**) are located at 2470 eV, 2471.5 eV and 2473 eV respectively. The peak positions of all the sulfates species are centered around 2481.5 eV (peak **c** & **c'**). Figure 10 shows the S K edge spectra in FLY mode, the peak positions for sample with ZDDP and functionalized nanoparticles (PHGM) align with that of ZnS and Zn/Fe sulfate model compounds. The difference in peak intensities clearly suggest that the tribofilm is rich in zinc sulfide and sulfur in the form of sulfates is relatively low. Whereas, the sample without nanoparticles (ZDDP 350 only) shows only one prominent peak which overlaps with peak position of sulfates and the other peaks overlapping with Zn/Fe sulfides appear very noisy. This tells us, for this sample, sulfur is present mostly in the form of sulfates and amount of sulfides is very low in the tribofilm. The S K edge TEY data is shown in figure 11 and the information regarding sulfur chemistry in the sample with functionalized nanoparticles is essentially the same as we got from FLY mode which indicates that sulfur is mainly present in the form of zinc sulfide in the tribofilm when ZDDP and PHGM is used and amount of sulfate is

significantly lower than sulfides. In addition, the TEY mode plot for sample with only ZDDP has a peak overlapping with zinc sulfide's peak position and there is no peak for sulfates.

Overall, the S K edge data from both FLY and TEY mode suggests that the sample with ZDDP and functionalized nanoparticles has a stable protective tribofilm which is rich in sulfur compared to the sample with only ZDDP where amount of sulfur is very low. In addition, the sulfur chemistry and its presence across the thickness of tribofilm is also very different in both the samples. Sample with nanoparticles has ample amount of zinc sulfide and zinc sulfate present in the film along with iron sulfide/sulfate. Whereas, the presence of sulfur for sample with only ZDDP is mainly in the form of iron bound sulfates and other species of sulfur such as zinc sulfide/sulfate, iron sulfide are present at a very low concentration and therefore they fail to provide with any friction and wear protection.

Another crucial piece of information that can be deduced from P and S K edge spectra is the relative abundance of P and S in the tribofilm.⁷⁰ As depicted in Figure 12, the amount of phosphorus in the tribofilm for the sample with ZDDP and functionalized PTFE nanoparticles is significantly higher than that of sulfur species. The data from FLY and TEY modes for the oil with ZDDP + PHGM suggests that, compared to the bulk (FLY data: P/S ratio, 3.05), the near-surface region of the tribofilm has a higher amount of phosphorus (TEY Data: P/S ratio, 3.59) which is present mainly in the form of medium- to longchain phosphates of zinc. However, for the sample with only ZDDP, the sulfur chemistry is clearly more abundant than the phosphorus chemistry, and its presence is almost similar in the bulk (FLY data: P/S ratio, 0.37) and near-surface (TEY data: P/S ratio, 0.43) regions of the film.

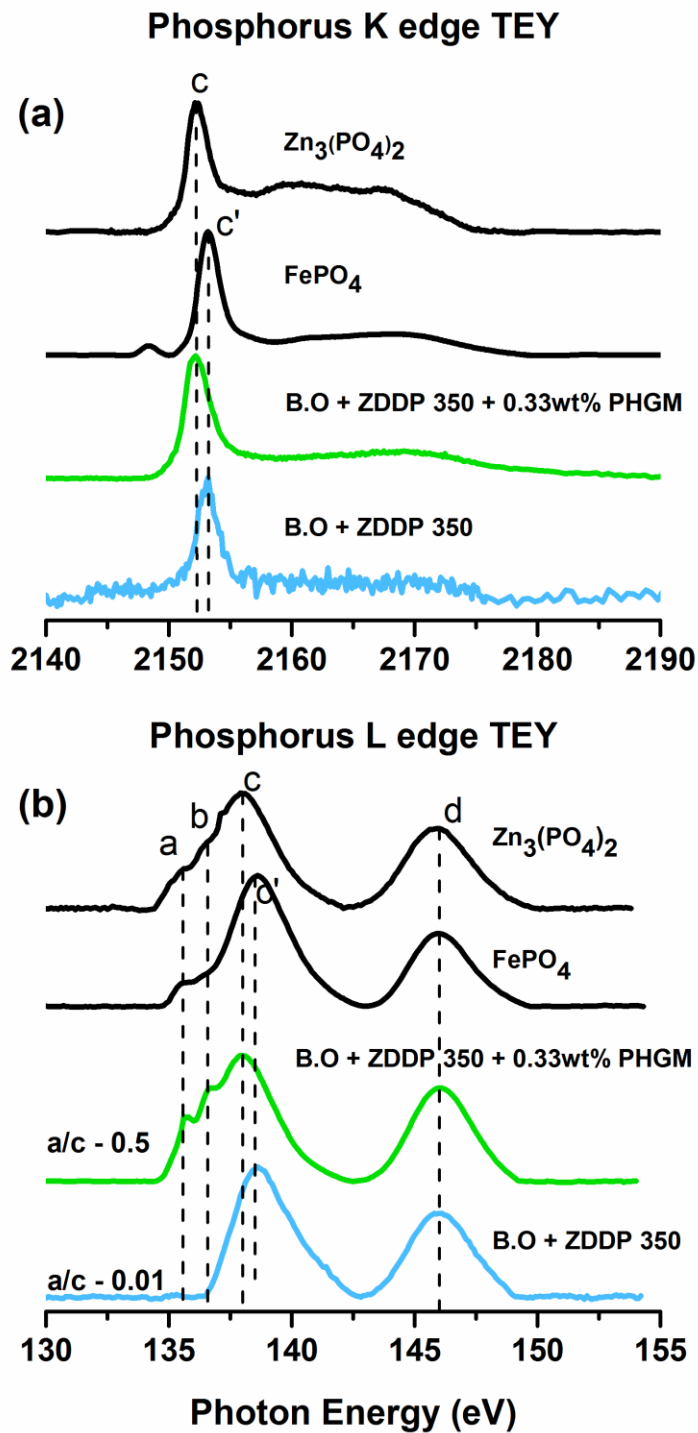


Figure 9. Phosphorus K and L edge XANES TEY spectra of model compounds and tribofilms generated with **B.O + ZDDP 350 + 0.33wt% PHGM** and **B.O + ZDDP 350**.

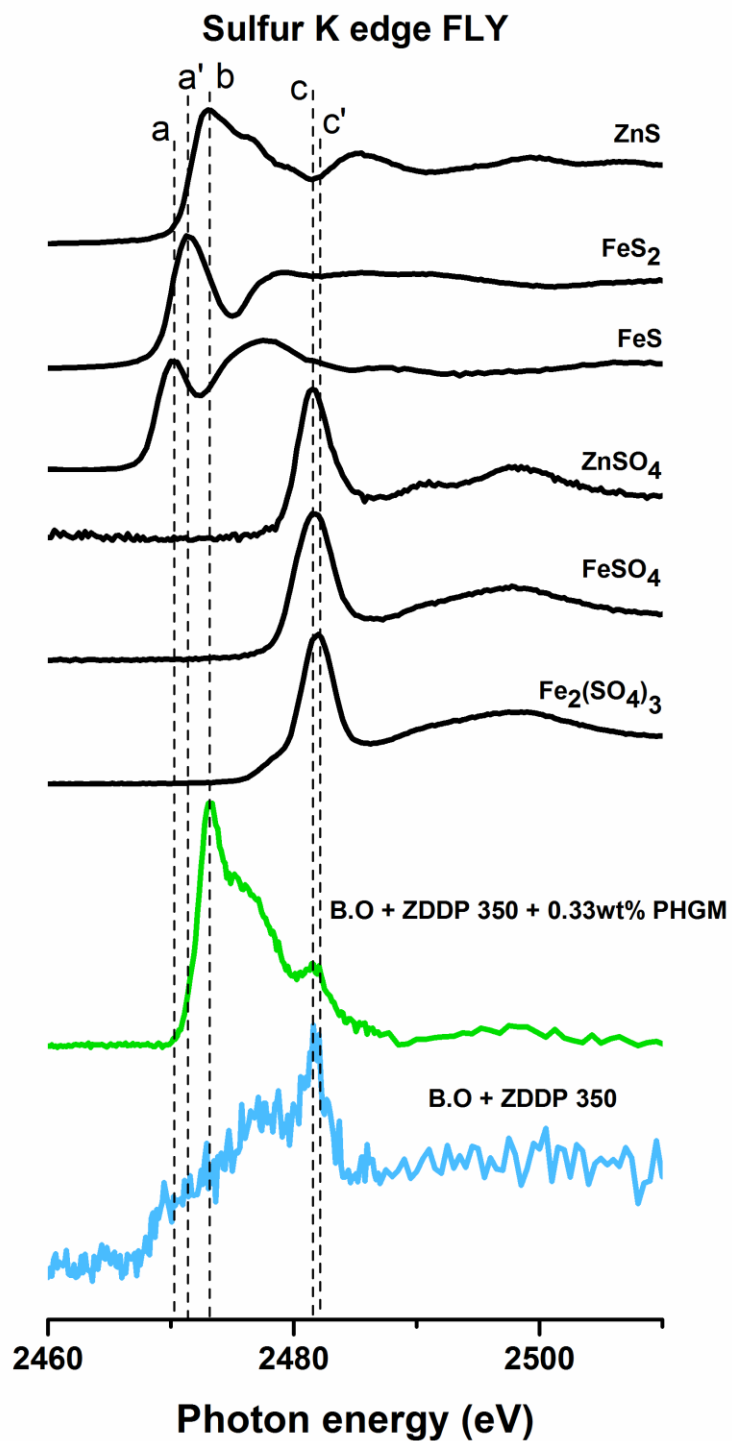


Figure 10. Sulfur K edge FLY XANES spectra of model compounds and tribofilms generated with **B.O + ZDDP 350 + 0.33wt% PHGM** and **B.O + ZDDP 350**.

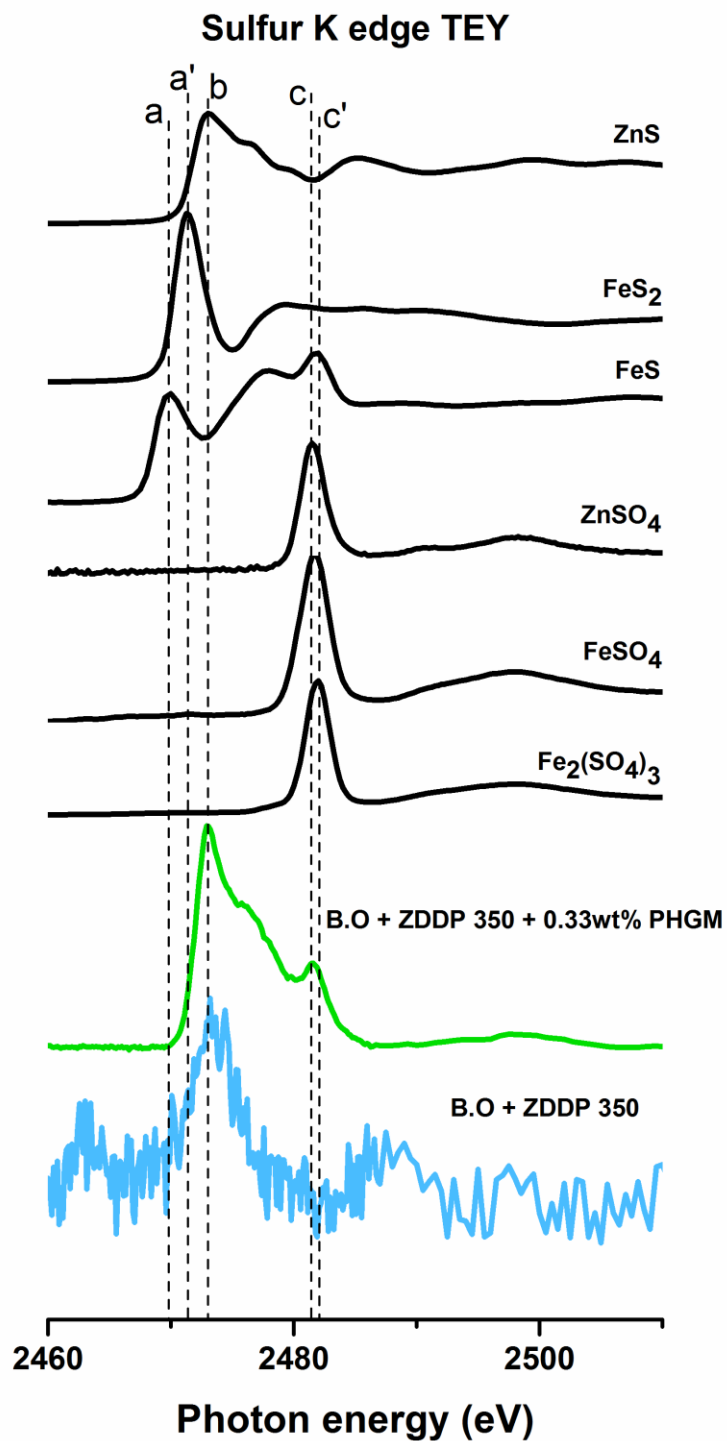


Figure 11. Sulfur K edge TEY XANES spectra of model compounds and tribofilms generated with **B.O + ZDDP 350 + 0.33wt% PHGM** and **B.O + ZDDP 350**.

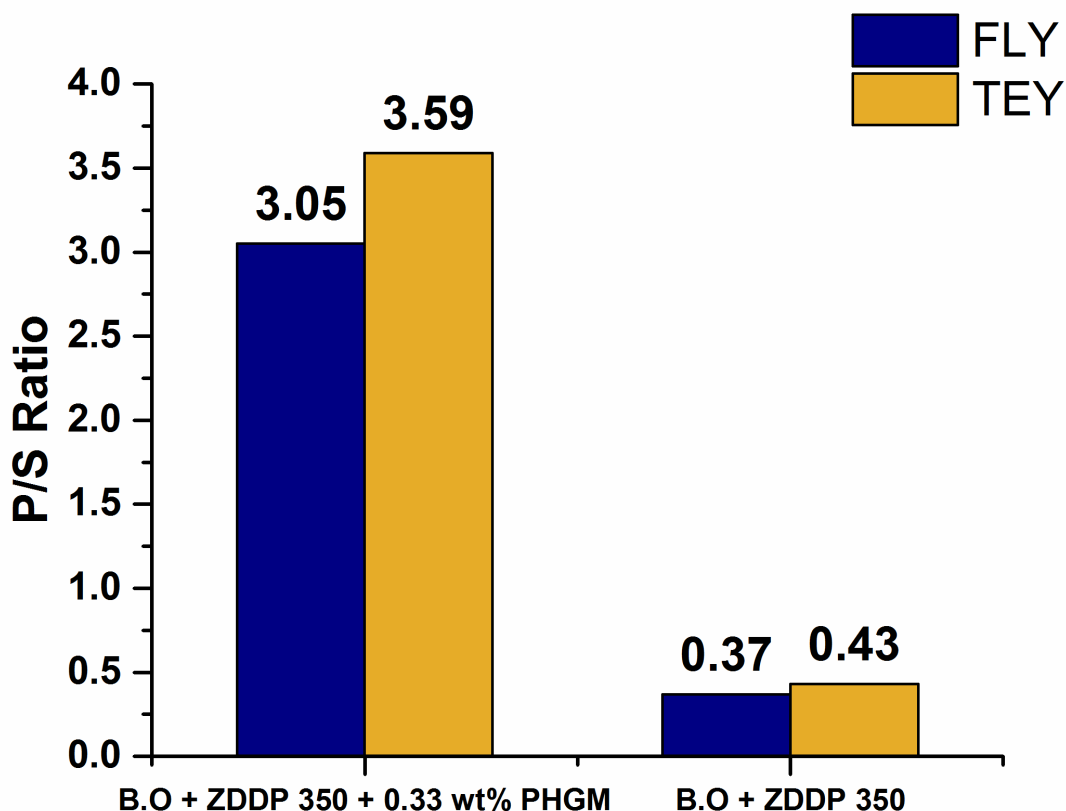


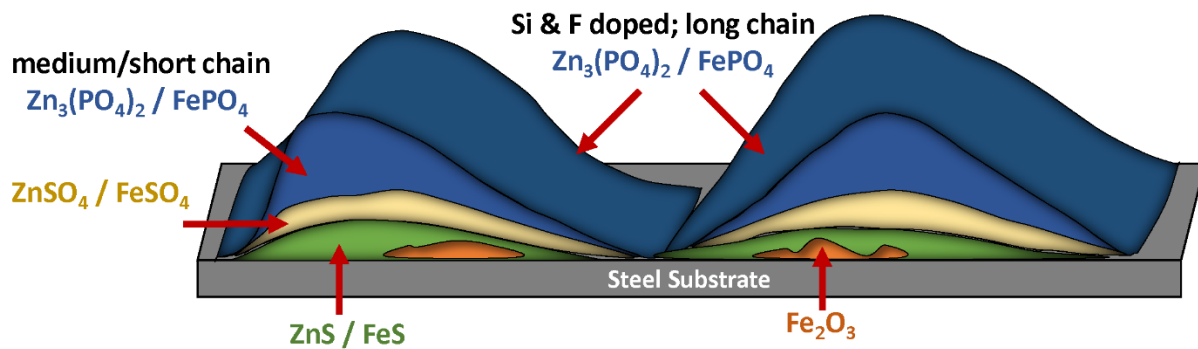
Figure 12. Relative P/S ratios for tribofilms generated with **B.O + ZDDP 350 + 0.33wt% PHGM** and **B.O + ZDDP 350**.

3.3 Phenomenological Modeling

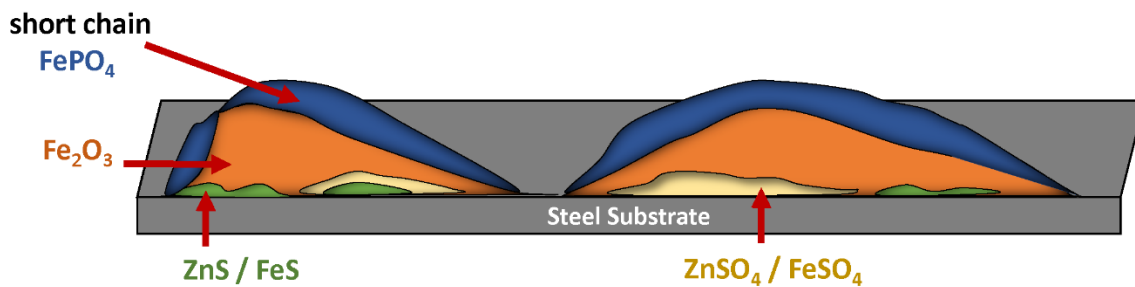
All the chemical information from XPS and XANES analysis was taken into account to develop phenomenological models for tribofilms for samples; a) B.O+ZDDP (350) + 0.33wt% PHGM and b) B.O+ZDDP 350, as shown in figure 13. XPS analysis provided us with critical information regarding the presence of silicon and fluorine chemistry doped into amorphous zinc phosphate glassy films. In addition, the distinctive chemical make-up of the tribofilms for both the samples was evident from oxygen, zinc, phosphorus and iron XPS spectra. XANES

characterization gave more insight into phosphorus and sulfur chemistry, their local chemical environment and relative amounts in the tribofilms. As shown in the figure 13 (a), the tribofilm for sample with ZDDP and plasma functionalized nanoparticles has Si and F doped long chain Zn/Fe phosphates in the top region and underneath it has short/medium chain phosphates. The sulfides and sulfates of Zn/Fe are mostly present in the bulk of the film and close to the steel substrate. However, the tribofilm for sample with only ZDDP has iron oxide as one of the main constituent (Fig. 13 (b)) and the contribution from phosphorus and sulfur chemistry is not very significant. The overall amount of sulfur species is higher than phosphorus and it is primarily present in the bulk of the film in the form of sulfate and sulfide of Zn/Fe. The phosphorus in the film is mostly iron phosphate.

The synergistic interaction of ZDDP and PTFE nanoparticles coated with siliceous chemistry contribute to the formation of phosphorus and sulfur rich protective tribofilm at the rubbing contacts. Whereas, ZDDP by itself at such low level of phosphorus fails to form any stable tribofilm at the surface to provide with anti-wear/anti-friction benefits. The presence of the stable tribofilms with phosphates of Zn and the presence of sulfides of Zn in the tribofilm formed with ZDDP+PHGM are contributing factors for the significantly improved wear and frictional performance even at 350 ppm of P in the oil.



a) B.O + ZDDP 350 + 0.33 wt% PHGM



b) B.O + ZDDP 350

Figure 13. Phenomenological models for tribofilms generated with (a) **B.O + ZDDP 350 + 0.33wt% PHGM** and (b) **B.O + ZDDP 350**.

4. CONCLUSIONS

The results obtained clearly reveal that the addition of the plasma functionalized PTFE nanoparticles to the base oil with ZDDP provide a very significant improvement in reducing wear, clearly outperforming samples having only ZDDP, or ZDDP plus un-functionalized particles. It is also shown that these functionalized particles provide improved tribological properties in base oils containing a two-fold reduction (from 700 ppm to 350 ppm P level) in ZDDP to that observed in samples devoid of these particles. However, compared to base oil containing higher amount of ZDDP (700 ppm P level), we observed significant improvement in only wear with friction coefficient being almost similar for both formulations. The improved wear performance is attributed from the stable tribofilm formation with polyphosphates of Zn doped with Si and F when ZDDP is used in combination with functionalized nanoparticles of PTFE. On the other hand oils with just ZDDP at 350 ppm resulted in primarily formation of oxides of Fe with very small amounts of phosphates of Zn and largely sulfates of Zn and Fe that are less protective. The improved wear performance coupled with the reduced concentration of ZDDP, should help reduce automobile catalyst deactivation due to phosphate glass deposits and reduce overall greenhouse gas emissions. Reduced friction can translate into improved fuel efficiency of internal combustion engines.

Acknowledgements: Support provided by Vanderbilt Chemicals is gratefully acknowledged. XANES experiments were conducted at the Canadian Light Source, Saskatoon, Saskatchewan, Canada that is supported by NSERC, NRC, CIHR and the University of Saskatchewan. Tribological tests were performed at Argonne National Laboratory. X-ray Photoelectron Spectroscopy facilities provided by the Department of Chemistry is gratefully acknowledged.

References

- (1) Wong, V. W.; Tung, S. C. Overview of Automotive Engine Friction and Reduction trends—Effects of Surface, Material, and Lubricant-Additive Technologies. *Friction* 2016, 4, 1-28.
- (2) Willermet, P. A. Some Engine Oil Additives and their Effects on Antiwear Film Formation. *Tribol. Lett.* 1998, 5, 41-47.
- (3) Holmberg, K.; Andersson, P.; Erdemir, A. Global Energy Consumption due to Friction in Passenger Cars. *Tribol. Int.* 2012, 47, 221-234.
- (4) Holmberg, K.; Andersson, P.; Nylund, N.; Makela, K.; Erdemir, A. Global Energy Consumption due to Friction in Trucks and Buses. *Tribol. Int.* 2014, 78, 94-114.
- (5) Singh, S. K.; Singh, S.; Sehgal, A. K. Impact of Low Viscosity Engine Oil on Performance, Fuel Economy and Emissions of Light Duty Diesel Engine. 2016.
- (6) Tormos, B.; Ramirez, L.; Johansson, J.; Bjorling, M.; Larsson, R. Fuel Consumption and Friction Benefits of Low Viscosity Engine Oils for Heavy Duty Applications. *Tribol. Int.* 2017, 110, 23-34.
- (7) Spikes, H. A. The History and Mechanisms of ZDDP. *Tribol. Lett.* 2004, 17, 469-489.
- (8) Sharma, V.; Erdemir, A.; Aswath, P. B. An Analytical Study of Tribofilms Generated by the Interaction of Ashless Antiwear Additives with ZDDP using XANES and Nano-Indentation. *Tribol. Int.* 2015, 82, 43-57.
- (9) Zhou, Y.; Qu, J. Ionic Liquids as Lubricant Additives: A Review. *ACS Appl. Mater. Interfaces* 2017, 9, 3209-3222.
- (10) Mosey, N.; Woo, T.; Kasrai, M.; Norton, P.; Bancroft, G.; Muser, M. Interpretation of Experiments on ZDDP Anti-Wear Films through Pressure-Induced Cross-Linking. *Tribol. Lett.* 2006, 24, 105-114.

- (11) Mosey, N.; Muser, M.; Woo, T. Molecular Mechanisms of Anti-Wear Pad Formation and Functionality of Lubricant Additives. *Science* 2005, 307, 1612-1612-1615.
- (12) Barnes, A. M.; Bartle, K. D.; Thibon, V. R. A. A Review of Zinc Dialkyldithiophosphates (ZDDPS): Characterisation and Role in the Lubricating Oil. *Tribol. Int.* 2001, 34, 389-395.
- (13) Somayaji, A.; Aswath, P. B. Antiwear Behavior of ZDDP and Fluorinated ZDDP in the Presence of Alkylated Diphenyl Amine Antioxidants. *Tribol. Trans.* 2008, 51, 4, 403-412.
- (14) Spedding, H.; Watkins, R. C. Antiwear Mechanisms of ZDDP's - 1. *Tribol. Int.* 1982, 15, 9-12.
- (15) Watkins, R. C. The Antiwear Mechanism of Zddp's. Part II. *Tribol. Int.* 1982, 15, 13-15.
- (16) Mourhatch, R.; Aswath, P. B. Tribological Behavior and Nature of Tribofilms Generated from Fluorinated ZDDP in Comparison to ZDDP Under Extreme Pressure Conditions---Part 1: Structure and Chemistry of Tribofilms. *Tribol. Int.* 2011, 44, 187-200.
- (17) Mourhatch, R.; Aswath, P. B. Nanoscale Properties of Tribofilms Formed with Zinc Dialkyl Dithiophosphate (ZDDP) Under Extreme Pressure Condition. *J. Nanosci. Nanotechnol.* 2009, 9, 2682-2691.
- (18) Martin, J. M.; Onodera, T.; Minfray, C.; Dassenoy, F.; Miyamoto, A. The Origin of Anti-Wear Chemistry of ZDDP. *Faraday Discuss.* 2012, 156, 311-323.
- (19) Buwono, H. P.; Minami, S.; Uemura, K.; Machida, M. Surface Properties of Rh/AlPO₄ Catalyst Providing High Resistance to Sulfur and Phosphorus Poisoning. *Ind. Eng. Chem. Res.* 2015, 54, 7233-7240.
- (20) Forzatti, P.; Lietti, L. Catalyst Deactivation. *Catal. Today* 1999, 52, 165-181.
- (21) Williamson, W. B.; Perry, J.; Gandhi, H. S.; Bomback, J. L. Effects of Oil Phosphorus on Deactivation of Monolithic Three-Way Catalysts. *Appl. Catal.* 1985, 15, 277-292.

- (22) Willermet, P. A.; Carter, R. O.; Schmitz, P. J.; Everson, M.; Scholl, D. J.; Weber, W. H. Formation, Structure, and Properties of Lubricant-Derived Antiwear Films. *Lubr. Sci.* 1997; 1997, 9, 325-348.
- (23) Sharma, V.; Doerr, N.; Aswath, P. Chemical-Mechanical Properties of Tribofilms and its Relation to Ionic Liquid Chemistry. *RSC Adv.* 2016, 6, 22341-22356.
- (24) Gosvami, N. N.; Bares, J. A.; Mangolini, F.; Konicek, A. R.; Yablon, D. G.; Carpick, R. W. Tribology. Mechanisms of Antiwear Tribofilm Growth Revealed in Situ by Single-Asperity Sliding Contacts. *Science* 2015, 348, 102-106.
- (25) Chen, X.; Elsenbaumer, R. L.; Aswath, P. B. Synthesis and Tribological Behavior of Ashless Alkylphosphorofluoridothioates. *Tribol. Int.* 2013, 69, 114-124.
- (26) Kim, B. H.; Jiang, J.; Aswath, P. B. Mechanism of Wear at Extreme Loads and Boundary Conditions with Ashless Anti-Wear Additives: Analysis of Wear Surfaces and Wear Debris. *Wear* 2011, 270, 181-194.
- (27) Najman, M. N.; Kasrai, M.; Bancroft, G. M. Chemistry of Anti-Wear Films from Ashless Thiophosphate Oil Additives. *Tribol. Lett.* 2004, 17(2), 217-229.
- (28) Mourhatch, R.; Aswath, P. B. Tribological Behavior and Nature of Tribofilms Generated from Fluorinated ZDDP in Comparison to ZDDP Under Extreme Pressure conditions—Part II: Morphology and Nanoscale Properties of Tribofilms. *Tribol. Int.* 2011, 44, 201-210.
- (29) Joly-Pottuz, L.; Dassenoy, F.; Belin, M.; Vacher, B.; Martin, J. M.; Fleischer, N. Ultralow-Friction and Wear Properties of IF-WS₂ Under Boundary Lubrication. *Tribol. Lett.* 2005, 18, 477-485.
- (30) Padgurskas, J.; Rukuiza, R.; Prosycevas, I.; Kreivaitis, R. Tribological Properties of Lubricant Additives of Fe, Cu and Co Nanoparticles. *Tribol. Int.* 2013, 60, 224-232.

- (31) Wu, Y. Y.; Tsui, W. C.; Liu, T. C. Experimental Analysis of Tribological Properties of Lubricating Oils with Nanoparticle Additives. *Wear* 2007, 262, 819-825.
- (32) Bakunin, V. N.; Suslov, A. Y.; Kuzmina, G. N.; Parenago, O. P.; Topchiev, A. V. Synthesis and Application of Inorganic Nanoparticles as Lubricant Components-a Review. *J. Nanopart. Res.* 2004, 6, 273-284.
- (33) Erdemir, A. Boron-Based Solid Nanolubricants and Lubrication Additives; In *Nanolubricants*; Wiley: New York, 2008; p 203-223.
- (34) Greco, A.; Mistry, K.; Sista, V.; Eryilmaz, O.; Erdemir, A. Friction and Wear Behaviour of Boron Based Surface Treatment and Nano-Particle Lubricant Additives for Wind Turbine Gearbox Applications. *Wear* 2011, 271, 1754-1760.
- (35) Kimura, Y.; Wakabayashi, T.; Okada, K.; Wada, T.; Nishikawa, H. Boron Nitride as a Lubricant Additive. *Wear* 1999, 232, 199-206.
- (36) Sharma, V.; Gabler, C.; Doerr, N.; Aswath, P. B. Mechanism of Tribofilm Formation with P and S Containing Ionic Liquids. *Tribol. Int.* 2015, 92, 353-364.
- (37) Otero, I.; Lopez, E. R.; Reichelt, M.; Villanueva, M.; Salgado, J.; Fernandez, J. Ionic Liquids Based on Phosphonium Cations as Neat Lubricants Or Lubricant Additives for a Steel/Steel Contact. *ACS Appl. Mater. Interfaces* 2014, 6, 13115-13128.
- (38) Ilie, F.; Covaliu, C. Tribological Properties of the Lubricant Containing Titanium Dioxide Nanoparticles as an Additive. *Lubricants* 2016, 4, 2.
- (39) Laad, M.; Jatti, V. K. S. Titanium Oxide Nanoparticles as Additives in Engine Oil. *J. King Saud Univ., Eng. Sci.* 2016, DOI: <http://dx.doi.org/10.1016/j.jksues.2016.01.008>.

- (40) Rosentsveig, R.; Gorodnev, A.; Feuerstein, N.; Friedman, H.; Zak, A.; Fleischer, N.; Tannous, J.; Dassenoy, F.; Tenne, R. Fullerene-Like MoS₂ Nanoparticles and their Tribological Behavior. *Tribol. Lett.* 2009, 36, 175-182.
- (41) Tannous, J.; Dassenoy, F.; Lahouij, I.; Le Mogne, T.; Vacher, B.; Bruhács, A.; Tremel, W. Understanding the Tribochemical Mechanisms of IF-MoS₂ Nanoparticles Under Boundary Lubrication. *Tribol. Lett.* 2011, 41, 55-64.
- (42) Li, X.; Cao, Z.; Zhang, Z.; Dang, H. Surface-Modification in Situ of Nano-SiO₂ and its Structure and Tribological Properties. *Appl. Surf. Sci.* 2006, 252, 7856-7861.
- (43) Jiao, D.; Zheng, S.; Wang, Y.; Guan, R.; Cao, B. The Tribology Properties of alumina/silica Composite Nanoparticles as Lubricant Additives. *Appl. Surf. Sci.* 2011, 257, 5720-5725.
- (44) Luo, T.; Wei, X.; Zhao, H.; Cai, G.; Zheng, X. Tribology Properties of Al₂O₃/TiO₂ Nanocomposites as Lubricant Additives. *Ceram. Int.* 2014, 40, 10103-10109.
- (45) Tao, X.; Jiazheng, Z.; Kang, X. The Ball-Bearing Effect of Diamond Nanoparticles as an Oil Additive. *J. Phys. D: Appl. Phys. D* 1996, 29, 2932.
- (46) Zhang, L.; Pu, J.; Wang, L.; Xue, Q. Synergistic Effect of Hybrid Carbon Nanotube-Graphene Oxide as Nanoadditive Enhancing the Frictional Properties of Ionic Liquids in High Vacuum. *ACS Appl. Mater. Interfaces* 2015, 7, 8592-8600.
- (47) Eswaraiyah, V.; Sankaranarayanan, V.; Ramaprabhu, S. Graphene-Based Engine Oil Nanofluids for Tribological Applications. *ACS Appl. Mater. Interfaces* 2011, 3, 4221-4227.
- (48) Kumar Dubey, M.; Bijwe, J.; Ramakumar, S. S. V. PTFE Based Nano-Lubricants. *Wear* 2013, 306, 80-88.
- (49) Dubey, M. K.; Bijwe, J.; Ramakumar, S. S. V. Nano-PTFE: New Entrant as a very Promising EP Additive. *Tribol. Int.* 2015, 87, 121-131.

- (50) Rico, E. F.; Minondo, I.; Cuervo, D. G. The Effectiveness of PTFE Nanoparticle Powder as an EP Additive to Mineral Base Oils. *Wear* 2007, 262, 1399-1406.
- (51) Wilson, B. Slick 50 – a Proven PTFE-based Boundary Lubricant for Engines. *Ind. Lubr. Tribol.* 1995, 47, 6-8.
- (52) Sunqing, Q.; Junxiu, D.; Guoxu, C. A Review of Ultrafine Particles as Antiwear Additives and Friction Modifiers in Lubricating Oils. *Lubr. Sci.* 1999, 11, 217-226.
- (53) Nehme, G. Interactions of Fluorinated Catalyst and Polytetrafluoroethylene in Two Different Plain Zinc Dialkyldithiophosphate Oils and One Fully Formulated Oil using Design of Experiment. *Lubr. Sci.* 2011, 23, 181-201.
- (54) Yasuda, H. K. Some Important Aspects of Plasma Polymerization. *Plasma Processes Polym.* 2005, 2, 293-304.
- (55) Beck, A. J.; Jones, F. R.; Short, R. D. Plasma Copolymerization as a Route to the Fabrication of New Surfaces with Controlled Amounts of Specific Chemical Functionality. *Polymer* 1996, 37, 5537-5539.
- (56) Yasuda, H.; Hsu, T. Some Aspects of Plasma Polymerization Investigated by Pulsed R.F. Discharge. *J. Polym. Sci., Polym. Chem. Ed.* 1977, 15, 81-97.
- (57) Rinsch, C. L.; Chen, X.; Panchalingam, V.; Eberhart, R. C.; Wang, J.; Timmons, R. B. Pulsed Radio Frequency Plasma Polymerization of Allyl Alcohol: Controlled Deposition of Surface Hydroxyl Groups. *Langmuir* 1996, 12, 2995-3002.
- (58) Aldana, P. U.; Vacher, B.; Le Mogne, T.; Belin, M.; Thiebaut, B.; Dassenoy, F. Action Mechanism of WS₂ Nanoparticles with ZDDP Additive in Boundary Lubrication Regime. *Tribol. Lett.* 2014, 56, 249-258.

- (59) Jenei, I. Z.; Svahn, F.; Csillag, S. Correlation Studies of WS₂ Fullerene-Like Nanoparticles Enhanced Tribofilms: A Scanning Electron Microscopy Analysis. *Tribol. Lett.* 2013, 51, 461-468.
- (60) Qu, J.; Barnhill, W. C.; Luo, H.; Meyer, H. M.; Leonard, D. N.; Landauer, A. K.; Kheireddin, B.; Gao, H.; Papke, B. L.; Dai, S. Synergistic Effects between Phosphonium-Alkylphosphate Ionic Liquids and Zinc Dialkyldithiophosphate (ZDDP) as Lubricant Additives. *Adv. Mater.*, 27: 4767–4774
- (61) Sharma, V.; Dorr, N.; Erdemir, A.; Aswath, P. Interaction of Phosphonium Ionic Liquids with Borate Esters at Tribological Interfaces. *RSC Adv.* 2016, 6, 53148-53161.
- (62) Meisel, A.; Leonhardt, G.; Szargan, R.; Källne, E. X-Ray Spectra and Chemical Binding; Springer: Verlag Berlin Heidelberg, 1989.
- (63) Bianconi, A.; Koningsberger, D.; Prins, R. X-Ray Absorption: Principles, Applications, Techniques of EXAFS, SEXAFS and XANES. In XANES Spectroscopy; Wiley: New York, 1988.
- (64) Najman, M. N.; Kasrai, M.; Bancroft, G. X-Ray Absorption Spectroscopy and Atomic Force Microscopy of Films Generated from Organosulfur Extreme-Pressure (EP) Oil Additives. *Tribol. Lett.* 2003, 14(4), 225-235.
- (65) Bakunin, V. N.; Kasrai, M.; Kuzmina, G. N.; Bancroft, G. M.; Parenago, O. P. Influence of Temperature and ZDDP Concentration on Tribochemistry of Surface-Capped Molybdenum Sulfide Nanoparticles Studied by XANES Spectroscopy. *Tribol. Lett.* 2007, 26, 33-43.
- (66) Harp, G.; Han, Z.; Tonner, B. X-ray Absorption Near Edge Structures of Intermediate Oxidation States of Silicon in Silicon Oxides during Thermal Desorption. *J. Vac. Sci. Technol., A* 1990, 8, 2566-2569.

- (67) Li, D.; Bancroft, G. M.; Kasrai, M.; Fleet, M. E.; Feng, X. H.; Tan, K. H. High-Resolution Si and P K- and L-Edge XANES Spectra of Crystalline SiP₂O₇ and Amorphous SiO₂-P₂O₅. *Am. Mineral.* 1994, 79, 785-788.
- (68) Najman, M. N.; Kasrai, M.; Bancroft, G. M.; Frazer, B. H.; DeStatio, G. The Correlation of Microchemical Properties to Antiwear (AW) Performance in Ashless Thiophosphate Oil Additives. *Tribol. Lett.* 2004, 17(4), 811-822.
- (69) Li, Y.; Pereira, G.; Kasrai, M.; Norton, P. R. Studies on ZDDP Anti-Wear Films Formed Under Different Conditions by XANES Spectroscopy, Atomic Force Microscopy and ³¹P NMR. *Tribol. Lett.* 2007, 28, 319-328.
- (70) Kim, B.; Sharma, V.; Aswath, P. B. Chemical and Mechanistic Interpretation of Thermal Films Formed by Dithiophosphates using XANES. *Tribol. Int.* 2017, 114, 15-26.

CHAPTER 3

TRIBOLOGICAL INTERACTION OF PLASMA FUNCTIONALIZED POLYTETRAFLUOROETHYLENE NANOPARTICLES WITH ZDDP AND IONIC LIQUIDS

Vinay Sharma, Jens Johansson, Richard Timmons, Braham Prakash and Pranesh B. Aswath

Abstract

Plasma functionalized polytetrafluoroethylene (PTFE) nanoparticles were employed to investigate their tribological interactions with zinc dialkyldithiophosphate (ZDDP) and ionic liquids (IL), as measured under boundary lubrication conditions. PTFE nanoparticles were coated with consecutive plasma deposited siliceous and methacrylate coatings to deliver chemistries at the rubbing interfaces. Separately, secondary ZDDP, phosphonium cation and phosphate anion IL and IL with dithiophosphate anion were mixed with the functionalized nanoparticles and evaluated for their compatibility and performance using a tribometer with cylinder on flat test configuration. Detailed comparative studies were carried out for seven separate formulations including base oil, oils with only additives, and oils with additives and functionalized PTFE particles. Results from these tests clearly reveal strong synergistic interactions of ZDDP and ILs with functionalized nanoparticles that provide favourable enhanced friction and wear performance. Comprehensive chemical analysis of the tribofilms were done using X-ray photoelectron spectroscopy (XPS) and X-ray absorption near edge structure spectroscopy (XANES). The data from these surface analyses reveal that functionalized PTFE nanoparticles collaborate synergistically with ZDDP and ILs to form silicon and fluorine doped tribofilms at the interactive surface, thus providing superior tribological performance compared to samples without nanoparticles.

Keywords: Additives, Thin Film, Synergism, XPS, XANES

1. Introduction

Engine oils play an important role in improving the longevity of mechanical parts of the engine, as well minimizing energy losses from mechanical friction. In order to develop an engine oil that can minimize both friction and wear, carrier base oils are typically blended with an additive package, one which usually represents about 10wt% of the final blend. These additives consist of a complex mix of different chemicals including antiwear compounds, friction modifiers, detergents, antioxidants, corrosion inhibitors, dispersants etc. [1-3] In view of the recent findings of negative environmental effects of such additives, an engine oil must satisfy guidelines provided by different regulatory bodies, such as the ILSAC (International Lubricants Standardization and Approval Committee for gasoline fueled vehicles).

These constantly updated regulations and guidelines have strongly promoted research in the oil lubrication industry to develop novel, more environmentally friendly additives, having similar or better tribological performance than the existing additives, including the currently widely employed zinc dialkyldithiophosphate (ZDDP). [2,4,5] ZDDP is one of the most studied and best performing antiwear additives for engine oils and has dominated the oil industry for more than sixty years. [6-9] Nevertheless, due to some of its undesirable and detrimental effects on the catalytic convertor, several research groups have focused on development of low phosphorus and metal free additives. [10-12] For example, the numerous candidate replacements of potential effective alternatives to ZDDP include ashless additives, ionic liquids, borate esters, inorganic nanomaterials, carbon derived nanostructures like carbon nanotubes and graphene. . [13-27] However, each of these potential additives also involve challenges, which need to be resolved, if they are to be ultimately used in lubricant oils. For example, ILs, being highly polar in nature involve solubility issues when mixed with generally used non-polar base oils. Similarly,

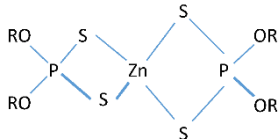
nanomaterials when used as such, pose issues such as agglomeration and poor dispersion in oils. Therefore, additional surface modification for nanomaterials is an essential and key step to make uniform and long standing oil formulations. [28-31] Other interesting alternate approaches to potential improved oil formulations involve use of mixtures of additives such as ionic liquids, nanoparticles etc., including their use in conjunction with ZDDP to deliver desired tribological properties. [19,32-37] Indeed, recent publications support the potential of such additive mixtures to provide enhanced friction and wear behavior. [38,39]

The present study is a significant extension of previously reported work involving development of plasma surface functionalized polytetrafluoroethylene (PTFE) nanoparticles for use as lubricant additive in oils. [40] In this prior study, it was clearly demonstrated that mineral base stock, containing plasma functionalized PTFE nanoparticles (coated with siliceous and methacrylate chemistry at 0.33wt%) and ZDDP at 350 ppm phosphorus treat rate, provided favorable synergistic interaction when studied under boundary lubrication conditions. Remarkable reductions in both coefficient of friction and wear volume loss values were observed. In the present work, tribological interaction of functionalized PTFE nanoparticles and two different ionic liquids, containing the phosphonium cation, were investigated. The experiments were conducted in an oil bath containing a mix of IL and coated nanoparticles. Friction and wear results obtained were compared with outcomes for base oil, oil with ZDDP and oil with ZDDP and nanoparticles. Extensive surface analytical studies, concentrating on the chemistry of the tribofilms formed, were carried using X-ray photoelectron spectroscopy (XPS) and X-ray absorption near edge structure spectroscopy (XANES). The results obtained provide valuable insights into the chemical make-up of the tribofilms formed.

2. Experimental

Polyfluortetraethylene (PTFE, $(CF_2CF_2)_n$) nanoparticles (MP1150; 200 nm), were purchased from the Dupont Corporation. Hexamethyldisiloxane (HMDSO, $(CH_3)_3SiOSi(CH_3)_3$) and glycidyl methacrylate ($C_7H_{10}O_3$) were procured from Sigma-Aldrich. Zinc dialkyldithiophosphate (ZDDP) was supplied by Oronite and the two ionic liquids, trihexyltetradecylphosphonium bis (2-ethylhexyl) phosphate and tetrabutylphosphonium O,O-diethyl-phosphoro-dithionate were provided by AC2T Research GmbH Austria. The functionalized PTFE nanoparticles were prepared using a home-built 360° rotating plasma reactor. This plasma deposition technique was employed to deposit thin polymeric films on the PTFE core nanoparticles. Two consecutive deposition processes were employed. Initially, a siliceous film was deposited from polymerization of the HMDSO monomer. This was followed by deposition of the second coating, produced from polymerization of glycidyl methacrylate monomer. This second coating was employed to help disperse the nanoparticles in the relatively non-polar lubricant oil. Additional details on the plasma polymerization set-up and processes used are described in a previous article. [40] The surface modified PTFE nanoparticles are referenced simply as PHGM in this report. Chemical structures of the other additives used in this study, namely the ZDDP and ionic liquids, are shown in table 1.

Table 1. Chemical structures of the additives used for the study.

Materials	Chemical Structures
Zinc dialkyl dithiophosphate (ZDDP)	

Trihexyltetradecylphosphonium bis (2-ethylhexyl) phosphate	
Tetrabutylphosphonium O,O-diethyl-phosphoro-dithionate	

All blends employed in the tribological evaluations of these additives were prepared using group III mineral oil, obtained from GS Caltex (Kixx Lubo 4 cSt). The phosphorus treat rate for all the additives was kept at 350 ppm. Table 2 shows the chemical composition details regarding the various formulations employed in this study, along with the code names adopted to identify each of these formulations throughout this manuscript.

Table 2. Details of the seven formulations used in this study.

S. No.	Formulation	Coded Name
I.	Base oil (group III base stock)	BO
II.	BO + ZDDP	ZD
III.	BO + ZDDP + 0.33 wt% Plasma Functionalized PTFE	ZD + PHGM
IV.	BO + Trihexyltetradecylphosphonium bis (2-ethylhexyl) phosphate	IL1
V.	BO + Trihexyltetradecylphosphonium bis (2-ethylhexyl) phosphate + 0.33 wt% Plasma Functionalized PTFE	IL1 + PHGM
VI.	BO + Tetrabutylphosphonium O,O-diethyl-phosphoro-dithionate	IL2
VII.	BO + + 0.33 wt% Plasma Functionalized PTFE	IL2 + PHGM

Tribological studies were carried out at the Luleå University of Technology, Sweden, using a reciprocating Cameron-Plint tribometer in a cylinder on flat test configuration. The steel flat was clamped in a temperature controlled oil bath, while the cylinder specimen was fastened to the reciprocating arm. The steel flats were 12 x 12 mm with a thickness of 1.7 mm, composed of hardened AISI 52100 steel and ground to a surface roughness of 40 nm Ra with a unidirectional lay. The pins (4 x 6 mm) used for the tests were AISI 52100 steel pins, as procured from RBC bearings. Prior to testing, the oil samples containing nanoparticles were sonicated for one hour to ensure a uniform dispersion of nanoparticles. Once finished, 2 ml of this blend was quickly put in the oil bath. Tests were run at a constant normal load of 82 N which resulted in a Hertzian contact pressure of approximately 500 MPa. In order to achieve boundary lubrication regime, the reciprocation speed was kept at 5 Hz with 5 mm stroke length. All the tests were run at 100⁰ C, for a duration of 1 hour. After completion of the test, the flat and cylinder samples were cleaned in an ultrasonic bath with heptane, after which they were rinsed in ethanol and dried in air. These samples were later preserved for surface characterization by submerging them into synthetic oil. Optical microscopy (Olympus STM6) was used to measure wear scar width on the test pins and to further calculate the wear volume losses. Wear surfaces generated on the steel flats from oils with additives were subjected to extensive surface characterization. For topographical information, worn surfaces were inspected by Hysitron TriboscopeTM in scanning probe microscopy (SPM) imaging mode XPS (Kratos Axis Ultra; monochromatic Al K_α X-ray source; power-150 W; spot size-300 μm x 700 μm) and XANES analyses were employed to provide a thorough chemical characterization of the tribofilms formed on the flat specimens. The XANES experiments were carried out at the Canadian Light Source in Saskatoon, Canada. A variable line spacing plane grating monochromator (VLS-PGM) beamline was used to obtain phosphorus L-edge analyses. A

soft X-ray microcharacterization beamline (SXRMB) was employed to identify the presence and coordination of silicon atoms (Si K-edge) in the tribofilms. Typical operating parameters for VLS-PGM and SXRMB beamline are shown in Table 3.

Table 3. Operating parameters for VLS-PGM and SXRMB beamlines.

Parameters	VLS-PGM	SXRMB
Energy range	5.5-250 eV	1.7 keV to 10 keV
Resolution	> 10,000 E/ Δ E	$\sim 3.3 \times 10^{-4}$ E/ Δ E
Beam Spot Size	100 μ m x 100 μ m	1 mm x 4 mm

3. Results

3.1 Friction and Wear Behavior: Figure 1 shows the coefficient of friction measurements obtained as a function of testing time for the seven oil formulations employed. As expected, the friction profile for sample with just base oil looks very unstable, exhibiting the highest values for coefficient of friction (CoF). In addition, the sample with only ZDDP (ZD) exhibits virtually similar friction behavior as base oil during the initial and final phase of the test, exhibiting COF values which are virtually the same as that of the base oil at the end of the test. In contrast, samples containing the other additives (i.e. PHGM and the ILs) all exhibited substantially lower COF values. For example, sample ZD + PHGM produced up to 25% reduction in coefficient of friction values compared to samples with only ZD and base oil. Similar friction benefits were reported for formulations containing ZDDP and plasma functionalized PTFE nanoparticles in our previous work where the tests were conducted with only 2-3 drops of formulation instead of using an oil bath as used in this study. [40] The samples containing just ionic liquids (IL1 and IL2) exhibit superior friction behavior compared to samples with only ZD and base oil. Among the two ionic

liquids, IL2 performs better than IL1. The friction outcome for sample with IL1 + PHGM nanoparticles is almost similar to that of IL1 alone and there is no substantial reduction in friction. However, sample IL2 + PHGM, clearly stands out as the best formulation in this study with respect to reduced coefficient of friction values. As shown in Figure 1, the presence of plasma functionalized PTFE nanoparticles with IL2 produced an approximate 18% reduction in CoF values when compared to IL2 alone, and almost 40% when compared to base oil and ZDDP only samples.

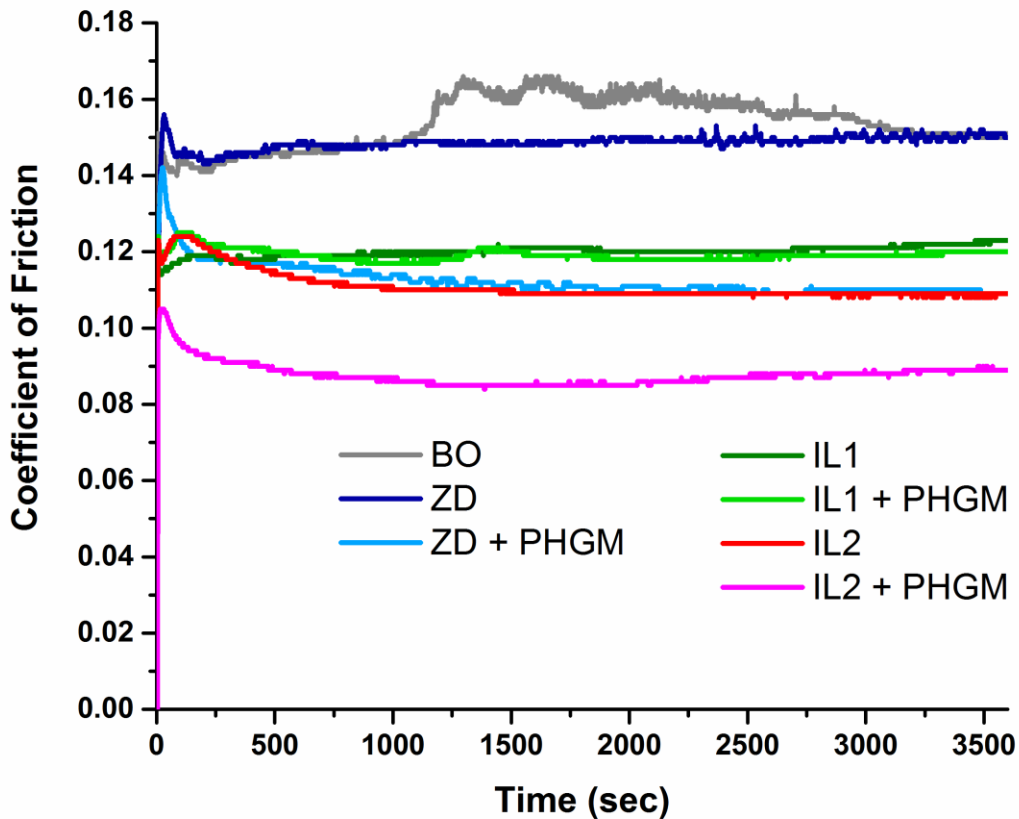


Figure 1. Coefficient of friction (CoF) as a function of time for the seven formulations: BO, ZD, ZD + PHGM, IL1, IL1 + PHGM, IL2 and IL2 + PHGM.

Figure 2 shows wear volume losses for pins from the seven different oil formulations examined. Optical microscopy was used to measure wear scar width, which was then subsequently employed to determine the wear volume loss, on the pin. Samples with just base oil (BO) gave the worst wear outcome. Additionally, and perhaps not too surprising, high wear volume loss was observed for the sample with only ZDDP (ZD) since the amount of phosphorus (350 ppm) employed was significantly lower than the 800 ppm level normally employed to provide sustainable and prolonged antiwear protective tribofilm formation. Notably, however, the sample with ZD + PHGM, exhibited the lowest wear volume among all 7 formulations tested, providing further confirmation of the synergistic tribological interaction of plasma functionalized PTFE nanoparticles with different additive chemistry, as previously reported. [19,38-40] Finally, both ionic liquids IL1 and IL2 exhibit superior antiwear performance than ZDDP at 350 ppm phosphorus treat rate. For samples with a mix of ionic liquid and functionalized PTFE nanoparticles i.e. IL1 + PHGM and IL2 + PHGM, the wear volume loss values show an additional drop of almost 25% compared to having only the IL present. Overall, the friction and wear outcomes from tribological testing of these different additive chemistries strongly advocate the utility of the plasma functionalized PTFE nanoparticles to provide synergetic benefits to lubrication oils containing ZDDP or ionic liquid additives in terms of lower friction and superior antiwear protection under boundary lubrication regime.

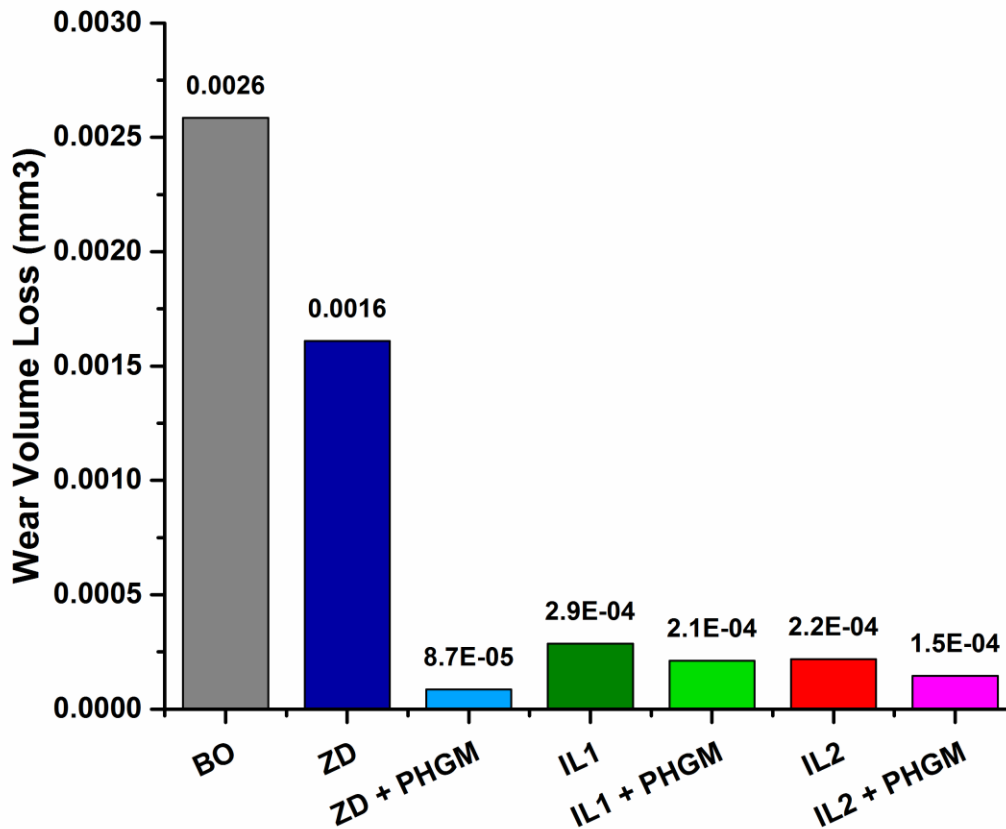


Figure 2. Wear volume losses for pins after tribological testing with BO, ZD, ZD + PHGM, IL1, IL1 + PHGM, IL2 and IL2 + PHGM.

3.2 Surface Topography: Figure 3 illustrates 3D images of the worn surfaces generated on the steel flats after tribological testing. The SPM imaging technique was employed to inspect an area of 60 x 60 μm on the wear surface to get these images. The SPM images (4: A & B) clearly show that worn surfaces for the samples with only ZDDP (ZD) and ZDDP with functionalized PTFE (ZD + PHGM) appear as typical ZDDP tribofilms but, nevertheless, several distinctive features are observable in contrasting these two surfaces. [41] The highlighted differences between the two images are the heights and lateral widths of the tribofilm patches. Sample ZD has small patches at

the surface, whereas ZD + PHGM has deep valleys suggesting thicker patches which are significantly bigger than ones on other sample. In addition, the tribofilm patches at the surface for sample with ZD + PHGM are more in number than the other. In the case of samples containing the ionic liquid additives, the wear surfaces with and without PHGM nanoparticles (4: C, D, E & F) look alike. This similarity, in the surface profiles of tribofilms from ionic liquids with and without functionalized particles, suggests that the friction and wear benefits could be the reflection of differences in chemical/mechanical properties of the tribofilms and these differences do not induce any drastic change in their physical architecture like we see in case of ZDDP with PHGM nanoparticles.

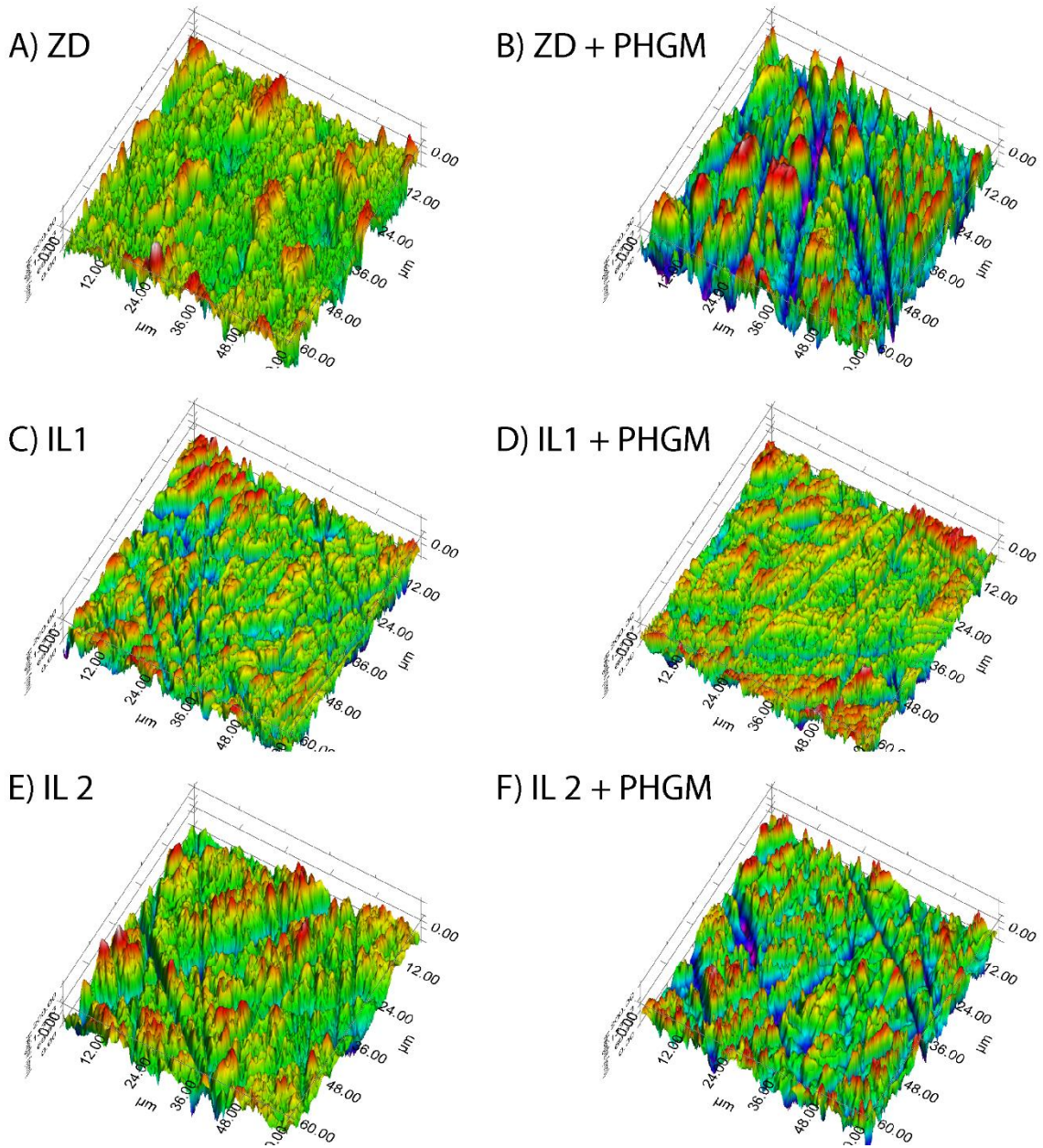


Figure 3. 3D SPM images of wear surfaces on flat specimens generated from BO, ZD, ZD + PHGM, IL1, IL1 + PHGM, IL2 and IL2 + PHGM.

3.3 Tribochemical Analysis: A thorough surface analysis was done for the tribofilms generated with different additive chemistries. XPS and XANES techniques were employed to find the chemical constituents of the tribofilms in an attempt to elucidate the role of different chemical species as contributors to the observed friction and anti-wear benefits.

3.3.1 XPS Characterization:

Figure 4 shows phosphorus, iron, oxygen and fluorine XPS spectra acquired from tribofilms on flat specimens from the different oil formulations. These spectra are useful in providing insights into the tribological properties and resulting lubrication mechanism of the additives used in this study. All the samples were initially subjected to plasma sputter cleaning for 10 minutes (beam energy-4.20 eV) and subsequently spectra were recorded.

Phosphorus (P) 2p

The plots in figure 4a reveal a strong presence of phosphorus in the tribofilms of all the samples employed. However, there are some notable evident shifts in the peak positions within these samples indicative of the chemical state of the phosphorus atom in the tribofilm. The plot for sample ZD has a strong signal at ~134.3 eV (peak **a**) which is attributed to the presence of zinc bound phosphates at the surface. For the sample with ZD + PHGM, it was observed that both zinc phosphates and long chain phosphates contribute to the overall phosphorus signal. [42,43] These findings are consistent with the information from SPM images where the sample with ZD + PHGM particles showed bigger patches of tribofilm at the surface. The spectra from samples with ionic liquids, with and without PHGM nanoparticles (IL1, IL1 + PHGM, IL2, IL2 + PHGM), are all similar in phosphorus intensity and peak position at ~ 133.8 eV (peak **a'**) which are attributed to the presence of iron phosphates in these tribofilms. [44]

Iron (Fe) 2p

The XPS spectra for the samples in figure 4b provides with some explicit information concerning the presence of iron atoms in the chemical make-up of the tribofilms and, at the same time, reveals some interesting secondary information regarding thickness of these tribofilms. There are two main peaks in these spectra. The first one, peak **a**, at ~706.7 eV, is attributed to metallic iron in the steel and the second peak **b**, at ~710.6 eV, is from iron oxides. [43,45] Since all the samples were subjected to plasma sputtering for same time period (10 min at beam energy 4.20 keV), the signal from metallic iron from steel (~ 706.7 eV) can be correlated to tribofilm thickness. [45] It is evident from figure 5b that the samples with ZD and ZD + PHGM have relatively similar thickness and as, as shown in figure 5a, the tribofilms are mostly composed of zinc phosphate and the contribution from iron oxide is very low, hence the weak signal. The plot for IL1 shows a more intense signal for metallic iron which suggests that the tribofilm formed was not thick enough in the first place and it also shows the presence of iron oxide in the tribofilm. Interestingly, the rest of the samples, IL1 + PHGM, IL2 and IL2 + PHGM, exhibit similar spectra for iron 2p. The contribution from metallic iron is weak which indicates that these tribofilms were thick enough to withstand sputter cleaning and limit the signal from steel surface.

Fluorine (F) 1s

XPS spectra for fluorine displays crucial information regarding role of plasma functionalized PTFE nanoparticles in providing enhanced friction and wear benefits for the additives. Figure 4c represents plots for samples containing additives with nanoparticles, obtained before and after sputter cleaning of the surfaces. Sample ZD + PHGM and IL1 + PHGM show presence of carbon bound fluorine (peak **b** ~ 689 eV) in the pre-sputtered surface scans whereas they exhibit relatively weak signals at ~ 685 eV, a peak attributable to metal fluorides, in the post

sputtered surface plots. [43,46,47] However, the sample with IL2 + PHGM shows an intense signal for metal fluorides in both pre and post sputtered surface scans. The overall information suggests that for samples ZD + PHGM and IL1 + PHGM, the PTFE nanoparticles provide with material transfer films at the top of the tribofilms and in the bulk, the fluorine from PTFE gets incorporated as metal fluoride. Whereas, for IL2 + PHGM, the fluorine from PTFE nanoparticles is only incorporated as metal fluoride throughout the thickness of the glassy tribofilm. It seems reasonable to assume that incorporation of these fluorine atoms into the glassy structure is helping to contribute to the antifriction and antiwear performance for the ZDDP and ionic liquids.

Oxygen (O) 1s

Figure 4d provides valuable information concerning the relative contribution of metal oxides and metal phosphates to the chemical architecture of the tribofilms. There are two peaks in each spectra and their relative intensities give important qualitative information. Peak **a** at ~ 530.2 eV is attributed to metal oxides which in this case are mostly oxides of iron and peak **b** at ~ 531.7 eV is due non-bridging (P-O-) oxygen ions associated with phosphorus. [43,48] In addition, there is a shift towards higher binding energy (peak **c** ~ 532.2 eV) for samples with ZD and ZD + PHGM, which is due to presence of both zinc cations and bridging (P-O-P) oxygen ions. Sample ZD shows strong a signal for zinc phosphate in the tribofilm and weak iron oxide signal whereas the sample with ZD + PHGM displays contribution from three different species including zinc phosphate, polyphosphates and iron oxide. The oxygen XPS spectra for IL1, IL1 + PHGM and IL2 appear almost identical and they suggest that the dominant chemical species in the tribofilms are iron phosphates with relatively low amount of iron oxides. However, for the sample with IL2 + PHGM, it looks like that even though iron phosphates are abundant in the tribofilm, the presence of iron

oxides are also very significant. The overall information from these spectra does not reveal any substantial differences between samples with and without PHGM nanoparticles.

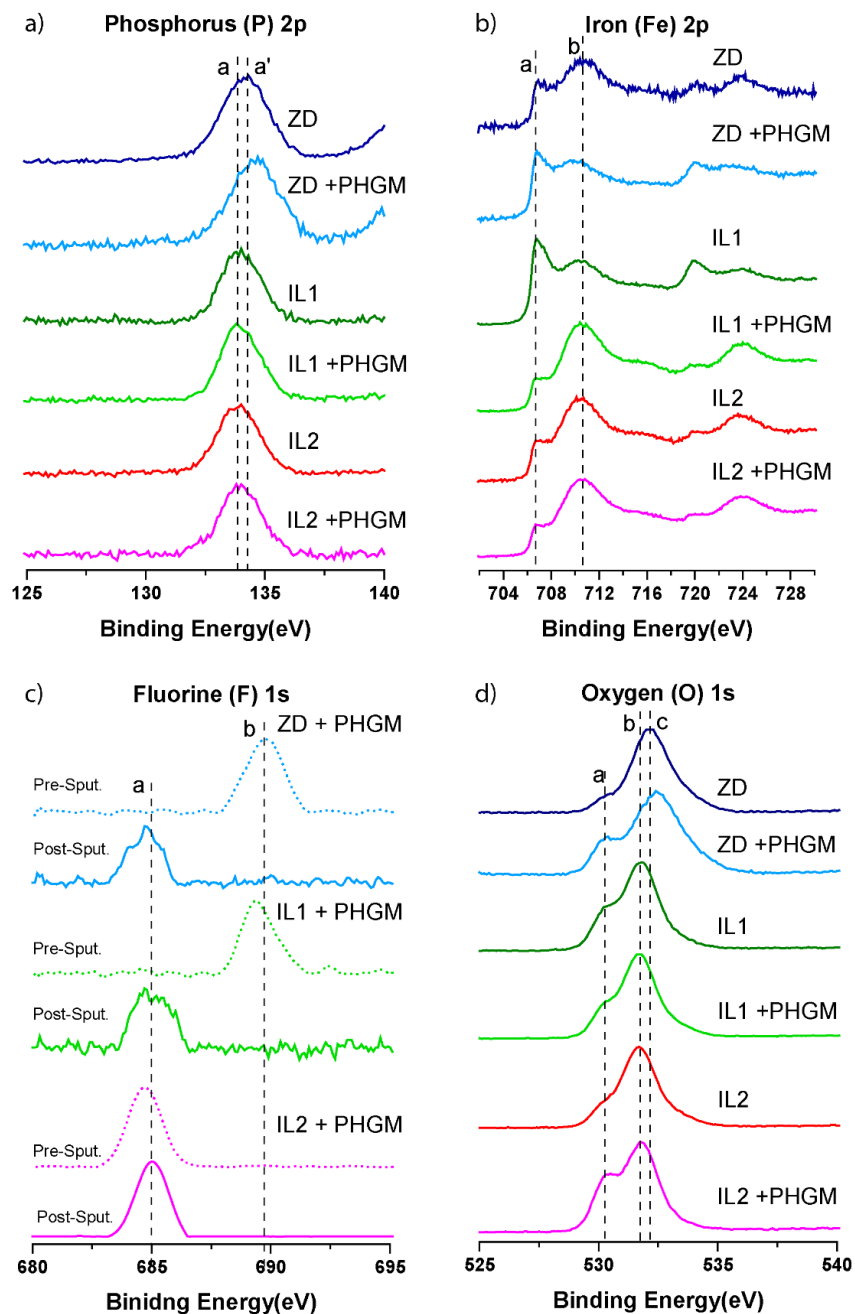


Figure 4. Phosphorus 2p, Iron 2p, Fluorine 1s and Oxygen 1s XPS spectra for ZD, ZD + PHGM, IL1, IL1 + PHGM, IL2 and IL2 + PHGM.

3.3.2 XANES Characterization: Whereas XPS spectra provide chemical information of external surfaces, X-ray absorption near edge spectroscopy provides the capability to acquire additional chemical information concerning sub-layers of the tribofilms, including important insights into the local coordination of individual elements. [9,49-51] Using the right X-ray energy and detector systems, it is possible to examine both the surface, as well as overall bulk, of the tribofilms to estimate qualitatively the distribution of different elements across the thickness of the film. The information from top 5-50 nm can be obtained using total electron yield (TEY) mode and information from the bulk can be gathered using fluorescence yield (FLY) detection mode. For this study, low energy X-ray beamline was employed to get phosphorus L-edge data in TEY mode and silicon K-edge analysis was done using high energy X-ray beamline in FLY detection mode. The collective information from XANES analyses, coupled with the XPS data, were used to provide an insight into the chemistry of the tribofilms formed from ZDDP and ionic liquids with plasma functionalized PTFE nanoparticles to help further understand the underlying lubrication mechanism.

Phosphorus L-edge

Figure 5a shows the phosphorus L-edge TEY spectra for zinc phosphate, iron phosphate, ZD + PHGM, IL1 + PHGM and IL2 + PHGM samples and this information as obtained from the top 5-15 nm of the tribofilms. Both model compounds (zinc and iron phosphate) used in this study have been extensively studied using XANES and all the peaks in the Fig 5A spectra (**a**, **b**, **c**, **c'** and **d**) have been precisely identified and reported in the literature. [50,52,53] In addition, the ratio (**a/c**) of relative intensities of peak **a** and **c** or **c'** can be used to determine the chain length of polyphosphates in the tribofilm under investigation. An a/c ratio of 0.3 to 0.4 suggests the presence of short chain phosphates; if the ratio is above 0.6 it indicates that long chain phosphates are

present. [19,54,55] In this study, the sample with ZD + PHGM has its main peak aligned with the peak position (c) of zinc phosphate model compound and has a/c ratio of 0.5. For samples IL1 + PHGM and IL2 + PHGM, the main peaks positions in the spectra are matching with iron phosphate's peak position (c') and the a/c ratios are 0.27 and 0.33 respectively. These results clearly show that phosphate species for the sample with ZDDP are bound to zinc and are medium chain polyphosphates whereas the tribofilms for samples with ionic liquids have short chain iron polyphosphates.

Silicon K-edge

Figure 5b illustrates silicon K-edge XANES spectra in FLY mode for calcium and sodium silicate model compounds and test samples with PHGM nanoparticles. The spectra for all three samples, ZD + PHGM, IL1 + PHGM and IL2 + PHGM display similar features and the signal intensities are also very low and noisy. The most prominent peak in the spectra for all four test samples match the main peak position (a) of the model compounds at ~ 1848 eV. These results are indicative of incorporation of siliceous chemistry from plasma functionalized nanoparticles into the tribofilm in some form of silicate but at a relatively low quantity. However, it is reasonable to assume that doping of tribofilms chemistry with even small amount of siliceous chemistry along with fluorine from functionalized PTFE nanoparticles is enough to provide remarkable tribological benefits. [40]

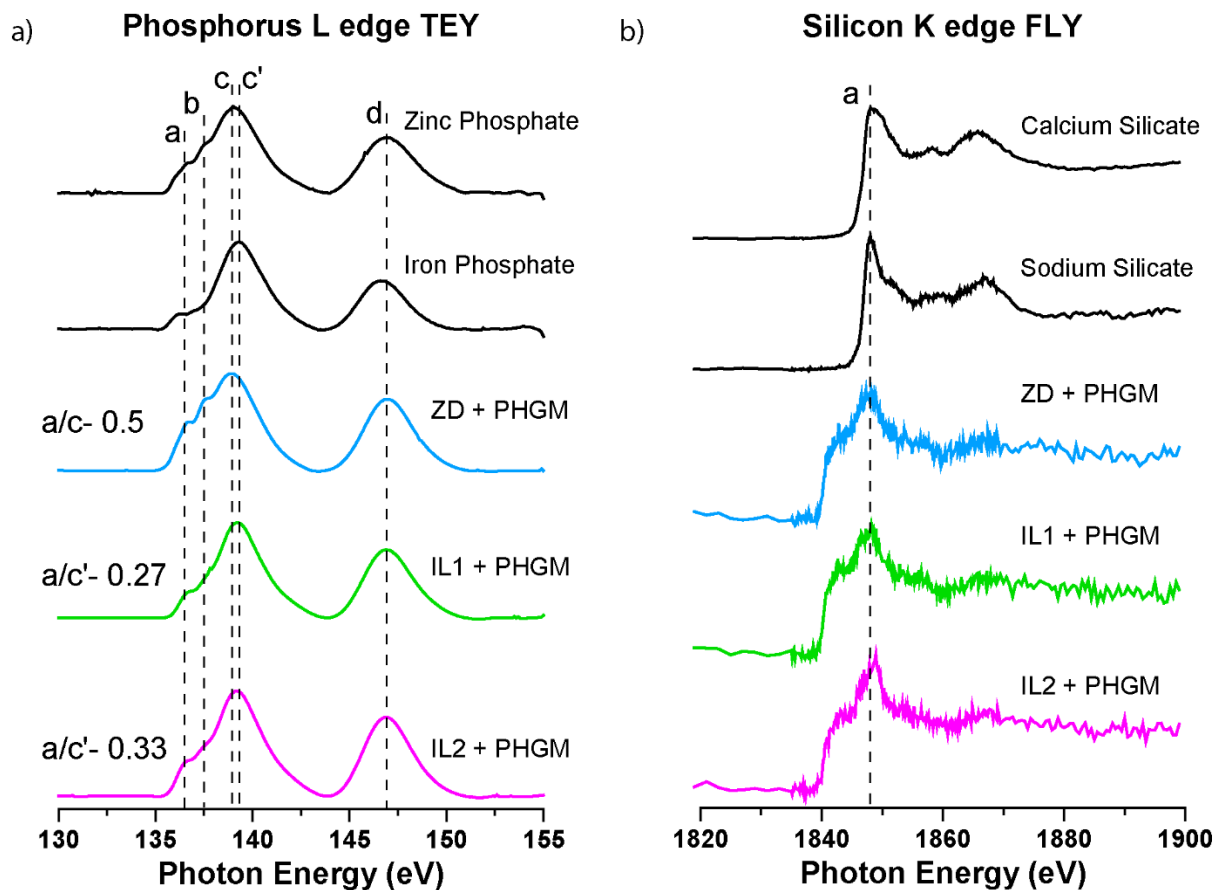


Figure 5. Phosphorus L-edge TEY and Silicon K-edge FLY XANES spectra for ZD + PHGM, IL1 + PHGM and IL2 + PHGM samples.

4. Discussion

Numerous research studies, during recent years, have investigated synergistic interaction of a wide variety of antiwear additives such as ZDDP, ashless-dithiophosphates, nanoparticles, ionic liquids, borate esters etc. when added to various lubrication oils and then subjected to rigorous tribological tests. [13-18,20-27] The overall evidence accumulated from these studies provide strong support that these additives can indeed lower friction coefficients and significantly decrease overall wear. The present work is a significant, extension of these studies in that an unusual combination of additives have been investigated. Specifically, we have included tests which involved combinations of ILs with nanoparticles, wherein the particles utilized were

molecularly surface tailored using a pulsed plasma polymerization deposition approach. Additionally the data obtained include comparison with oil formulations which contained the more traditional ZDDP additive.

As evidenced in the results section, very large scale reductions in both friction coefficients and wear were achieved with ILs and mixtures of ILs plus functionalized PTFE samples, even in the absence of added ZDDP. From the XPS and XANES data reported, it is clear that highly effective tribological films can be obtained without having to resort to ZDDP addition. As noted earlier, the elimination of ZDDP would represent a major advance in terms of environmental considerations, particularly helping to reduce unwanted engine emissions and extend the lifetimes of catalytic converters. It is also of interest to note that the tribofilms formed from ZDDP + PHGM, as well as ILs +PHGM, combinations contain polyphosphate chains as shown in Fig 5a, although these chains are somewhat shorter for the samples containing the ILs. Nevertheless, these shorter chains appear to be very effective in terms of wear outcomes. An additional, and conceivably, important finding is the presence of silicon atoms in the films, presumably contributed by the HMDSO polymeric film deposited on the PTFE particles. Finally, we note that all samples which included the functionalized PTFE nanoparticles produced films which contained some amount of fluorine atoms, the ZDDP +PHGM and IL1 + PHGM samples contained it in both organic and inorganic (metal fluoride) forms, but in the IL2 + PHGM samples, it is mostly in the form of metal fluorides. It is interesting to note that the latter sample provided the best overall outcome in terms of CoF and wear results. However, at this point in time, it is not clear why the IL2 +PHGM combination resulted in increased fluorine incorporation in the tribofilm, but may simply reflect the different chemical reactivity of this IL.

5. Conclusions

We conclude by noting that both the phosphonium cation, ionic liquids exhibited significantly better friction and wear behavior than zinc dialkyldithiophosphate at 350 ppm phosphorus treat rate. However, when used with plasma functionalized polytetrafluoroethylene (PTFE) nanoparticles, sample with tetrabutylphosphonium O, O-diethyl-phosphoro-dithionate ionic liquid (IL2 + PHGM) displayed lowest values for coefficient of friction and sample with ZDDP (ZD + PHGM) gave lowest wear volume loss. Among the two ILs, the one with both phosphorus and sulfur chemistry (IL2) performed better than the other, with and without functionalized PTFE nanoparticles. Surface analysis information from XPS and XANES experiments suggests that tribofilms from ILs are mostly composed of short chain, iron phosphates and for ZDDP samples, the chemistry is dominated by the presence of medium to long chain, zinc phosphates. Interestingly, the role of functionalized PTFE nanoparticles in forming the protective film is clearly revealed by presence of inorganic/organic fluorine and silicon chemistry in the surface films. Tribofilms from functionalized PTFE with ZDDP and IL1 contain both carbon bound and iron bound fluorine along with small amount of siliceous chemistry. Whereas, for IL2 with functionalized nanoparticles, it is observed that in the tribofilm, fluorine is present only in the form of metal fluorides along with other phosphates and silicates. All the results reported in this study establish synergistic interaction of ZDDP and ionic liquids with plasma tailored PTFE nanoparticles that provide with enhanced friction and wear properties due to incorporation of small amount of fluorine and silicon chemistry in the tribofilms.

Acknowledgments

XANES experiments were conducted at the Canadian Light Source, Saskatoon, Saskatchewan, Canada that is supported by NSERC, NRC, CIHR and the University of Saskatchewan. Tribological tests were performed at Argonne National Laboratory. X-ray Photoelectron Spectroscopy facilities provided by the Department of Chemistry is gratefully acknowledged.

References

- [1] R. Syed, A Comprehensive Review of Lubricant Chemistry, Technology, Selection, and Design, ASTM International, West Conshohocken, PA, 2009.
- [2] Barnes AM, Bartle KD, Thibon VRA. A review of zinc dialkyldithiophosphates (ZDDPS): characterization and role in the lubricating oil. Tribol. Int. 2001;34: 389-95.
- [3] Willermet PA. Some engine oil additives and their effects on antiwear film formation. Tribol Lett 1998;5:41-7.
- [4] Martin JM, Onodera T, Minfray C, Dassenoy F, Miyamoto A. The origin of anti-wear chemistry of ZDDP. Faraday Discuss 2012;156:311-23.
- [5] Barnes AM, Bartle KD, Thibon VRA. A review of zinc dialkyldithiophosphates (ZDDPS): characterisation and role in the lubricating oil. Tribol Int 2001;34:389-95.
- [6] Fujita H, Spikes HA. The formation of zinc dithiophosphate antiwear films. Proc Inst Mech Eng Part J 2004;218:265-77.
- [7] Spikes HA. The history and mechanisms of ZDDP. Tribol Lett 2004;17:469-489.
- [8] Varlot K, Kasrai M, Martin JM, Vacher B, Bancroft GM, Yamaguchi ES et al. Antiwear film formation of neutral and basic ZDDP: influence of the reaction temperature and of the concentration. Tribol Lett 2000; 01;8:9-16.

- [9] Mourhatch R, Aswath PB. Tribological behavior and nature of tribofilms generated from fluorinated ZDDP in comparison to ZDDP under extreme pressure conditions---Part 1: Structure and chemistry of tribofilms. *Tribol Int* 2011;44:187-200.
- [10] Lin YC, So H. Limitations on use of ZDDP as an antiwear additive in boundary lubrication. *Tribol Int* 2004;37:25-33.
- [11] Williamson WB, Perry J, Gandhi HS, Bomback JL. Effects of oil phosphorus on deactivation of monolithic three-way catalysts. *Applied Catalysis* 1985;15:277-92.
- [12] Angelo B, Kirchner K. The poisoning of noble metal catalysts by phosphorus compounds-chemical processes, mechanisms and changes in the catalyst. *Chemical Engineering Science* 1980;35:2089-91.
- [13] Phillips WD. Ashless phosphorous-containing lubricating oil additives. In: Rudnick LR, editor. *Lubricant Additives-Chemistry and Applications*, 2nd Edition, Chemical Industries 124, Danvers, MA, U.S.A.: CRC Press; 2009, p. 63-121.
- [14] Kim B, Sharma V, Aswath PB. Chemical and mechanistic interpretation of thermal films formed by dithiophosphates using XANES. *Tribol Int* 2017;114:15-26.
- [15] Chen X, Elsenbaumer RL, Aswath PB. Synthesis and Tribological Behavior of Ashless Alkylphosphorofluoridothioates. *Tribol Int* 2013;69:114-24.
- [16] Zhou Y, Qu J. Ionic Liquids as Lubricant Additives: A Review. *ACS Appl Mater Interfaces* 2017;9:3209-22.
- [17] González R, Bartolomé M, Blanco D, Viesca J, Fernández-González A, Battez AH. Effectiveness of phosphonium cation-based ionic liquids as lubricant additive. *Tribol Int* 2016;98:82-93.

- [18] Otero I, Lpez ER, Reichelt M, Villanueva M, Salgado J, Fernndez J. Ionic Liquids Based on Phosphonium Cations As Neat Lubricants or Lubricant Additives for a Steel/Steel Contact. ACS Appl Mater Interfaces 2014;6:13115-28.
- [19] Sharma V, Dorr N, Erdemir A, Aswath P. Interaction of phosphonium ionic liquids with borate esters at tribological interfaces. RSC Adv 2016;6:53148-61.
- [20] Shah FU, Glavatskih S, Antzutkin ON. Boron in tribology: from borates to ionic liquids. Tribology letters 2013;51:281-301.
- [21] Taher M, Shah FU, Filippov A, de Baets P, Glavatskih S, Antzutkin ON. Halogen-free pyrrolidinium bis (mandelato) borate ionic liquids: some physicochemical properties and lubrication performance as additives to polyethylene glycol. RSC Advances 2014;4:30617-23.
- [22] Shen G, Zheng Z, Wan Y, Xu X, Cao L, Yue Q et al. Synergistic lubricating effects of borate ester with heterocyclic compound. Wear 2000;246:55-8.
- [23] Nicholas G. Demas, Robert A. Erck, Cinta Lorenzo-Martin, Oyelayo O. Ajayi, and George R. Fenske. Experimental Evaluation of Oxide Nanoparticles as Friction and Wear Improvement Additives in Motor Oil. Journal of Nanomaterials 2017;Volume 2017 (2017), Article ID 8425782.
- [24] Bakunin VN, Suslov AY, Kuzmina GN, Parenago OP, Topchiev AV. Synthesis and Application of Inorganic Nanoparticles as Lubricant Components-a Review. Journal of Nanoparticle Research 2004;6:273-84.
- [25] Zhmud B, Pasalskiy B. Nanomaterials in Lubricants: An Industrial Perspective on Current Research. Lubricants 2013;1.
- [26] Gautam Anand and PS. A review on graphite and hybrid nano-materials as lubricant additives. IOP Conference Series: Materials Science and Engineering 2016;149:012201.

- [27] - Salah N, - Abdel-wahab MS, - Alshahrie A, - Alharbi ND, - Khan ZH. - Carbon nanotubes of oil fly ash as lubricant additives for different base oils and their tribology performance. - RSC Adv:- 40295.
- [28] Chen CS, Chen XH, Xu LS, Yang Z, Li WH. Modification of multi-walled carbon nanotubes with fatty acid and their tribological properties as lubricant additive. Carbon 2005;43:1660-6.
- [29] Li X, Cao Z, Zhang Z, Dang H. Surface-modification in situ of nano-SiO₂ and its structure and tribological properties. Appl Surf Sci 2006;252:7856-61.
- [30] YANG G, CHAI S, XIONG X, ZHANG S, YU L, ZHANG P. Preparation and tribological properties of surface modified Cu nanoparticles. Transactions of Nonferrous Metals Society of China 2012;22:366-72.
- [31] - Kong L, - Sun J, - Bao Y. - Preparation, characterization and tribological mechanism of nanofluids. - RSC Adv:- 12599.
- [32] Landauer AK, Barnhill WC, Qu J. Correlating mechanical properties and anti-wear performance of tribofilms formed by ionic liquids, ZDDP and their combinations. Wear 2016;354:78-82.
- [33] Qu J, Barnhill WC, Luo H, Meyer HM, Leonard DN, Landauer AK et al. Synergistic Effects Between Phosphonium-Alkylphosphate Ionic Liquids and Zinc Dialkyldithiophosphate (ZDDP) as Lubricant Additives. Adv Mater 2015.
- [34] Zhang L, Pu J, Wang L, Xue Q. Synergistic Effect of Hybrid Carbon Nanotube-Graphene Oxide as Nanoadditive Enhancing the Frictional Properties of Ionic Liquids in High Vacuum. ACS Appl Mater Interfaces 2015;7:8592-600.

- [35] Fox M, Priest M. Tribological properties of ionic liquids as lubricants and additives. Part 1: synergistic tribofilm formation between ionic liquids and tricresyl phosphate. *Proc Inst Mech Eng Part J* 2008;222:291-303.
- [36] Morina A, Neville A, Priest M, Green JH. ZDDP and MoDTC interactions and their effect on tribological performance – tribofilm characteristics and its evolution. *Tribology Letters* 2006;24:243-56.
- [37] Bakunin VN, Kasrai M, Kuzmina GN, Bancroft GM, Parenago OP. Influence of temperature and ZDDP concentration on tribochemistry of surface-capped molybdenum sulfide nanoparticles studied by XANES spectroscopy. *Tribology Letters* 2007;26:33-43.
- [38] Tomala A, Vengudusamy B, Rodr guez Ripoll M, Naveira Suarez A, Rem kar M, Rosentsveig R. Interaction Between Selected MoS₂ Nanoparticles and ZDDP Tribofilms. *Tribology Letters* 2015;59:26.
- [39] Aldana PU, Vacher B, Le Mogne T, Belin M, Thiebaut B, Dassenoy F. Action Mechanism of WS₂ Nanoparticles with ZDDP Additive in Boundary Lubrication Regime. *Tribology Letters* 2014;56:249-58.
- [40] Sharma V, Timmons R, Erdemir A, Aswath PB. Plasma-Functionalized Polytetrafluoroethylene Nanoparticles for Improved Wear in Lubricated Contact. *ACS Appl Mater Interfaces* 2017;9:25631-41.
- [41] Warren OL, Graham JF, Norton PR, Houston JE, Michalske TA. Nanomechanical properties of films derived from zinc dialkyldithiophosphate. *Tribology Letters* 1998;4:189-98.
- [42] Onyiriuka EC. Zinc phosphate glass surfaces studied by XPS. *Journal of Non-Crystalline Solids* 1993;163:268-73.

- [43] Wagner C, Muilenberg G. Handbook of X-ray photoelectron spectroscopy. : Perkin-Elmer, 1979.
- [44] Wang Y, Sherwood PMA. Iron (III) Phosphate (FePO₄) by XPS. Surface Science Spectra 2002;9:99-105.
- [45] Gonzalez Y, Lafont MC, Pebere N, Chatainier G, Roy J, Bouissou T. A corrosion inhibition study of a carbon steel in neutral chloride solutions by zinc salt/phosphonic acid association. Corrosion Science 1995;37:1823-37.
- [46] Totolin V, Minami I, Gabler C, Dörr N. Halogen-free borate ionic liquids as novel lubricants for tribological applications. Tribology International 2013;67:191-8.
- [47] Tang Y, Guan X, Wang J, Gao N, McPhail MR, Chusuei CC. Fluoride adsorption onto granular ferric hydroxide: Effects of ionic strength, pH, surface loading, and major co-existing anions. Journal of Hazardous Materials 2009;171:774-9.
- [48] Yu X, Day DE, Long GJ, Brow RK. Properties and structure of sodium-iron phosphate glasses. Journal of Non-Crystalline Solids 1997;215:21-31.
- [49] Meisel A, Leonhardt G, Szargan R, Källne E. X-ray spectra and chemical binding. : Springer, 1989.
- [50] Sharma V, Erdemir A, Aswath PB. An analytical study of tribofilms generated by the interaction of ashless antiwear additives with ZDDP using XANES and nano-indentation. Tribol Int 2015;82:43-57.
- [51] Mourhatch R, Aswath PB. Tribological behavior and nature of tribofilms generated from fluorinated ZDDP in comparison to ZDDP under extreme pressure conditions—Part II: Morphology and nanoscale properties of tribofilms. Tribol Int 2011;44:201-10.

- [52] Harp G, Han Z, Tonner B. X-ray absorption near edge structures of intermediate oxidation states of silicon in silicon oxides during thermal desorption. *Journal of Vacuum Science & Technology A* 1990;8:2566-9.
- [53] Li D, Bancroft GM, Kasrai M, Fleet ME, Feng XH, Tan KH. High-resolution Si and P K- and L-edge XANES spectra of crystalline SiP_2O_7 and amorphous $\text{SiO}_2\text{-P}_2\text{O}_5$. *Am Mineral* 1994;79:785-8.
- [54] Najman MN, Kasrai M, Bancroft GM, Frazer BH, DeStatio G. The correlation of microchemical properties to antiwear (AW) performance in ashless thiophosphate oil additives. *Tribol Lett* 2004;17(4):811-22.
- [55] Sharma V, Gabler C, Doerr N, Aswath PB. Mechanism of tribofilm formation with P and S containing ionic liquids. *Tribol Int* 2015;92:353-64.

CHAPTER 4

SYNERGISTIC EFFECTS OF PLASMA FUNCTIONALIZED TiO₂ NANOPARTICLES AND ZDDP ON FRICTION AND WEAR UNDER BOUNDARY LUBRICATION

Vinay Sharma, Richard B. Timmons, Ali Erdemir and Pranesh B. Aswath

Submitted to: ACS Applied Nano Materials (Oct., 2017)

Abstract

Interaction of zinc dialkyl dithiophosphate (ZDDP) with titanium dioxide nanoparticles and plasma functionalized TiO₂ was investigated, under boundary lubrication conditions, to evaluate tribological performance of these additives when employed in a mineral base oil. A pin on reciprocating flat test configuration was selected to determine the tribological properties of the individual additives and mixtures in the oil. Friction coefficients, wear loss and electrical contact resistance (ECR) data from seven different formulations were measured. Tribofilms generated were subjected to extensive surface analysis using X-ray photoelectron spectroscopy (XPS) and X-ray absorption near edge structure spectroscopy (XANES) to determine tribochemistry variations. Results from tribological tests, coupled with chemical characterization of the tribofilms, suggest that both ZDDP and TiO₂ nanoparticles, by themselves, form effective protective films at the rubbing surfaces. However, when used as a mix in the oil, they surprisingly behave antagonistically in terms of providing anti-wear films, resulting in severely increased wear. In contrast, TiO₂ nanoparticles coated with boron rich plasma films showed relatively better anti-wear performance than when the uncoated ones were used singularly in the oil or as a mix with ZDDP.

Keywords: Tribology, TiO₂ nanoparticles, Plasma functionalization, ZDDP

1. Introduction

In recent years, reflecting significant advances in the fields of nanomaterials and nanotechnology, there has been a dramatic increase in research involving nanoadditives to lubricants to help reduce friction and wear in a wide range of important applications. In fact, published works involving nanoparticle additives have documented significant improved anti-wear and anti-friction performances.^[1-4] Overall, the variety of nanoadditives employed can be broadly categorized as metal, metal sulfides/oxides and carbon derived.^[5-10] Among them, WS₂, MoS₂, CuS, graphite/graphene, boron based, TiO₂, and PTFE have shown improved performance under a wide variety of tribological test conditions.^[3,9,11-25] Studies have included comparison of the tribological benefits of different nanoadditives with the best industrially established lubricant additives. In particular, these studies have examined the potential of using nanoadditives to replace, or minimize currently employed non-particle additives, by providing improved performance and, at the same time, being more environmentally friendly.

For tribological systems experiencing a boundary lubrication regime such as the piston ring liner in automobile engines with direct contact of surface asperities of interacting interfaces, the chemical properties and efficacy of the additives to form protective tribofilms become exceedingly important. One of the most researched and currently widely used additive in the lubrication industry is zinc dialkyldithiophosphate (ZDDP). It is one of the best anti-wear additives and also provides a secondary benefit of working as an antioxidant in the engine oil.^[26-30] ZDDP is known to provide exceptional anti-wear benefits by forming sacrificial protective tribofilms at the rubbing surfaces. These films are primarily composed of long to medium chain phosphates of zinc at the surface, and other iron and zinc bound sulfur/phosphorus species in the bulk of the tribofilm.^[31-34] However, ZDDP poses a major drawback by creating sludge in the oil and the volatile species of

phosphorus and sulfur, resulting from its decomposition. These volatile P and S effluents reduce the efficiency of the catalytic converter, thus directly increasing the amount of harmful emissions.^[35,36]

In light of these concerns, a broad range of alternative approaches have been explored in recent times to improve tribological benefits, while simultaneously reducing harmful side effects on the environment. One such widely sought approach would be to substantially reduce the amount of ZDDP in the oil by addition of an environmentally friendly nanoadditive to maintain and, hopefully, even enhance tribological performances. Numerous recent published papers have focused on understanding the interaction of nanoadditives with ZDDP for such applications.^[11,17,37-41]

The present study investigates the tribological compatibility of ZDDP with TiO₂ nanoparticles and plasma surface functionalized TiO₂ nanoparticles when used together as an additive mix in the oil. In previous work, we have reported the tribological benefits of plasma functionalized PTFE nanoparticles.^[42] Herein we report detailed examination of the potential benefits of employing TiO₂ nanoparticles to achieve the goal noted above. It includes studies of pure and surface modified TiO₂ nanoparticles. In the latter case, plasma enhanced chemical vapor deposition was employed to deposit films on TiO₂ nanoparticles using trimethylboroxine and glycidyl methacrylate monomers. The outer methacrylate layer serves the purpose of particle dispersion in the oil as well as protects the underlying boron rich film until it reaches the interacting surfaces. This study also includes systematic assessment of the separate individual additives in order to draw comparative conclusions. For tribological evaluation of the respective additives and the additive mix, pin on reciprocating flat (line contact) test configuration was used. Friction and electrical contact resistance (ECR) data were recorded during the test procedure and optical

microscopic techniques were employed to calculate wear volume loss from the post-test specimens. The tribofilms generated on the rubbed interfaces were subjected to extensive chemical surface characterization using X-ray photoelectron spectroscopy (XPS) and X-ray absorption near edge spectroscopy (XANES). The information obtained from these spectroscopic surface analyses identified the chemical architecture of the tribofilms.

The outcomes of this study reveal that under similar test conditions, ZDDP, TiO₂ nanoparticles and functionalized TiO₂ nanoparticles, employed separately by themselves, display good anti-wear performance via creation of different effective tribofilms. However, when ZDDP and uncoated TiO₂ additives are used as a mixture, they exhibit surprisingly antagonistic behavior that leads to severe wear. In sharp contrast, the mix of boron coated TiO₂ additives and ZDDP display a synergistic interaction which leads to an early incubation of a very stable tribofilm providing good wear performance. XPS and XANES data revealed the chemical make-up of the tribofilms and this information was further used to create phenomenological schematics.

2. Results and Discussion

2.1 Friction and Wear outcomes: **Figure 1** shows friction spectra collected for seven different oil formulations whose details are listed in **Table 1** of the experimental section. These friction plots are dynamic representation of tribofilm formation and exclusion throughout the duration of the test. Samples with ZDDP at 700 ppm P level (B), TiO₂ nanoparticles only (D) and TiBGM (boron and methacrylate coated TiO₂) nanoparticles only (F) exhibited the lowest and almost same coefficient of friction values towards the end of the 1 hour tests. However, the friction profiles for samples D and F were the most stable ones throughout the test compared to rest of the samples. Sample with reduced amount of ZDDP i.e. 350 ppm P level (C) performed better than the base oil (A) in terms of friction outcomes but showed relatively higher coefficient of friction values

compared to other oil samples containing additives. The sample with base oil, ZDDP at 350 ppm P level and TiO₂ nanoparticles (E) displayed the most dramatic friction behavior. For the initial 30 mins of the test, the coefficient of friction remained high and relatively unstable and then started to decrease. After 40 mins, the friction profile stayed relatively smooth exhibiting values essentially comparable to that of samples B and D. Sample G with ZDDP at 350 ppm P level and TiBGM nanoparticles showed an unsteady friction profile for the initial 20 mins and then remained very stable, with coefficient of friction values similar to that of sample C, after longer test times.

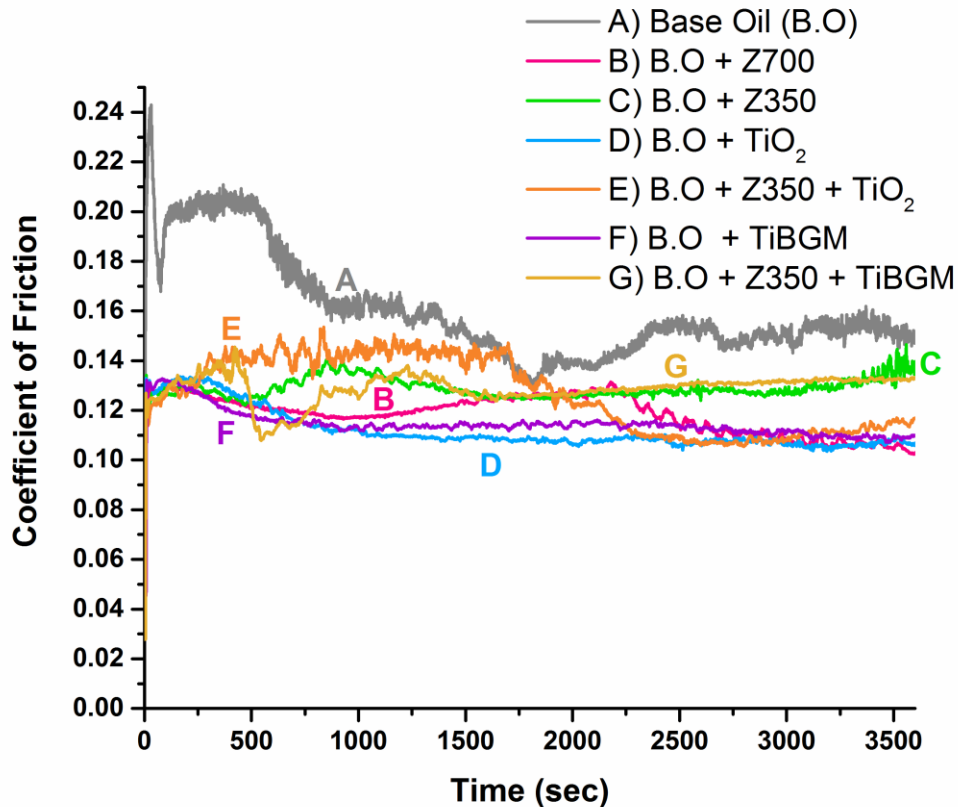


Figure 1. Coefficient of friction as a function of time for sample **A)** Base Oil (B.O) ; **B)** B.O + ZDDP at 700 ppm P level; **C)** B.O + ZDDP at 350 ppm P level; **D)** B.O + 0.33wt% TiO₂; **E)** B.O + ZDDP at 350 ppm P level + 0.33wt% TiO₂; **F)** B.O + 0.33wt% TiBGM; **G)** B.O + ZDDP at 350 ppm P level + 0.33wt% TiBGM.

The wear scar formed on the steel pin from each test was measured using optical microscopy and this value was used to calculate the wear volume loss. **Figure 2** represents the wear volumes outcomes for the steel pins after tribological testing. As expected, sample A, having just base oil displayed the worst wear outcomes and sample B with ZDDP at 700 ppm P level gave the best wear protection. Interesting wear results were observed for the rest of the samples. Sample C with ZDDP at 350 ppm P level showed increased wear as compared to sample B. In contrast, sample D with TiO₂ nanoparticles gave wear volume loss values only slightly higher than sample B but lower than 50% of sample C's value. The results for sample E, containing both ZDDP at 350 ppm P level and TiO₂ nanoparticles, was quite surprising as the wear volume value was almost 4 fold higher than sample C and 12 fold higher than sample D. In sharp contrast, the functionalized TiO₂ nanoparticles (TiBGM) exhibited better anti-wear performance in the oil when used by themselves (F), as well as when used with ZDDP (G). Whereas some well-known additives, such as ionic liquids, borate esters, tungsten disulfide nanoparticles etc., have shown favorable synergistic interaction with ZDDP,^[11,31,43-45] in this study, ZDDP exhibited unanticipated antagonistic behavior when used with TiO₂ nanoparticles under boundary lubrication conditions. However, when TiO₂ nanoparticles coated with boron chemistry were employed with ZDDP, they negated the hostile interaction and resulted in providing wear outcomes almost similar to ZDDP (350 ppm P level) by itself. This reflects the benefit of having extra anti-wear chemistry in the form of plasma film at the rubbing contacts which is being delivered via nanoparticles. Similar benefits of plasma functionalized PTFE nanoparticles were reported in our previous work.^[42]

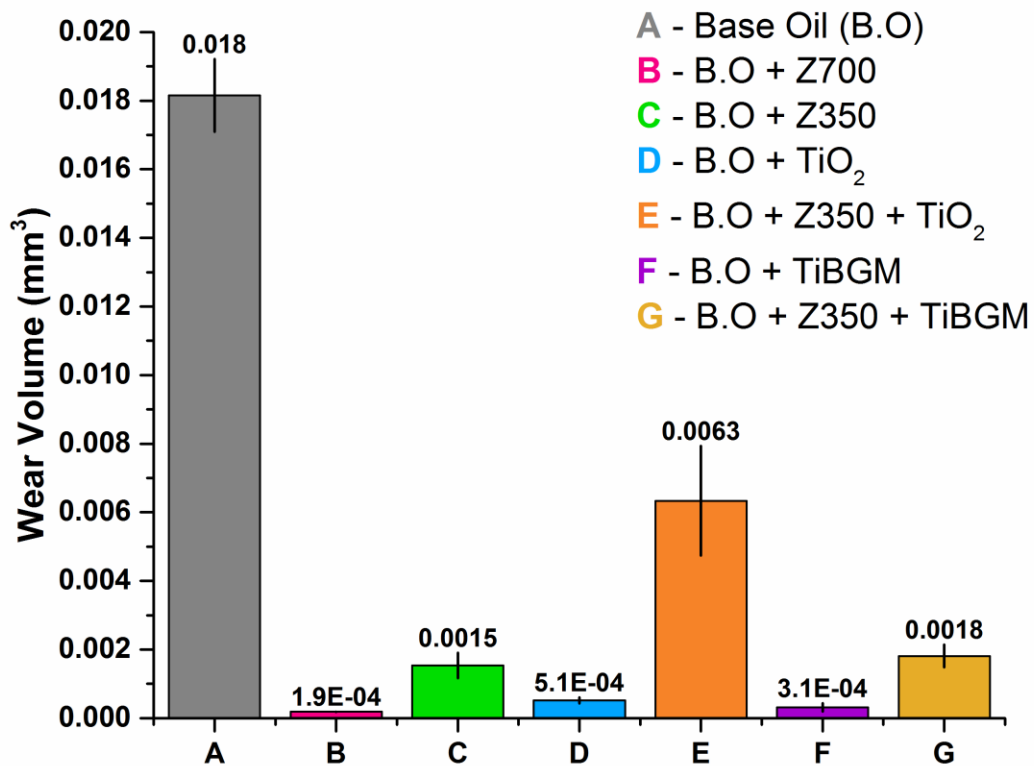


Figure 2. Wear volume losses for sample **A**) Base Oil (B.O) ; **B**) B.O + ZDDP at 700 ppm P level; **C**) B.O + ZDDP at 350 ppm P level; **D**) B.O + 0.33wt% TiO₂; **E**) B.O + ZDDP at 350 ppm P level + 0.33wt% TiO₂; **F**) B.O + 0.33wt% TiBGM; **G**) B.O + ZDDP at 350 ppm P level + 0.33wt% TiBGM.

Surface profiling for steel pins was performed using a white light interferometer. **Figure 3** shows the 3D representation of the worn surfaces after tribological testing. The wear profiles obtained for all seven samples are reasonably consistent with the findings of friction coefficient measurements, as noted above. Notably, sample E's pin surface reveals severe wear and, looks very different than that of sample G's surface as it is virtually flat and thus similar to that of sample

A. The improved wear protection provided by functionalized TiO_2 nanoparticles in presence of ZDDP is visually evident in the 3D pictures.

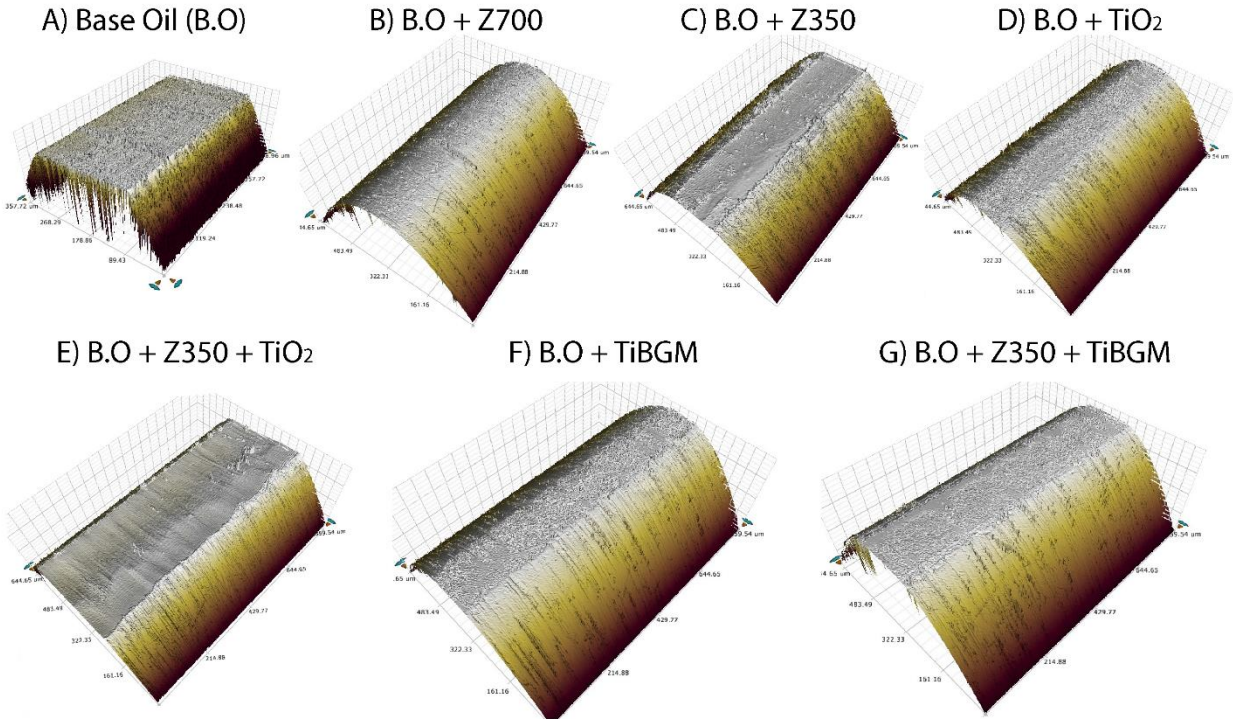


Figure 3. 3D profiles of the worn surfaces after tribological testing for sample **A)** Base Oil (B.O) ; **B)** B.O + ZDDP at 700 ppm P level; **C)** B.O + ZDDP at 350 ppm P level; **D)** B.O + 0.33wt% TiO_2 ; **E)** B.O + ZDDP at 350 ppm P level + 0.33wt% TiO_2 ; **F)** B.O + 0.33wt% TiBGM; **G)** B.O + ZDDP at 350 ppm P level + 0.33wt% TiBGM.

2.2 Electrical contact resistance (ECR) data: The ECR measurements provide a convenient way to examine the dynamics of tribofilm formation by lubricant additives between the interacting steel surfaces.^[31,43] The tribofilms formed by ZDDP are mostly glassy films of short to long chain phosphates and behave as insulating thin films. **Figure 4** shows the ECR data as a function of time for all the samples containing additives. The potential applied between the steel pin and the flat was 100 mV and the voltage drop (left y-axis) recorded for each test is represented with dots in

these plots. In addition, to compare the extent and subtleties of tribofilm formation from these different formulations, the line plot (white curve) in each graph shows normalized integrated voltage drop (right y-axis) wherein the maximum value of potential drop for sample A i.e. base oil with ZDDP at 700 ppm P level was used for data normalization. It is evident from the figure that ZDDP at 700 ppm P level rapidly forms a stable tribofilm and it stays there throughout the test, whereas for ZDDP at 350 ppm P level (B) the data points are much more scattered thus showing tribofilm forming and breaking over time. These data are in accord with the aforementioned wear outcomes (Figure 2 and 3). The voltage drop data points for samples with TiO₂ nanoparticles (C) also look dispersed, but the majority of them are in the upper half of the plot, showing the continuous presence of a thin protective film between the rubbing surfaces. The ECR data for the sample containing both reduced ZDDP and TiO₂ nanoparticles (D) also compliment the wear volume loss results. The data points in this plot are very discrete thus revealing the inability of the additive mix to form a stable protective tribofilm between the two surfaces. Only towards the end of the test was some indication of film formation observed. The ECR data for sample with only TiBGM nanoparticles (E) has more numerous data points in the high 90-100 mV region of the plot, compared to sample C, thus suggesting the formation of a more stable tribofilm at the surface due to the presence of additional boron species. Similarly, ECR data for the sample containing both TiBGM nanoparticles and ZDDP (F) demonstrate the additional benefits from boron chemistry to form protective film at the surface. The data points show the presence of a very stable tribofilm after just the initial 10 mins and it remains throughout the duration of the test, just like sample A. The significant differences in the ECR plots for sample D and F reveal that the presence of boron chemistry from functionalized particles reduces the

incubation time for tribofilm formation and this film remains effective until the end of test, unlike the tribofilm for sample B that fails before the completion of the test.

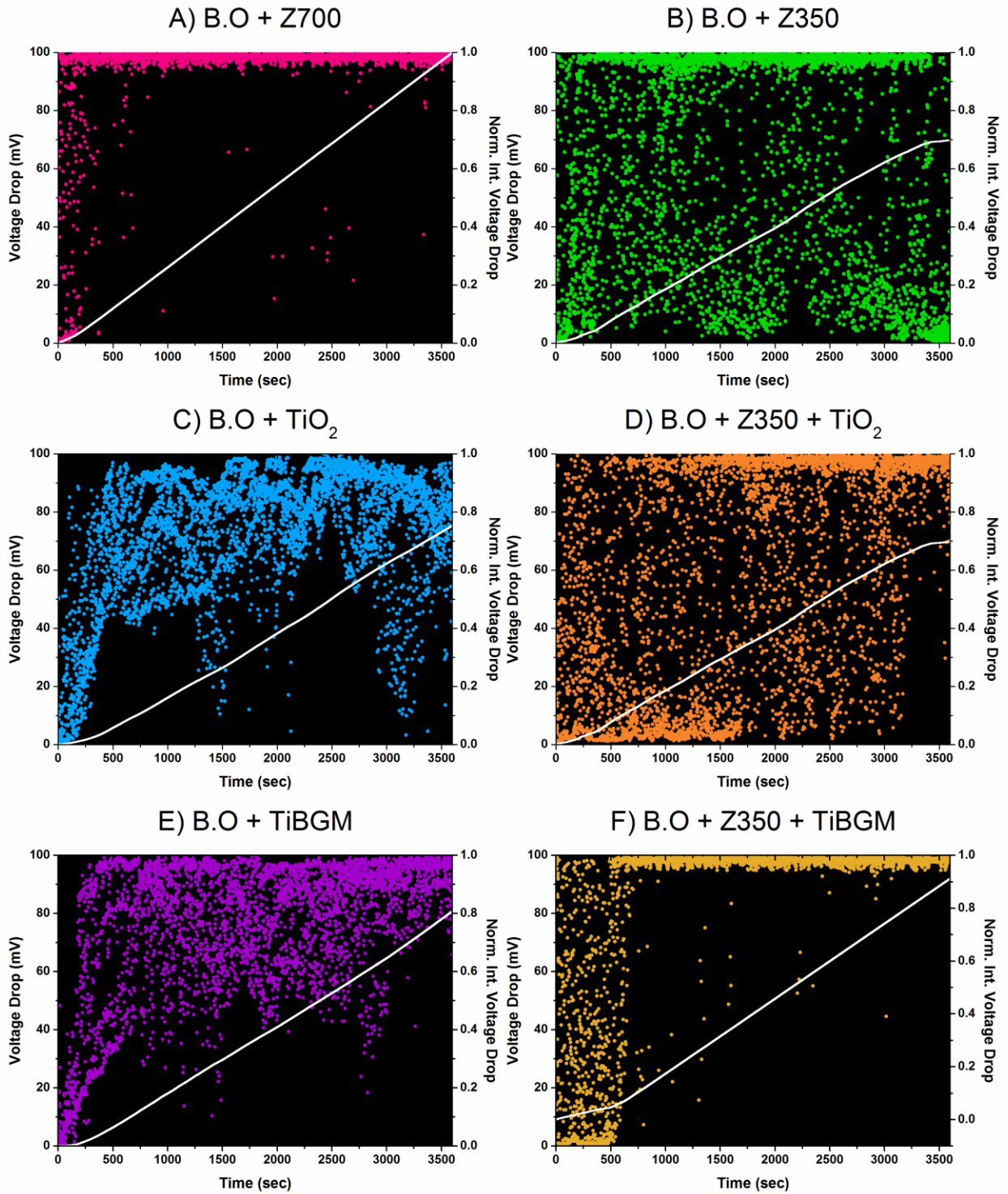


Figure 4. Electrical contact resistance (ECR) data plots recorded during tribological testing of sample **A)** B.O + ZDDP at 700 ppm P level; **B)** B.O + ZDDP at 350 ppm P level; **C)** B.O + 0.33wt% TiO₂; **D)** B.O + ZDDP at 350 ppm P level + 0.33wt% TiO₂; **E)** B.O + 0.33wt% TiBGM; **F)** B.O + ZDDP at 350 ppm P level + 0.33wt% TiBGM.

2.3 Tribofilm Characterization: Highly surface sensitive spectroscopic techniques were used to perform a comprehensive examination of the tribofilms to understand their chemical make-up. The flat steel specimens from tribological testing were subjected to XPS and XANES analysis to obtain a comparative study of the tribochemistry from different additives.

2.3.1 XPS analysis of the Tribofilms: **Figure 5** shows XPS spectra obtained for phosphorus, iron, zinc, titanium and oxygen elements in the tribofilms of the samples. The plots for each element shows the contrasting differences in its chemical state and relative quantitative amounts presence in the tribofilms of the selected samples. For the sample with only ZDDP (at 350 ppm P level) we observe sharp peaks for phosphorus 2p (133.8 eV) and zinc 2p (1022.4 eV & 1045.3 eV) and a very weak signal for iron 2 p. In addition, there is no signal in titanium 2p spectra, as expected. In the case of the sample having only TiO₂ nanoparticle additives, there are no peaks for phosphorus and zinc in the spectra as these elements are not present in the oil itself. We do observe a signal for iron 2 p spectra (710.9 eV & 724.8 eV) and it is slightly more intense than the sample with only ZDDP. There are intense peaks for titanium 2p signal (458.4 eV & 464 eV) in the spectra which indicates the presence of a titanium rich tribofilm at the surface. The phosphorus and zinc XPS spectra for the sample which showed the worst wear outcomes, i.e. oil with both ZDDP and TiO₂ nanoparticles, do not show any significant peaks, suggesting the inability of ZDDP to form zinc phosphate rich protective tribofilm, presumably due to the presence of TiO₂ nanoparticles in the oil. Additionally, the sharp iron peaks observed indicates the absence of a stable film at the

surface as the steel substrate is apparently exposed. The weak signal in titanium 2p spectra indicates that a small amount of titanium is present at the sample surface but apparently not sufficient to provide significant wear protection. A strong signal for titanium and a weak signal for iron in XPS spectra for the sample with TiBGM nanoparticles again shows the presence of titanium rich film at the surface. The phosphorus, iron, titanium and zinc spectra from sample with TiBGM nanoparticles and ZDDP establish the advantageous role of boron rich plasma coating on TiO₂ nanoparticles in promoting the formation of protective films. There is a fairly strong signal in phosphorus and zinc spectra suggesting that the tribofilm is rich in zinc and other metal phosphates. A weak signal for iron shows that major contribution to the chemical make-up of the film is from zinc and titanium which is protecting the surface from wear.

The information from oxygen 1s spectra reveals the overall chemical nature of the tribofilms formed with different additive chemistries and gives an insight into the contribution of different chemical species. The sample with only ZDDP shows intense peak for metal phosphates (~ 531.7 eV) and weak signals for metal oxides (~ 530.1 eV) and other organic (C=O) species (~ 533.6 eV) in the tribofilm. The oxygen spectra for the sample with only TiO₂ nanoparticles shows intense peaks for metal oxides which is mostly coming from titanium bound to oxygen and small contribution from iron oxide. In contrast, the sample with both ZDDP and TiO₂ nanoparticles reveals that the metal oxide peak is primarily from iron bound to oxygen, which is consistent with the information from iron 2p spectra. The peak between 531-532 eV must be due to metal carbonates or other oxygen vacancies and not from phosphates as there is no signal in phosphorus spectra for this sample. The oxygen spectra for the sample with only TiBGM nanoparticles has a strong peak for a Ti-O bond and in addition, the signal also has contribution from boron bound oxygen around 533 eV. Again, there is broad peak in the 531 to 532 eV energy range which would

possibly be due to some carbonate species as there is no phosphorus in this sample as well. The sample with TiBGM nanoparticles and ZDDP has an oxygen spectra resembling that of the ZDDP sample, with some additional contributions from oxygen bound to titanium, iron and boron. Overall, from the XPS results, it is evident that ZDDP, TiO₂ nanoparticles and TiBGM nanoparticles by themselves are capable of forming protective films at the surface and provide anti-wear performance. However, when ZDDP and TiO₂ nanoparticles are used together in a mix, they work antagonistically and fail to form any kind of stable tribofilms and, as a result, poor wear outcomes. However, in contrast, when functionalized TiO₂ nanoparticles are used with ZDDP, they form a very stable tribofilm primarily composed of phosphates with small but significant contribution from other species of titanium and boron.

A) B.O + Z350 B) B.O + TiO₂ C) B.O + Z350 + TiO₂ D) B.O + TiBGM E) B.O + Z350 + TiBGM

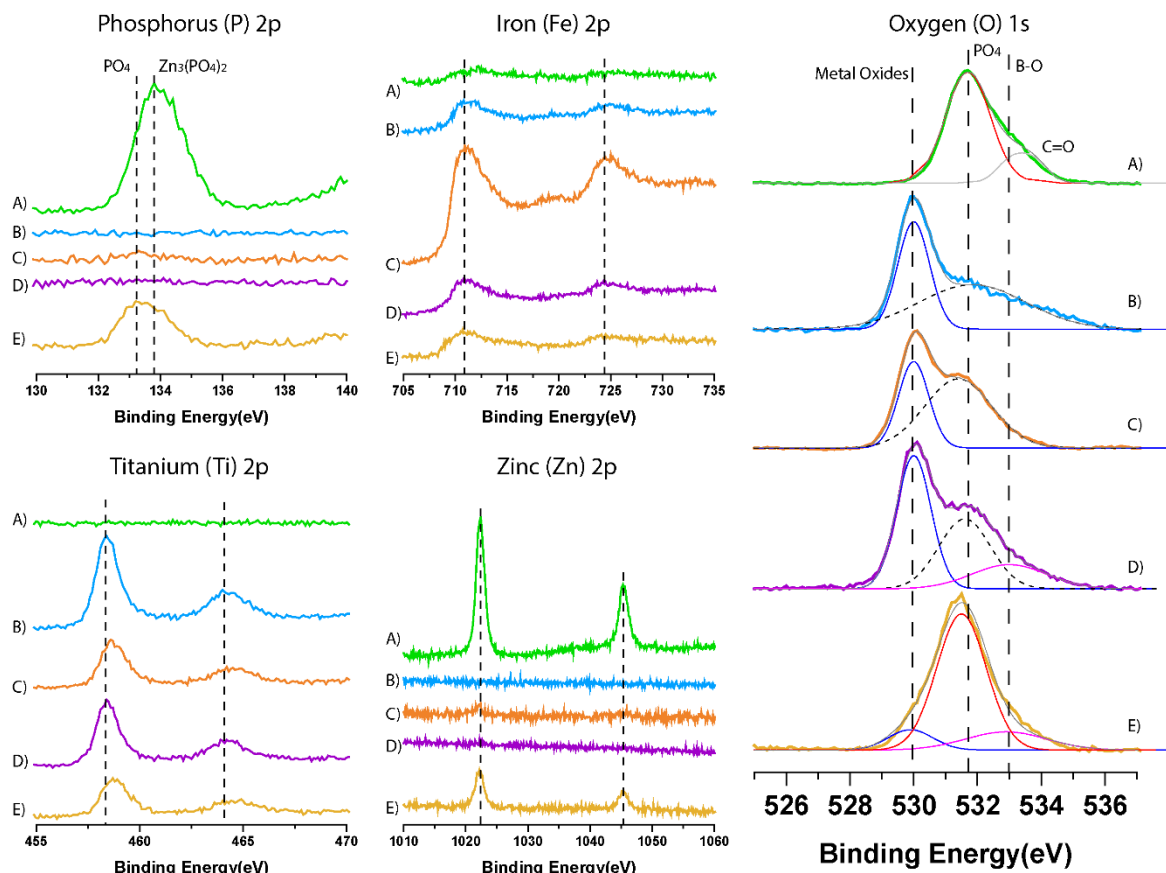


Figure 5. XPS spectra (P 2p, Fe 2p, Zn 2p, Ti 2p & O 1s) for samples **A)** B.O + ZDDP at 350 ppm P level, **B)** B.O + 0.33wt% TiO₂ and **C)** B.O + ZDDP at 350 ppm P level + 0.33wt% TiO₂; **D)** B.O + 0.33wt% TiBGM; **E)** B.O + ZDDP at 350 ppm P level + 0.33wt% TiBGM.

2.3.2 XANES analysis of the Tribofilms: X-ray absorption near edge spectroscopy is a powerful

surface analysis technique which has been extensively used to study the chemistry of tribofilms.^{[46-}

^{51]} It provides crucial information about the element's local coordination environment, as well as

its geometric make-up, within the film. Depending on the energy of the x-ray and the detection

mode used, both surface and bulk of the tribofilms can be examined. The total electron yield (TEY)

detection mode provides information from the top 5-50 nm of the film, whereas the fluorescence

yield (FLY) mode helps to study the bulk of the tribofilm. In this study, XANES was used to compliment the findings of XPS spectroscopy and also to provide a better insight into the mechanism of tribofilm formation from the different additives under investigation.

Phosphorus L edge

Figure 6(a) shows the P L-edge spectra in TEY mode for model compounds and samples A to E. The sampling depth in this case is about 5-15 nm. The P L-edge spectra for zinc and iron phosphate model compounds have been thoroughly studied and the significance and identity of each of the peaks (**a**: 136.6 eV, **b**: 137.7 eV, **c**: 139.3 eV, **d**: 147.2 eV & **c'**: 139.6 eV), are well documented in the literature.^[52,53] It is evident, from the plots, that the sample with only ZDDP (A) has its peaks aligned exactly with the peak positions for zinc phosphate. Whereas, for the sample with both ZDDP and TiO₂ nanoparticles (C), the signal is very weak and it is difficult to tell whether it is from iron or zinc phosphates in the film. These results further confirm the incompatibility between ZDDP and TiO₂ nanoparticles in terms of promoting effective tribology films, thus resulting in severe wear, as noted earlier. However, for the sample containing functionalized nanoparticles and ZDDP (E), the peak intensities reveal the strong presence of phosphates in the tribofilm. The peak positions hint at iron phosphates being the dominant species at the surface and the contribution from zinc/boron phosphates is limited.

Zinc L edge

The Zn L-edge TEY spectra in **Figure 6(b)** confirm the results from P L-edge spectra as well as Zn 2p XPS spectra. Again, the sample with only ZDDP (A) shows the strong presence of zinc in the tribofilm as the peaks match well with the zinc phosphate model compound's peaks (**a**: 1031 eV & **b**: 1054.3 eV). The tribosurfaces generated from the mix of ZDDP and TiO₂

nanoparticles (C) have no signal for zinc at all. Interestingly, the spectra for sample E which contains plasma functionalized TiO₂ nanoparticles (TiBGM) with ZDDP, has its peak positions matching with that of zinc phosphate model compound. This adds more to the information obtained from phosphorus L-edge data and establishes that tribofilm for this sample contains both zinc and iron phosphates.

Boron K edge

Boron K-edge TEY spectra provide valuable information regarding the role of plasma functionalized TiO₂ nanoparticles in this study. **Figure 6(c)** shows the spectra for boron model compounds and samples B to E. As expected, the samples with unaltered TiO₂ nanoparticles (B and C) did not show any signal for boron. The peak positions and intensities in TEY spectrum from the sample with only functionalized nanoparticles (D) reveal the presence of borates in the tribofilm. The features in the spectra match that of borates of iron from the literature.^[54] However, the features in the spectra from sample with both TiBGM nanoparticles and ZDDP (E) are quite distinct from model compounds, as well as from sample (D). There is a strong peak at 196.5 eV and it has a shoulder on the lower energy side at 194.5 eV which matches with hydrogen borate's peak **a**. This distinct peak position suggests the presence of a complex metal borate complex as zinc, iron and titanium are also present in the tribofilm.^[54,55]

Iron L edge

The Fe L-edge TEY spectra in **Figure 6(d)**, shows plots for four different model compounds namely: Fe₂O₃, FePO₄, FeSO₄ and FeS. The sample with only ZDDP (A) has its main peak positions (**b**: 712.7 eV & **d**: 714.6 eV) aligning with those of the FePO₄ model compound. However, due to the contribution from other iron species, such as FeS and Fe₂O₃ in the tribofilm,

the intensity for peak **d** is higher than that of peak **b**. The sample with only TiO₂ nanoparticles (B), ZDDP and TiO₂ nanoparticles (C) and TiBGM nanoparticles (D) have their main peak position superimposing the Fe₂O₃ model compound's peak **c** (714.2 eV). However, the features in the signal for sample with both ZDDP and TiBGM nanoparticles (E) show that iron is primarily present in the form of phosphate/sulfate/sulfide. This yet again establishes that ZDDP with TiO₂ nanoparticles combination fails to provide any wear protection and the tribofilm at the surface is mainly rich in iron oxide. In contrast, in the presence of functionalized nanoparticles TiBGM, the boron chemistry provides an additional benefit by promoting the formation of stable phosphate rich protective films at the surface.

Titanium L edge

As shown in **Figure 6(e)**, the Ti L-edge TEY spectra adds some vital information regarding the titanium atoms present in the tribofilms for different test samples. It provides additional information regarding the local chemical and geometric arrangement of titanium which was not available from the Ti 2p XPS spectra. The shapes, positions and heights for peaks **a** (~ 462 eV) and **b** (463.7 eV) in the Ti L-edge spectra from the TiO₂ model compound and test samples look quite dissimilar. However, the positions and shapes for peaks **c** (467.4 eV) and **d** (469.4 eV) from the test samples are consistent with the TiO₂ model compound. The variations in the features of peak **a** and **b** suggests that the titanium present in the tribofilms of the test samples no longer exists in anatase phase and during the test it apparently experienced chemical and structural transformation to a higher site symmetry.^[56-59] The spectra from the samples with only TiO₂ nanoparticles (B), ZDDP with TiO₂ nanoparticles (C) and ZDDP with TiBGM nanoparticles are consistent with the transformation of low symmetry anatase TiO₂ into a higher symmetry titanate,^[57,59] it appears that the tribofilm has titanium in the form of iron titanate, i.e. ilmenite (FeTiO₃).

However, in the case of sample C and E, it is not possible to distinguish between the presence of iron titanate or zinc titanate in the tribofilm.

Oxygen K edge

Figure 6(f) shows the O K-edge TEY spectra for six model compounds (Fe_2O_3 , FePO_4 , FeSO_4 , $\text{Zn}_3(\text{PO}_4)_2$, ZnSO_4 and TiO_2) and three test samples. XANES spectra for oxygen K edge gives us information from the bulk of the tribofilm. It has been reported, in previous works of Aswath et al. [32,60], that the zinc bound phosphates species are predominantly present in the top region of the tribofilms and iron phosphates/sulfates exist in the bulk. Likewise, the O K-edge plot for the sample with only ZDDP (A) has its main features aligned with those of iron sulfate (d: 538.9 eV) and iron phosphate model compounds. The peak itself is very broad and this hints to the contribution from zinc bound phosphorus/sulfur species. The spectrum does not show any peaks at iron oxide peak positions. The contrasting differences in O K-edge spectra for the samples reflect the overall chemistry of their respective tribofilms. The spectra for samples B and D have peak positions matching with those of TiO_2 model compound (e: 531.9 eV & f: 534.5 eV). This suggests that the titanium bound oxygen species dominate in the tribofilm and the contribution from Fe-O species is very limited. In addition, due to the aforementioned transformation of anatase TiO_2 to titanate form i.e. FeTiO_3 , the features on the higher energy side (~537 eV to 550 eV) are very distinctive compared to the model compound.^[59] For sample C (containing both ZDDP and TiO_2 nanoparticles), the two peaks in the lower energy side of the spectrum (530 to 537 eV) are close to the peaks from Fe_2O_3 (b: 531.5 eV) and FePO_4 (c: 532.4 eV) model compounds and represent the rich iron content in the tribofilm. The Ti L-edge XANES spectra and Ti 2p XPS spectra provide sufficient evidence to validate the presence of titanium in the tribofilm and therefore the Ti-O species are also contributing to the overall metal-oxygen signal in the spectrum. The features in

the high energy range are also credited to the Ti-O bonds in the tribofilm as they look similar to that of sample B. However, the spectrum from sample containing both ZDDP and functionalized TiO₂ nanoparticles (E) has the main intense peak close to iron phosphate/sulfate peak positions. The smaller peaks in the lower energy side do not exactly match with TiO₂ model compound peaks and this could be due to formation of a complex glass structure involving trace amount of titanium, boron and zinc along with profusely existing iron phosphates/sulfates.

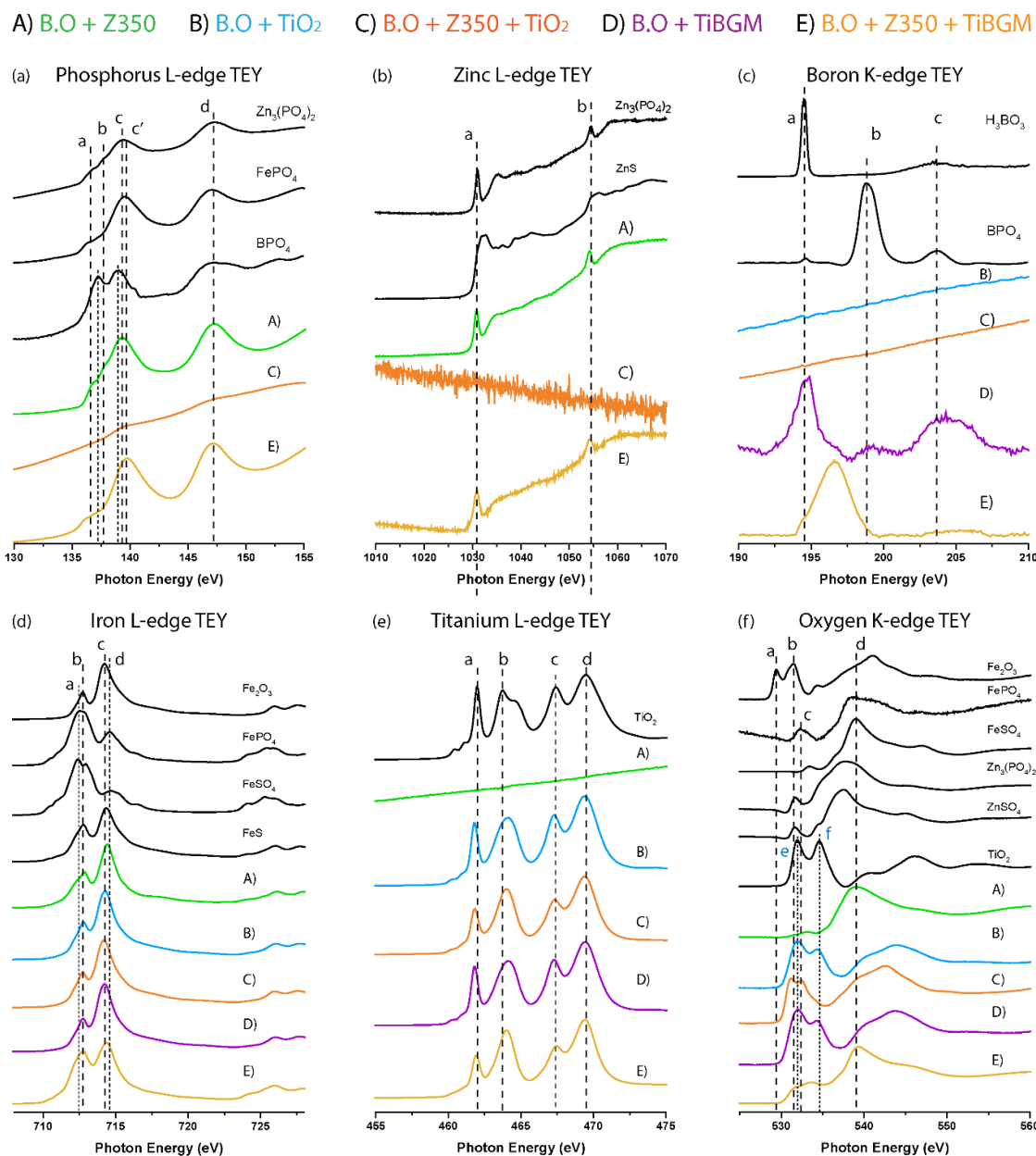


Figure 6. (a) Phosphorus L edge TEY, (b) Zinc L edge TEY and (c) Boron K edge TEY (d) Iron L edge TEY (e) Titanium L edge TEY (f) Oxygen K edge TEY XANES spectra for samples A) B.O + ZDDP at 350 ppm P level, B) B.O + 0.33wt% TiO₂ and C) B.O + ZDDP at 350 ppm P level + 0.33wt% TiO₂; D) B.O + 0.33wt% TiBGM; E) B.O + ZDDP at 350 ppm P level + 0.33wt% TiBGM.

2.4 Schematics for Tribofilms: Figure 7 shows the phenomenological schematics of the tribofilms for samples subjected to XPS and XANES analysis. Chemical information, from both techniques, were extrapolated to develop these representations. Figure 7(A) shows the tribofilm generated from the sample with only ZDDP at 350 ppm of phosphorus. The typical components of a ZDDP tribofilm are shown in the figure containing long to medium chain zinc phosphates at the top and underneath there are phosphate/sulfate/sulfide species of zinc. In the bulk of film, iron bound species dominate the chemistry of the film. For the sample with only TiO₂ nanoparticles, Ti L-edge and Fe L-edge XANES data provided the foundation for Figure 7(B). It represents an arrangement of the chemical species in the tribofilm where it has trace amount of iron oxide in the bulk and above it there is strong presence of iron bound titanium. Figure 7(C) provides insight into the chemical architecture of the tribofilms formed from the mixture of ZDDP and TiO₂ nanoparticles in the oil. Consistent with the spectroscopic data, the model 7(C) shows a large quantity of iron throughout the thickness of the tribofilm, which is primarily available in the form of iron oxides and a smaller amount of iron phosphates. As the Ti L-edge and O K-edge XANES spectra suggest, there is also a trace quantity of titanium present in the form of titanate in the tribofilm as well. Again, the information from boron K-edge, iron L-edge and titanium L-edge XANES spectra helped in modelling the schematic of the tribofilm for the sample with plasma functionalized nanoparticles, as shown in Figure 7(D). As evident in the XANES data, iron titanates are the dominant chemical species in the tribofilm with a trace amount of iron borates. Finally, Figure 7(E) represents the model of tribofilm for sample containing both ZDDP and functionalized TiO₂ nanoparticles (TiBGM). The phosphorus, zinc and iron data from both XPS and XANES support the presence of phosphates of iron and zinc in the upper region of the tribofilm. The boron and titanium XANES spectra suggest that a complex glassy structure is

present at the surface where titanium is forming titanates and boron is making borates with available iron and zinc. In the bulk of the tribofilms, iron is present in the form of sulfates/sulfides along with short chain phosphates. Information from both XPS and XANES spectra were employed to expose the incompatibility of combined ZDDP and TiO₂ additives, as well as to understand the role of plasma functionalized TiO₂ additives in promoting the formation of stable tribofilms with ZDDP.

For the sample containing functionalized TiO₂ nanoparticles the contribution of boron bound iron species to the tribofilm is not very significant compared to titanium bound iron species. This is because the amount of available boron chemistry from the functionalized TiO₂ nanoparticles at the tribological interface is limited. In addition, iron titanate (FeTiO₃) has a lower standard enthalpy of formation (-1153.9 kJ/mol) compared to iron borate (FeBO₃; >1800 kJ/mol) and therefore the interaction between iron and titanium species is thermodynamically favored in this case. For sample with both functionalized TiO₂ nanoparticles and ZDDP, we have additional chemical species present at the interface including P, S and Zn along with Fe, Ti and B. Due to the lower enthalpy of formation values for iron-sulfur and iron-oxygen species (FeS: -102 kJ/mol, FeS₂: -178 kJ/mol, Fe₂O₃: -824.2 kJ/mol) they form first at the surface along with zinc bound sulfur species (ZnS: -204.6 kJ/mol; ZnSO₄: -980.14 kJ/mol). The other chemical species that were found using XPS and XANES studies, including zinc phosphate, iron phosphate, titanates and borates of Zn and Fe, have significantly higher enthalpy of formation and they form a complex glass structure where the phosphorus chemistry predominates over titanium and boron chemistry.

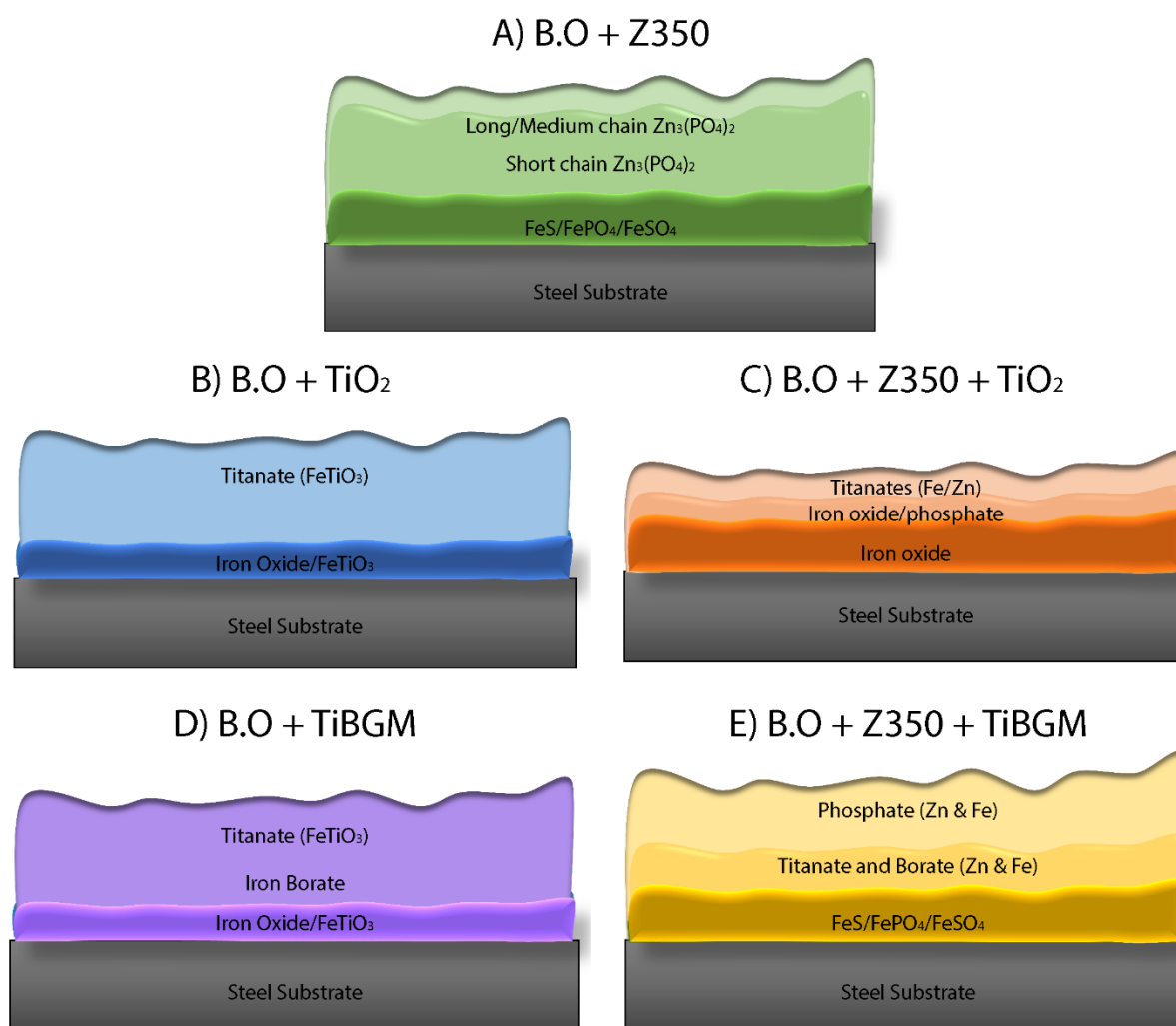


Figure 7. Schematics of tribofilms generated from samples **A)** B.O + ZDDP at 350 ppm P level, **B)** B.O + 0.33wt% TiO_2 and **C)** B.O + ZDDP at 350 ppm P level + 0.33wt% TiO_2 ; **D)** B.O + 0.33wt% TiBGM; **E)** B.O + ZDDP at 350 ppm P level + 0.33wt% TiBGM.

3. Conclusion

This study demonstrates that TiO_2 nanoparticles exhibit promising anti-wear and anti-wear properties when used as additives in the base oil. However, the TiO_2 particle data also revealed some completely unexpected aspects. When a mixture of ZDDP (350 ppm P) and TiO_2

nanoparticles was employed surprisingly worst wear protection and wear volume loss value were observed since these combined additives failed to promote the formation of a stable tribofilm. However, in the case of plasma surface modified TiO₂ nanoparticles, better anti-wear performance was observed by themselves and also when used with 350ppm of ZDDP in the oil. In terms of TiO₂ surface modification, it was discovered that the introduction of boron atoms can play a prominent role in promoting the formation of protective anti-wear films at the surface. Detailed XPS and XANES spectroscopic analysis were provided to elucidate the chemistry of the tribofilms and how these chemistries varied from the various oil formulations employed in this study. Notably, the plasma surface modification technique employed in this work, to introduce boron atoms, is applicable to providing a very wide range of additional nanoparticle surface films containing other potential film forming atoms.

4. Experimental Section

Titanium dioxide (TiO₂) nanoparticles (avg. size: 25 nm), trimethylboroxine and glycidyl methacrylate were procured from Sigma Aldrich USA. The secondary Zinc dialkyl dithiophosphate (ZDDP) used for this study is approx. 30% neutral and 70% basic in nature. ^[61] To achieve uniform deposition of plasma films on TiO₂ nanoparticles as well as to address the particle aggregation problem, they were subjected to a homebuilt 360° rotating plasma reactor. Trimethylboroxine was employed as the organic monomer to deposit boron rich thin films on TiO₂ nanoparticles via plasma polymerization. The deposition process was carried out using a continuous wave (CW) plasma for initial 1 hour, followed with sequential lower duty cycle pulsed plasma deposition from 50:20 (plasma on time : plasma off time, in milliseconds) to 50:50, 15 mins each. Typical plasma operating parameters are as following: Pressure - 100 mT; Power - 60 W; monomer flow rate - 2 sccm; RF frequency - 13.56 MHz. Afterwards, another plasma coating

was deposited on top of these particles using glycidyl methacrylate as the monomer. This process was run for 1 hour at 100 W peak power at 100 mT pressure. A pulsed plasma with 20:50 duty cycle was employed throughout the deposition. The TiO₂ nanoparticles coated with boron and methacrylate chemistry are referred as TiBGM nanoparticles in the text. Further details on the plasma process employed are provided in reference 42.

The base oil used as the carrier for additives to perform the tribological testing is a group III base stock (GS Caltex Kixx Lubo 4 cSt). Details regarding the oil formulations used in this study are shown in **Table 1**.

Table 1. Details of oil formulations used for tribological tests.

Test	Formulation	Coded Name
A.	Group III Base oil	Base Oil (B.O)
B.	B.O + ZDDP at 700 ppm of Phosphorus	B.O + Z700
C.	B.O + ZDDP at 350 ppm of Phosphorus	B.O + Z350
D.	B.O + 0.33 wt% TiO ₂ nanoparticles	B.O + TiO ₂
E.	B.O + ZDDP at 350 ppm of Phosphorus + 0.33 wt% TiO ₂ nanoparticles	B.O + Z350 +TiO ₂
F.	B.O + 0.33 wt% TiBGM nanoparticles	B.O + TiBGM
G.	B.O + ZDDP at 350 ppm of Phosphorus + 0.33 wt% TiBGM nanoparticles	B.O + Z350 +TiBGM

ZDDP was used at two different phosphorus levels: i) 700 ppm and ii) 350 ppm. To make a homogenous suspension of TiO₂ nanoparticles in the base oil, they were subjected to probe sonication for 15 mins right before the start of the test and 2-3 drops of this mix was used to lubricate the surface of the steel sample. The flat (14mm X 14 mm; R_a 13 nm) and pin (4mm X 6mm) samples used in the study were 52100 hardened steel. The specifics regarding tribological testing are as following: load-82 N; hertzian contact pressure-500 MPa; speed-5Hz; temperature-100⁰ C; stroke length-6 mm; duration-60 min. A high-frequency reciprocating cylinder on flat configuration, which mimics the line contact in automobile engine's piston ring on liner interaction, was employed for tribological testing. The testing conditions were preferably chosen to observe the additives performance under boundary lubrication conditions. The test setup was built in-house at Argonne National Lab and it was equipped to record both friction and electrical contact resistance data (ECR). In order to collect the ECR data, a potential (100 mV) was applied between the two conducting surfaces which in this case are steel flat and pin. During the test, the two surfaces move against each other, and the additives in the oil form a protective film which ultimately cuts-off the electrical circuit. As a result, an electric potential builds up across the two surfaces and it is measured along with the friction data as a function of time. The pre-test sample cleaning procedure involved step-by-step cleaning with Stoddard, isopropanol and acetone in a sonication bath to remove any contaminants from the surfaces. Post-test samples were first gently rinsed with heptane and then optical microscopy (Olympus STM6) and white light interferometry (Bruker Contour GT) were used to conduct wear volume calculations, and to examine the 3D surface profile. Each time, the sample was subjected to a characterization technique it was rinsed with heptane and then again lubricated with polyalphaolefin (PAO) oil after analysis.

Surface sensitive techniques namely, XPS (Kratos Axis Ultra; monochromatic Al K α X-ray source) and XANES were used to identify the chemical make-up of the tribofilms. XPS provides chemical information from the top 5-8 nm of the surface and it was used to identify the elements and their relative presence in the tribofilms. The XPS spectra were recorded at following run-time parameters; power: 150 W; spot size: 300 μm x 700 μm . XANES experiments were performed at SGM (spherical grating monochromator) and VLS-PGM (variable line spacing-plane grating monochromator) beamlines at the Canadian Light Source in Saskatoon Canada. These beamlines were employed to identify the different chemical species in the tribofilms, such as oxygen (K edge), iron (L edge), titanium (L edge), zinc (L edge) and phosphorus (L edge) and their local coordination environments. Typical operating parameters for SGM are: energy-200-2000 eV; photon resolution->5000 E/ Δ E; spot size-50 μm x 50 μm and for VLS-PGM beamline are: energy-5.5-250 eV; photon resolution-> 10,000 E/ Δ E; spot size-100 μm x 100 μm .

Acknowledgments

XANES experiments were conducted at the Canadian Light Source, Saskatoon, Saskatchewan, Canada that is supported by NSERC, NRC, CIHR and the University of Saskatchewan. Tribological tests were performed at Argonne National Laboratory. X-ray Photoelectron Spectroscopy facilities provided by the Department of Chemistry is gratefully acknowledged.

References

- [1] V. N. Bakunin, A. Y. Suslov, G. N. Kuzmina, O. P. Parenago, A. V. Topchiev, *J. Nanopart. Res.* **2004**, *6*, 273.
- [2] B. Zhmud, B. Pasalskiy, *Lubricants* **2013**, *1*, 95.

- [3] G. Anand, P. Saxena, *IOP Conf. Ser.: Mater. Sci. Eng.* **2016**, *149*, 1.
- [4] Q. Sunqing, D. Junxiu, C. Guoxu, *Lubr. Sci.* **1999**, *11*, 217.
- [5] Y. Y. Wu, W. C. Tsui, T. C. Liu, *Wear* **2007**, *262*, 819.
- [6] J. Padgurskas, R. Rukuiza, I. Prosycevas, R. Kreivaitis, *Tribol. Int.* **2013**, *60*, 224.
- [7] N. G. Demas, R. A. Erck, C. L. Martin, O. O. Ajayi, and G. R. Fenske, *J. Nanomater.* **2017**, *2017*. (DOI:<https://doi.org/10.1155/2017/8425782>)
- [8] J. Chen, *Tribol. Lett.* **2010**, *38*, 217.
- [9] L. Joly-Pottuz, F. Dassenoy, M. Belin, B. Vacher, J. M. Martin, N. Fleischer, *Tribol. Lett.* **2005**, *18*, 477.
- [10] X. Tao, Z. Jiazheng, X. Kang, *J. Phys. D.* **1996**, *29*, 2932.
- [11] P. U. Aldana, B. Vacher, T. Le Mogne, M. Belin, B. Thiebaut, F. Dassenoy, *Tribol. Lett.* **2014**, *56*, 249.
- [12] C. Drummond, N. Alcantar, J. Israelachvili, R. Tenne, Y. Golan, *Adv. Funct. Mater.* **2001**, *11*, 348.
- [13] I. Z. Jenei, F. Svahn, S. Csillag, *Tribol. Lett.* **2013**, *51*, 461.
- [14] M. Ratoi, V. B. Niste, J. Walker, J. Zekonyte, *Tribol. Lett.* **2013**, *52*, 81.
- [15] X. Zhang, B. Luster, A. Church, C. Muratore, A. A. Voevodin, P. Kohli, S. Aouadi, S. Talapatra, *ACS Appl. Mater. Interfaces*, **2009**, *1*, 735.
- [16] M. I. De Barros, J. Bouchet, I. Raoult, T. Le Mogne, J. M. Martin, M. Kasrai, Y. Yamada, *Wear* **2003**, *254*, 863.

- [17] S. D. Bagi, P. B. Aswath, *Lubricants* **2015**, 3, 687.
- [18] X. Kang, B. Wang, L. Zhu, H. Zhu, *Wear* **2008**, 265, 150.
- [19] D. Berman, S. A. Deshmukh, S. K. R. S. Sankaranarayanan, A. Erdemir, A. V. Sumant, *Adv. Funct. Mater.* **2014**, 24, 6640.
- [20] C. S. Chen, X. H. Chen, L. S. Xu, Z. Yang, W. H. Li, *Carbon* **2005**, 43, 1660.
- [21] A. Greco, K. Mistry, V. Sista, O. Eryilmaz, A. Erdemir, *Wear* **2011**, 271, 1754.
- [22] Y. Kimura, T. Wakabayashi, K. Okada, T. Wada, H. Nishikawa, *Wear* **1999**, 232, 199.
- [23] S. Ingole, A. Charanpahari, A. Kakade, S. S. Umare, D. V. Bhatt, J. Menghani, *Wear* **2013**, 301, 776.
- [24] F. Ilie, C. Covaliu, *Lubricants* **2016**, 4, 2. (DOI [10.3390/lubricants4020012](https://doi.org/10.3390/lubricants4020012))
- [25] M. Laad, V. K. S. Jatti, *J. King Saud Univ., Eng. Sci.* 2016. (<http://dx.doi.org/10.1016/j.jksues.2016.01.008>)
- [26] H. Spedding, R. C. Watkins, *Tribol. Int.* **1982**, 15, 9.
- [27] H. A. Spikes, *Tribol. Lett.* **2004**, 17, 469.
- [28] A. M. Barnes, K. D. Bartle, V. R. A. Thibon, *Tribol. Int.* **2001**, 34, 389.
- [29] J. M. Martin, T. Onodera, C. Minfray, F. Dassenoy, A. Miyamoto, *Faraday Discuss.* **2012**, 156, 311.
- [30] N. J. Mosey, T. K. Woo, M. H. Müser, *Prepr. - Am. Chem. Soc., Div. Pet. Chem.* **2005**, 50, 332.

- [31] V. Sharma, A. Erdemir, P. B. Aswath, *Tribol. Int.* **2015**, 82, 43.
- [32] R. Mourhatch, P. B. Aswath, *Tribol. Int.* **2011**, 44, 187.
- [33] N. J. Mosey, M. H. Müser, T. K. Woo, *Science* **2005**, 307, 1612.
- [34] N. N. Gosvami, J. A. Bares, F. Mangolini, A. R. Konicek, D. G. Yablon, R. W. Carpick, *Science* **2015**, 348, 102.
- [35] W. B. Williamson, J. Perry, H. S. Gandhi, J. L. Bomback, *Appl. Catal.* **1985**, 15, 277.
- [36] H. P. Buwono, S. Minami, K. Uemura, M. Machida, *Ind. Eng. Chem. Res.* **2015**, 54, 7233.
- [37] A. Morina, A. Neville, M. Priest, J. H. Green, *Tribol. Lett.* **2006**, 24, 243.
- [38] G. Nehme, *Lubr. Sci.* **2011**, 23, 181.
- [39] Y. Olomolehin, R. Kapadia, H. Spikes, *Tribol. Lett.* **2010**, 37, 49.
- [40] L. G. Yu, E. S. Yamaguchi, M. Kasrai, G. M. Bancroft, *Can. J. Chem.* **2007**, 85, 675.
- [41] A. Morina, A. Neville, M. Priest, J. H. Green, *Tribol. Int.* **2006**, 39, 1545.
- [42] V. Sharma, R. Timmons, A. Erdemir, P. B. Aswath, *ACS Appl. Mater. Interfaces* **2017**.
(DOI: 10.1021/acsami.7b06453)
- [43] V. Sharma, N. Dorr, A. Erdemir, P. Aswath, *RSC Adv.* **2016**, 6, 53148.
- [44] A. K. Landauer, W. C. Barnhill, J. Qu, *Wear* **2016**, 354, 78.
- [45] J. Qu, W. C. Barnhill, H. Luo, H. M. Meyer, D. N. Leonard, A. K. Landauer, B. Kheireddin, H. Gao, B. L. Papke, S. Dai, *Adv. Mater.* **2015**, 27, 4767.

- [46] M. Nicholls, M. N. Najman, Z. Zhang, M. Kasrai, P. R. Norton, P. U. P. A. Gilbert, *Can. J. Chem.* **2007**, *85*, 816.
- [47] B. Kim, R. Mourhatch, P. B. Aswath, *Wear* **2010**, *268*, 579.
- [48] V. N. Bakunin, M. Kasrai, G. N. Kuzmina, G. M. Bancroft, O. P. Parenago, *Tribol. Lett.* **2007**, *26*, 33.
- [49] Y. Li, G. Pereira, M. Kasrai, P. R. Norton, *Tribol. Lett.* **2007**, *28*, 319.
- [50] A. Meisel, G. Leonhardt, R. Szargan, E. Källne, *X-ray spectra and Chemical Binding*, Springer-Verlag Berlin Heidelberg, Germany **1989**.
- [51] A. Bianconi, D. Koningsberger, R. Prins, *X-Ray Absorption: Principles, Applications, Techniques of EXAFS, SEXAFS and XANES*, Wiley, New York, 1988.
- [52] G. Harp, Z. Han, B. Tonner, *J. Vac. Sci. Technol., A* **1990**, *8*, 2566.
- [53] D. Li, G. M. Bancroft, M. Kasrai, M. E. Fleet, X. H. Feng, K. H. Tan, *Am. Mineral.* **1994**, *79*, 785.
- [54] M. E. Fleet, S. Muthupari, *Am. Mineral.* **2000**, *85*, 1009.
- [55] M. E. Fleet, S. Muthupari, *J. Non-Cryst. Solids* **1999**, *255*, 233.
- [56] F. M. F. de Groot, M. O. Figueiredo, M. J. Basto, M. Abbate, H. Petersen, J. C. Fuggle, *Phys. Chem. Miner.* **1992**, *19*, 140.
- [57] G. van der Laan, *Phys. Rev. B: Condens. Matter Mater. Phys.* **1990**, *41*, 12366.
- [58] H. Thakur, R. Kumar, P. Thakur, N. B. Brookes, K. K. Sharma, A. P. Singh, Y. Kumar, S. Gautam, K. H. Chae, *J. Appl. Phys.* **2011**, *110*, 083718.

[59] D. Kim, M. Lee, S. Song, D. H. Kim, T. J. Park, D. Cho, *J. Phys. Chem. C* **2016**, *120*, 18674.

[60] R. Mourhatch, P. B. Aswath, *Tribol. Int.* **2011**, *44*, 201.

[61] K. Parekh, X. Chen, P. B. Aswath, *Tribol. Lett.* **2009**, *34*, 141.

CHAPTER 5

GENERAL CONCLUSIONS

Automobiles have long become an inherent part of our life and any scientific advances in this field will obviously have potential far reaching beneficial effects. For example, one-third of the fuel energy consumed is used to overcome friction in the engine, transmission, tires, and brakes. Thus, any new lubrication technology that reduces these frictional losses, increases longevity of the engine parts and lowers automobiles negative environmental effect, will be of both scientific and socio-economic importance. Over the years, with the advent of new engine designs and strict environmental regulations, there has been an increasing demand for novel lubricant additives which can perform under more extreme conditions and, at the same time, help reduce the harmful emissions.

The objective of this dissertation study was to explore and develop a novel approach to improved lubrication, one which involved a convergence of tribology and plasma polymerization techniques. In this approach, an innovative idea was implemented whereby nanoparticles are molecularly tailored using plasma polymerization techniques and these novel nano-additives were then evaluated for their tribological benefits in lubricant oils. Their performance was compared with the best anti-wear additive in the field, i.e. ZDDP, to estimate the commercial feasibility of these new additives. The study involved a thorough scientific effort to elucidate both physical and chemical phenomena involved in these processes.

Initially this technique was employed using PTFE nanoparticles, wherein core shell nano-additives were synthesized by depositing silica rich plasma coatings on nanoparticles. An additional methacrylate coating was deposited on top of the functionalized nanoparticles, using the

same plasma deposition method, to protect the siliceous chemistry and to achieve stable dispersion of these nanoparticles in the oil. These plasma functionalized PTFE nanoparticles were then mixed with oils containing a reduced amount of ZDDP and these oil formulations were then evaluated for their tribological performance. Results of the experiments strongly suggest that functionalized PTFE synergistically interact with reduced amount of ZDDP and provided superior anti-wear and anti-friction properties compared to ZDDP itself. Chemical analysis of the tribofilms revealed that these plasma modified particles promoted the formation of fluorine and silicon doped phosphate films at the tribological contacts.

Following the compatibility experiments between functionalized PTFE nanoparticles and ZDDP, more experiments were conducted along the same lines wherein functionalized nanoparticles were blended with oils containing ionic liquids. The objective was to investigate the interaction between these nanoparticles and ionic liquids and also to compare their tribological performance with blends containing ZDDP. Again, it was observed that functionalized PTFE nanoparticles interacted synergistically with the ionic liquid additives and displayed enhanced anti-wear and anti-friction behavior.

In order to examine the general extent and applicability of this technique, the same method was employed to make core-shell nano-additives with TiO_2 nanoparticles and boron rich monomer (TMB). The plasma functionalized TiO_2 nanoparticles were then investigated for their tribological properties and their interaction with reduced amount of ZDDP. The results of this study also showed synergistic interaction between boron functionalized TiO_2 nanoparticles and ZDDP.

The overall outcomes of this dissertation work establish plasma functionalization of nanoparticles as an effective way of delivering chemistries at tribological interfaces for superior anti-wear and anti-friction benefits. The knowledge acquired from this study adds a new dimension

to the lubricants additive research. Ideally, it can result in substantial reduction in the use of ZDDP or, even more ideally, possibly entirely eliminate its use via replacement with more environmentally friendly additives. An important inherent feature of the present work is that, in principle, the plasma surface functionalization readily permits an extremely wide range of surface chemistry modifications to virtual any nanoparticle, as based simply on an appropriate choice of monomer. Additionally, it will accommodate usage of mixtures of different nanoparticles, with each particle surface modified to provide specific atoms to molecularly tailor the compositions of the requisite tribological films.